WA School of Mines: Minerals, Energy and Chemical Engineering

Carbon Dioxide Capture using Gas Hydrates Technology

Hossein Dashti

This thesis is presented for the Degree of
Doctor of Philosophy
of
Curtin University

January 2019

توانا بود هر که دانا بود

ز دانش دل پیر برنا بود

“Mighty is he who has knowledge; By knowledge the old hearts grow young again.”- Ferdowsi (c. 940–1020)

Declaration

To the best of my knowledge and belief, this thesis contains no material previously published by any other person except where due acknowledgement has been made. This thesis contains no material, which has been accepted for the award of any degree or diploma in any university.

Full Name: Hossein Dashti

Signature:

Date: 06/01/2019

Abstract

Carbon dioxide (CO_2) capture has been a significant topic of research and development activities over the past two decades. As a highly potential novel alternative to adsorption, absorption or membrane technologies, hydrate-based CO_2 capture (HBCC) has received increasing attention within related industries, due to such advantages as the mild operating pressure and temperature that is required, the ease of regeneration and its unique separation mechanism. The kinetics of the gas hydrate formation is one the important challenging topics in order to have a better understanding of the mechanism of this process. The current thesis consists of three main technical modelling parts in order to enhance our understanding from the kinetics of the HBCC process.

A wide range of studies has been reported in the past decade on the improvement of the separation efficiency by using chemical additives. While most of these studies have shown improved kinetics, thermodynamics and/or separation efficiency at the laboratory scale, there has been no quantitative analysis of the energy consumption for viable industrial applications. Comparison of the effectiveness of chemical additives from separate studies or groups also is impossible. The present thesis is focused on the modelling of the hydrate-based CO_2 separation process and provides a quantitative approach that is new in its analysis of the effectiveness of chemical additives in relation to the energy required and the kinetic parameters involved in the process.

The second part of this thesis aims to conduct a model-based investigation on the kinetics of the HBCC process. A variation to the shrinking core model (SCM) was developed for the analysis of this heterogeneous system under varying boundary conditions. The results revealed that while the CO_2 diffusion through the hydrate layer is the dominant controlling mechanism, for a realistic scenario in which a time-dependent bulk gas concertation exists the model results would better match the experimental data by incorporating the effects of the reaction rate into the diffusion-based model. Sensitivity analysis was performed, showing that increasing diffusivity through the hydrate layer significantly decreases the full conversion time of the water. Moreover, the effect of temperature change was investigated, and it was found that lower temperatures slowed the hydrate growth rate. The model was proven to be a

computationally effective and time-efficient predictive tool without a need for high-speed computers for the large-scale (reactor) applications.

Due to the complexity of the multi-physics and multi-scale nature of the process, the technology has not been sufficiently understood for the real-life scale applications. The hydrate formation mechanisms and rate, in particular, need further fundamental studies to achieve relevant insights into the process design and intensification. High fidelity numerical models are crucial to capture and explain the dominant physicochemical mechanisms involved in the process. The third part of this thesis presents a new variation of the SCM allowing to capture the practically observed features of the CO_2 hydration process that has not been exploited by far, that is, the nucleation phase behavior. Accordingly, the most significant contribution of the current work, in contrast to the literature, is to propose and demonstrate an efficient and fast predictive tool for the CO_2 hydrate nucleation process. Moreover, a model-based estimation of the induction time, as a critical parameter in CO_2 hydrate rate estimation and control, is presented. Additionally, the temperature history profile over the nucleation and growth phases is simulated and compared against the experimental data from the literature.

Acknowledgements

I would like to express my sincere gratitude and special appreciation to Dr Amirpiran Amiri for his helpful and valuable supervision, support, feedback, insight and patience during my PhD at Curtin University. He supervised me in two main chapters of my thesis, and without his support, I could have never achieved my goals.

I wish to thank Professor Vishnu Pareek, my thesis Chairperson, for his valuable advice.

I foremost dedicate this thesis to my mother and father for their unconditional love, support and encouragement throughout this journey from a long distance.

List of publications

Chapter 2:

1. Dashti H, Yew LZ, Lou X. Recent advances in gas hydrate-based CO_2 capture. Journal of Natural Gas Science and Engineering. 2015; 23:195-207, Elsevier (Cited by 84).

Chapter 3:

2. Dashti H, Lou X. Gas Hydrate-Based CO_2 Separation Process: Quantitative Assessment of the Effectiveness of Various Chemical Additives Involved in the Process. Energy Technology. 2018, Carbon Dioxide Management and Other Technologies, 3-16, Springer (Cited by 2).

Chapter 4:

3. Dashti H, Thomas D, Amiri A, Lou X. Variations to the shrinking core model for effective kinetics modelling of the gas hydrate-based CO_2 process. Computer Aided Chemical Engineering. 2019, Elsevier (Accepted paper).

Chapter 5:

4. Dashti H, Thomas D, Amiri A. Modeling and analysis of hydrate-based CO_2 capture with nucleation stage prediction capability, The Journal of Cleaner Production. 2019; 231: 805-816, Elsevier.

Awards

Chapter 2 was presented, as an invited address by Professor Xia Lou, the 147th Annual Meeting & Exhibition of the Minerals, Metals & Materials Society, Phoenix, Utah USA and received the TMS LMD/EPD Energy Best Paper Award – Professional. The full paper was published in: Sun. et al. (eds) Energy Technology 2018. TMS 2018. The Minerals, Metals & materials Series. Springer, Cham Pp 3-16 (Online ISBN 978-3-319-72362-4; Print ISBN 978-3-319-723621-7).

Statement of contribution of others

The work presented in this thesis was primarily designed, executed, interpreted, and written by the thesis candidate, Hossein Dashti, under the supervision of Professor Xia Lou, and Dr Amirpiran Amiri (Lecturer at Aston University and Adjunct Lecturer at Curtin University) who has provided strong support in the work of the shrinking core model. Specific contributions by colleagues are described below.

Chapter 2: A literature review: Recent advances in gas hydrate-based CO_2 capture

Hossein Dashti continued the initial work on the review of the carbon dioxide (CO_2) hydrate formation by Leonel Zhehao Yew, an honours research student in the same group, and further progressed it into a manuscript for publication with critical guidance of Professor Xia Lou.

Chapter 3: Energy consumption estimation: Gas Hydrate-based CO_2 Capture Processes

Hossein Dashti designed and conducted the modelling of this chapter under the supervision of Professor Xia Lou. The writing of the manuscript was conducted by Hossein Dashti and critically reviewed by Professor Xia Lou.

Chapter 4: Kinetic modelling of the gas hydrate-based CO_2 processes: Variations to the shrinking core model
Chapter 5: Kinetic modelling of the gas hydrate-based CO_2 processes: a multistage shrinking core model

Hossein Dashti designed and developed the models for these two chapters under the supervision of Dr Amirpiran Amiri. Daniel Thomas, a taught MEng student at Aston University, conducted a portion of these two chapters and he used a portion of these works in his MEng Research Project report. Hossein Dashti's contribution in these works has been major and significant. The manuscripts were written by Hossein Dashti and critically reviewed by Dr Amirpiran Amiri and Professor Xia Lou.

Table of Contents

List of Figures

List of Tables

Chapter 2

Chapter 3

Chapter 5

Chapter 1. Introduction

1.1. Background

Carbon dioxide (CO_2) emissions from different chemical process industries are responsible for the rapid rise in global temperatures recorded in the last century. Separation of CO_2 from different industrial sources is one of the main challenges. As a highly potential alternative to the existing methods such as adsorption and absorption, hydrate-based CO_2 capture (HBCC) has received increasing attention within related industries, due to such advantages as the mild operating pressure and temperature that is required, the ease of regeneration and its unique separation mechanism.

Gas hydrates are solid clathrates made up of small gas molecules such as CO_2, nitrogen (N_2), hydrogen (H_2) and water molecules connected by hydrogen bonds which are formed under specific thermodynamic conditions of low temperature and high pressure (Sloan & Koh, 2008). CO_2 will form structure I hydrate at pressures higher than 4.5 MPa and temperatures lower than 283 K. The formation process includes two main steps: hydrate nucleation and growth. The nucleation stage is the initiation of the clathrate hydrate particles, and this stage follows by the growth stage in which the considerable increase in gas consumption occurs (Sloan & Koh, 2008).

The HBCC process is achieved through the differences of affinity with water between CO_2 and other gases in the hydrate cages when hydrate crystals are formed from a mixture of these gases (Eslamimanesh, Mohammadi, Richon, Naidoo, & Ramjugernath, 2012). These result in a solid hydrate phase enriched with CO_2 and a gaseous phase with concentrated other gases. The hydrate phase can then be dissociated, and accordingly, CO_2 can be recovered. High operation pressure is required to form hydrate crystals which lead to an increase in operating costs and energy consumption. The hydrates formation kinetics and the hydration capacity, as well as the hydration selectivity, are critical for the ultimate application of hydrates technology. Chemical additives such as tetrahydrofuran (THF) have been found useful to reduce the operating pressure as well as enhancing CO_2 recovery and gas storage capacity.

Different experimental and modelling studies focused on the investigation of the thermodynamic aspects of the gas hydrate formation such as prediction of the pressure and temperature of gas hydrate formation and dissociation (Maghsoodloo Babakhani, Bouillot, Ho-

Van, Douzet, & Herri, 2018). However, the kinetics of HBCC process is still not fully understood, and it needs to be investigated from both experimental and modelling point of view (Ke, Svartaas, & Chen, 2018; Khurana, Yin, & Linga, 2017; Warrier, Khan, Srivastava, Maupin, & Koh, 2016; Yin, Khurana, Tan, & Linga, 2018). The complexity of the gas hydrate formation especially in the understanding of the nucleation and growth step in this process leads to develop different modelling approaches to have a better understanding from the HBCC process. Further, using different chemical additives in order to enhance the effectiveness of the HBCC process is another challenge. It is significantly important to science and research as it develops a fundamental understanding about the CO_2 gas hydrates and the influence of various chemical additives to the formation kinetics conditions.

1.2. Project objectives and significance

The significance of the CO_2 capture and storage is one of the best solutions for the CO_2 emission into the atmosphere and consequently global warming. HBCC process is one of the new solutions for the CO_2 capture however the kinetics of this process is still not understood well, and it needs further experimental and modelling works to enhance our understanding from this process. This thesis presents an original contribution to improve the understanding of the kinetics of the gas hydrate formation process with emphasis on the CO_2 hydrate formation.

This study intends to address these critical problems using a fundamental approach. Specifically:

1) This thesis attempts to firstly develop a methodology to quantitatively analyse the effectiveness of the chemical additives in relation to the required energy and the controlling kinetic parameters which can be applied into the industrial application of the HBCC process.
2) Secondly, develop a variation of the shrinking core model (SCM) under varying boundary condition in order to identify the controlling kinetic mechanisms during HBCC process.
3) Develop a multi-stage SCM to simulate gas hydrate nucleation and growth process.
4) Prediction of the temperature history profile during gas hydrate nucleation and growth process using multi-stage SCM.

1.3. Research method

The techniques developed and improved in the current thesis is focussed on addressing the kinetics of the gas hydrate formation with more emphasis on the CO_2 hydrate formation which can be adapted to other gas hydrate formers.

Firstly, as the literature review of the current thesis, compared the separation mechanisms, as well as the advantages and limitations of HBCC process, with a strong focus on the reviewing of the chemical (additives) and mechanical (mixing) approaches that have been investigated to improve the CO_2 separation efficiency and energy consumption through HBCC technology. Further, the challenges for future research to further improve HBCC technology, making it industrially feasible and sustainable have been discussed.

Secondly, the energy analyses of this process with/without chemical additives are developed based on the following steps:

1) A literature review is done on the chemical additives capabilities in order to enhance the effectiveness of the HBCC process.
2) An energy analysis model has been developed in order to investigate the energy consumption during the HBCC with/without chemical additives. MATLAB coding is used for numerical calculations.
3) Validate the proposed model against the literature data and apply the model in the presence of the different chemical additives.

It is worth mentioning that the work in this chapter has considered the end point temperature and pressure for all chemical additives in the simulation. The results are comparable. Further work in Chapters 4 and 5 will focus on the improvement of the models to consider the entire process rather than the end points.

Following the above work, the multi-stage SCM was developed in order to simulate the kinetics of the HBCC with the capability to model the nucleation and the growth stage. The research in this stage includes:

1) A literature review is done on the different kinetic models based on the SCM in order to identify the weakness of the previous models. Each chapter of this thesis presents a part of the literature review in its own Introduction section.
2) A variation to the SCM was developed for the analysis of this heterogeneous system under varying boundary conditions. Further, the SCM modelling tried to identify the

controlling kinetic mechanism through the HBCC process using the fundamental equation in SCM.

3) Develop a new variation of a multi-stage SCM in order to simulate the nucleation and growth stage during the gas hydrate formation and examine the proposed model against the experimental. It is proposed and demonstrated an efficient and fast predictive tool for the CO_2 hydrate nucleation process. Moreover, a model-based estimation of the induction time, as a critical parameter in CO_2 hydrate rate estimation and control, is presented. Additionally, the temperature history profile over the nucleation and growth phases is simulated and compared against the experimental data from the literature.
4) Develop a multi-stage SCM in order to simulate the temperature profile change during the gas hydrate formation process and examine the results with the experimental data with emphasis on the HBCC process.

1.4. Thesis structure

The thesis is composed of six chapters:

1) In the first chapter (Introduction), the through a brief introduction the whole objective of this thesis has been summarised.
2) The second chapter is the literature review of the recent advances in gas hydrate-based CO_2 capture process.
3) The third chapter is focused on the modelling of the hydrate-based CO_2 separation process and provides a quantitative approach that is new in its analysis of the effectiveness of chemical additives in relation to the energy required and the kinetic parameters involved in the process.
4) The fourth chapter aims to conduct a model-based investigation on the kinetics of the HBCC process. A variation to the SCM was developed for the analysis of this heterogeneous system under varying boundary conditions. Further, the SCM modelling tried to identify the controlling kinetic mechanism through the HBCC process.
5) The fifth chapter presents a new variation of the SCM allowing to capture the practically observed features of the CO_2 hydrate formation process that has not been exploited by far, that is, the nucleation phase behaviour.
6) In the last chapter, the conclusions of the thesis and the possible future works are presented.

Overall, the thesis work firstly has developed an energy-based model in order to illustrate the efficient application of the HBCC with more emphasis on the presence of the chemical additives which can be later use for the large-scale application of the HBCC process, secondly this thesis for the first time developed a multi-stage kinetic model based on the SCM in order to simulate the nucleation and growth stages during gas hydrate formation which was compared with the experimental data and therefore, it is a foundation for future research towards enhancing our understanding of the hydrate nucleation behaviour-based on the predictive models at various scales.

1.5. References

Eslamimanesh, A., Mohammadi, A. H., Richon, D., Naidoo, P., & Ramjugernath, D. (2012). Application of gas hydrate formation in separation processes: A review of experimental studies. *The Journal of Chemical Thermodynamics, 46*, 62-71. doi:http://dx.doi.org/10.1016/j.jct.2011.10.006

Ke, W., Svartaas, T. M., & Chen, D. (2018). A Review of Gas Hydrate Nucleation Theories and Growth Models. *Journal of Natural Gas Science and Engineering*. doi:https://doi.org/10.1016/j.jngse.2018.10.021

Khurana, M., Yin, Z., & Linga, P. (2017). A review of clathrate hydrate nucleation. *ACS Sustainable Chemistry & Engineering*. doi:10.1021/acssuschemeng.7b03238

Maghsoodloo Babakhani, S., Bouillot, B., Ho-Van, S., Douzet, J., & Herri, J.-M. (2018). A review on hydrate composition and capability of thermodynamic modeling to predict hydrate pressure and composition. *Fluid Phase Equilibria, 472*, 22-38. doi:10.1016/j.fluid.2018.05.007

Sloan, E. D., & Koh, C. A. (2008). *Clathraye Hydrates of Natural Gases* (third ed. Vol. 119). New York: Taylor & Francis Group.

Warrier, P., Khan, M. N., Srivastava, V., Maupin, C. M., & Koh, C. A. (2016). Overview: Nucleation of clathrate hydrates. *J Chem Phys, 145*(21), 211705. doi:10.1063/1.4968590

Yin, Z., Khurana, M., Tan, H. K., & Linga, P. (2018). A review of gas hydrate growth kinetic models. *Chemical Engineering Journal, 342*, 9-29. doi:10.1016/j.cej.2018.01.120

Chapter 2. A literature review: Recent advances in gas hydrate-based CO_2 capture

This chapter is published as a journal paper in the Journal of Natural Gas Science and Engineering, 23 (2015): 195-207.

Journal of Natural Gas Science and Engineering 23 (2015) 195–207

Contents lists available at ScienceDirect

Journal of Natural Gas Science and Engineering

journal homepage: www.elsevier.com/locate/jngse

Review article

Recent advances in gas hydrate-based CO_2 capture

Hossein Dashti [1], Leonel Zhehao Yew [1], Xia Lou*

Department of Chemical Engineering, Curtin University, Kent Street, Bentley, WA 6102, Australia

ARTICLE INFO

Article history:
Received 5 December 2014
Received in revised form
21 January 2015
Accepted 22 January 2015
Available online 30 January 2015

Keywords:
CO_2 capture
Hydrate-based CO_2 capture
Semi-clathrate hydrates
Chemical additives
Mechanical methods

ABSTRACT

Hydrate-based CO_2 capture (HBCC) has received increasing attention, due to such advantages as the mild operating pressure and temperature, the ease of regeneration and its unique separation mechanism. This review paper is focused on the chemical additives and the mechanical methods that have been investigated to improve the CO_2 separation efficiency and energy consumption through HBCC technology. Detailed comparisons of the effects of various chemical additives and mechanical methods on gas consumption, operating conditions, hydrate induction time and CO_2 recovery are critically reviewed. The limitations and challenges of HBCC, in comparison with the conventional methods for CO_2 capture also are discussed.

1. Introduction

Carbon dioxide (CO_2) capture is a continuous process which requires a significant amount of energy to operate. It contributes to around 70–90% of the total operating cost of the three-stage carbon capture and storage system that is commonly used for the reduction of CO_2 emissions (Herzog and Golomb, 2004). Current CO_2 capture employs adsorption, absorption and membrane technologies which are low in efficiency and usually require multiple stages. Continuous efforts have been made to search for alternative methods in the area of CO_2 capture so that the overall operating cost of the carbon capture can be reduced.

CO_2 is captured from the effluent of power plants either post combustion or pre-combustion. Post-combustion capture refers to the treatment of flue gas before being released into the atmosphere. The flue gas consists of approximately 15–20% CO_2 and 5% O_2, with the balance being N_2, and it is emitted from a full combustion process. Pre-combustion capture refers to the capture of CO_2 from the fuel gas, which is the partially combusted fuel containing approximately 40% CO_2 and 60% H_2. The high CO_2 content in the fuel gas allows more efficient capture. However, it can only be employed in an integrated gasification combined cycle (IGCC) power plant where the fuel is pre-treated to produce CO_2/H_2 syngas and the CO_2 is separated from the syngas while the H_2 is fed into the combustion process. Post-combustion CO_2 capture is less effective than the pre-combustion method. However, it can be retrofitted to any plant without much modification (Spigarelli and Kawatra, 2013). Regardless, the gas systems that are discussed in this paper are mostly CO_2, or CO_2/N_2, or CO_2/H_2.

Hydrate-based CO_2 capture (HBCC) technology is a novel process that has received enormous attention, both from the industry and academic researchers, during the last two decades. The technology operates at mild pressures and temperatures, through a unique separation mechanism that is easy to regenerate and capable of separating gas mixtures, which might not be achievable via conventional technologies (Englezos and Lee, 2005). A significant number of studies have reported on the potential application of gas hydrates technology in CO_2 capture. These include some early work that was mostly focused on phase equilibrium studies of pure CO_2 hydrates, and more recent work that has focused closely on investigations of various chemical additives and mechanical methods for enhancement of the efficiency of CO_2 capture and separation. This paper will review the recent developments and research activities conducted on HBCC with a focus on chemical additives and mechanical approaches that are able to improve the selectivity, efficiency and kinetics of this technology. An introduction to the principles and significance of gas hydrates technology will be followed by detailed discussions of the current progress in technological improvements through the application of various chemical additives and mechanical methods. The key effects of the chemicals and mechanical methods, as well as the major outcomes

* Corresponding author.
E-mail address: x.lou@curtin.edu.au (X. Lou).
[1] These authors contributed equally to this work.

http://dx.doi.org/10.1016/j.jngse.2015.01.033
1875-5100/

of the research activities, will be summarised. In addition, the paper will give an account of the costs, limitations and challenges that are associated with HBCC, in comparison with the conventional technologies.

2. Hydrate-based CO_2 capture technology

2.1. Gas hydrates

Gas hydrates are solid clathrates made up of gas molecules (guests), such as methane (CH_4), CO_2, N_2 and H_2, that are caged within a cavity of hydrogen-bonded water molecules (host). They form under the favourable thermodynamic conditions of low temperature and high pressure, and they exhibit various structures depending on the size and chemical properties of the guest molecules (Sloan and Koh, 2008). Most small gas molecules, such as CO_2 and CH_4, form structure I (S_I). Structure II (S_{II}) hydrates form with larger gas molecules such as N_2 (Davidson et al., 1986) and propane. With the mixture of both small and large gas molecules, such as methane + cycloheptane, the structure H (S_H) may form (Sloan, 2003). The crystal structures of these hydrates consist of different water cavities. The most common forms of water cavity include the irregular dodecahedron ($4^35^66^3$) and the pentagonal dodecahedron (5^{12}), as well as the tetrakaidecahedron ($5^{12}6^2$), the hexakaidecahedron ($5^{12}6^4$) and the icosahedron ($5^{12}6^8$) that are often collectively described as $5^{12}6^m$, with $m = 2, 4, 8$ (Sloan and Koh, 2008). The term "5^{12}" is used to indicate that a relatively smaller cavity contains 12 pentagonal faces, whereas the term "$5^{12}6^m$" denotes a larger cavity with 12 pentagonal and m hexagonal faces, while "$4^35^66^3$" illustrates a medium cavity which contains 3 tetragonal, 6 pentagonal and 3 hexagonal faces. A combination of 5^{12} and $5^{12}6^2$ is more commonly seen in S_I, while the combination of 5^{12} and $5^{12}6^4$ is more commonly seen in S_{II}. In S_H, a combination of 5^{12}, $4^35^66^3$ and $5^{12}6^8$ has been observed.

Formation of gas (in particular methane) hydrates has been a significant problem for the upstream oil and gas industry because they clog pipelines, valves, wellheads and processing facilities, thus reducing production and causing safety problems. Extensive research activities have been undertaken in order to prevent or mitigate the formation of gas hydrates (Kelland, 2006). Research on the enhancement of gas hydrate formation began in the late 19th century after discovering the positive applications of gas hydrates for gas storage, separation, sequestration and desalination (Sloan and Koh, 2008).

2.2. Gas hydrate-based CO_2 capture

CO_2, as a small nonpolar hydrocarbon, forms S_I hydrates with a formula of $CO_2 \cdot nH_2O$ ($n = 5.75$) when coming into contact with water molecules below the equilibrium temperature and above the equilibrium pressure (Sloan and Koh, 2008). Upon dissociation, one volume of CO_2 hydrates can release 175 volumes of CO_2 gas at standard temperature and pressure conditions, which is potentially useful for the separation of the CO_2 from flue gas. The equilibrium phase diagram of CO_2 hydrates is presented in Fig. 1, which is constructed using an equation from experimental data reported by Kamath (1984). The figure also shows that other gases, such as N_2, H_2, and O_2, form hydrates under different equilibrium conditions. The equilibrium curve of H_2 was obtained from Dyadin et al. (1999).

As one can see from the equilibrium diagrams, CO_2 has the lowest hydrate-forming pressure in comparison with other components in flue gas. Separating CO_2 from the other gases can be achieved by first forming a solid hydrate phase that is enriched with CO_2. Dissociating the hydrates, after separating the hydrate phase from the gaseous phase, leads to the recovery of CO_2 that is much higher in concentration than the initial feed. Studies have shown that the concentration of CO_2 in the hydrate phase is at least four times greater than that in the gas phase (Duc et al., 2007). This hydrate-based CO_2 capture process is illustrated in a flow diagram displayed in Fig. 2. In brief, the gas mixture is sent to the hydrate formation reactor, in which CO_2 hydrates form as the pressure increases and temperature decreases. The hydrate slurry is separated from the CO_2-lean gas in the separator and sent to a hydrates dissociation reactor, from which purified CO_2 is collected, and the CO_2-rich gas is recycled for further processing.

2.3. Parameters describing the HBCC process

The efficiency of hydrate-based CO_2 separation is often described by such parameters as hydrate induction time, gas consumption, hydrate equilibrium pressure, CO_2 recovery or split fraction (S.Fr.) and separation factor (S.F.).

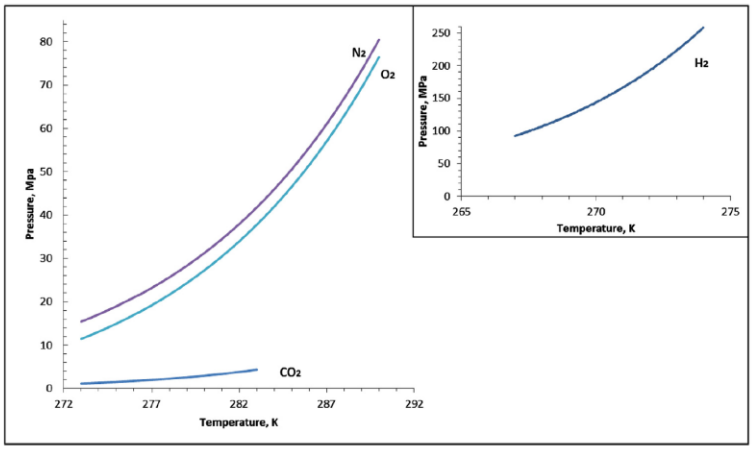

Fig. 1. The equilibrium phase diagrams of different hydrate formers.

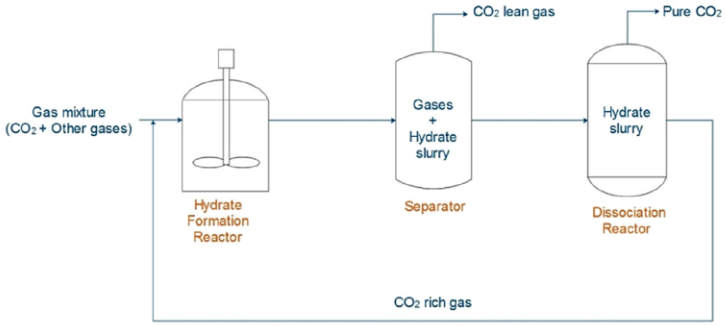

Fig. 2. Flow diagram of a HBCC processing unit.

The hydrate *induction time* is the time taken for crystal nuclei to form that are not visible to macroscopic probes. In practice, the induction time is determined at the time the consumption of hydrate-forming gases becomes observable (Sloan and Koh, 2008). Total *gas consumption* is the maximum amount of gas enclathrated during the hydration process. It is measured in moles, which includes all compositions within the gas mixture. The amount of gas that has been consumed during hydrate formation can be calculated using Eq. (1) and Eq. (2) (Linga et al., 2007c):

$$\Delta n_g = n_{g,0} - n_{g,t} = \frac{P_0 V}{Z_0 RT} - \frac{P_t V}{Z_t RT} \tag{1}$$

$$\Delta n_g^i = n_{g,0}^i - n_{g,t}^i = \frac{y_0^i P_0 V}{Z_0^i RT} - \frac{y_t^i P_t V}{Z_t^i RT} \tag{2}$$

where $n_{g,0}$ and $n_{g,t}$ are the total number of moles at time t = 0 and at any time t, respectively, Z is the compressibility factor calculated by the equation of the state, P is the pressure of the hydrate formation reactor, T is the temperature of the liquid phase, R is the ideal gas constant, i refers to component i of the gas mixture and y is the mole fraction in the gas phase. The volume of gas (V) is assumed to be constant throughout the hydrate formation process.

High gas consumption does not always mean high CO_2 consumption because the gas consumed might contain mostly gases other than CO_2. High separation efficiency is required for CO_2 capture, which is governed by two common factors: the *CO_2 recovery* or *split fraction* (S.Fr.) and the *separation factor* (S.F.). Split fraction refers to the percentage recovery of CO_2 and is determined using Eq. (3) (Linga et al., 2007c):

$$S.Fr. = n_{CO_2}^H \Big/ n_{CO_2}^{feed} \tag{3}$$

where $n_{CO_2}^H$ is the number of moles of CO_2 in the hydrate phase, and $n_{CO_2}^{feed}$ is the number of moles of CO_2 in the feed gas.

For a flue gas mixture containing CO_2 and another gas (A), the value of the *separation factor* is calculated using the following equation (Linga et al., 2007c):

$$S.F. = \frac{n_{CO_2}^H \times n_A^{gas}}{n_{CO_2}^{gas} \times n_A^H} \tag{4}$$

where $n_{CO_2}^H$ and n_A^H denote the number of moles of CO_2 and another gas (A) in the hydrate phase, respectively, $n_{CO_2}^{gas}$ is the number of moles of CO_2 in the residual gas phase and n_A^{gas} is the number of moles of A in the residual gas phase.

For CO_2 capture, a short induction time and high gas consumption, combined with high separation factor, are highly desirable. In practice, this is a challenging goal. Higher operating pressure leads to fast/high gas consumption; however, it does not guarantee a high CO_2 recovery and separation factor, since gases other than CO_2 may also form hydrates at the same time. In addition, the required high pressure leads to an increase in compression costs due to the high energy consumption. Over the past two decades, research has been focused on the methods and processes that would lower the operating pressure, while increasing the hydrate formation rate and the selectivity to CO_2 gas. Various chemical additives have been extensively studied to improve the CO_2 capture/separation efficiency. Mechanical methods also have been investigated to improve the contact area and mass transfer between gas and water so as to enhance gas consumption and reduce induction time. The following sections will discuss these chemical additives and mechanical methods, with the focus being on their thermodynamic and kinetic effects on the CO_2 hydrate formation process and the ultimate separation efficiency.

2.4. Chemical additives

Chemical additives act as hydrate promoters that may reduce the equilibrium hydrate formation pressure, shorten the induction time, increase the hydration rate, enhance gas uptake and improve the selectivity of CO_2 in hydrate cages. The chemical additives are generally divided into two classes: kinetic promoters and thermodynamic promoters. Kinetic promoters are mostly surfactants that increase the rate of hydrate formation without taking part in the hydrate formation itself. Commonly used surfactants in hydrate forming systems include sodium dodecyl sulphate (SDS), Tween-80 (T-80) and dodecyl-trimethyl-ammonium chloride (DTAC). Thermodynamic promoters are small molecules that take part in hydrate formation by competing with gas molecules for hydrate cages. The most investigated thermodynamic promoters include tetrahydrofuran (THF), cyclopentane (CP), propane (C_3H_8) and tetra-n-butyl ammonium bromide (TBAB), among which THF, CP and C_3H_8 form hydrate crystals without changing the structure of the water cavity, while TBAB takes part in the process through the formation of a semi-clathrate structure by breaking the water cage (Eslamimanesh et al., 2012). The chemical structures of these promoters are presented in Table 1. The mechanisms, kinetics and thermodynamic effects of these chemical additives on the efficiency of CO_2 separation are discussed in the following sections.

Table 1
The chemical structures of various chemical additives and surfactants.

Chemical additives		Chemical structure
Thermodynamic promoters	Tetrahydrofuran (THF)	
	Propane	
	Cyclopentane (CP)	
	Tetra-n-butyl ammonium bromide (TBAB)	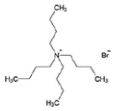
Kinetic promoters (Surfactants)	Tween-80 (T-80)	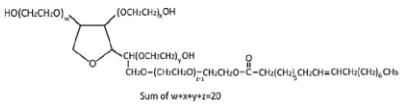 Sum of w+x+y+z=20
	Dodecyl-trimethyl-ammonium chloride (DTAC)	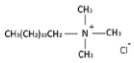
	Sodium dodecyl sulphate (SDS)	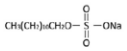

2.4.1. Tetrahydrofuran

Tetrahydrofuran (THF) is one of the most commonly studied chemical additives in hydrate-based CO_2 capture technology. THF forms the S_{II} hydrate (Hawkins and Davidson, 1966) that contains 16 small cavities (5^{12}) and 8 large cavities ($5^{12}6^4$) per unit lattice at thermodynamic conditions of 0.1 MPa and 277.6 K (Strobel et al., 2009). Although CO_2 naturally forms the S_I hydrate with water, the presence of THF induces the formation of S_{II} hydrates for all gas components in flue gas (Park et al., 2013), in which CO_2 occupies both the small cages, competing with N_2 or H_2, and the large cages, while competing with THF (Kang and Lee, 2000).

The most significant impact of THF on hydrate-based CO_2 capture includes the drastic reduction of both hydration pressure and induction time. As a consequence, large amounts of hydrates form, which include CO_2 hydrates, along with H_2 or N_2 hydrates depending on the composition of the gas mixtures. The CO_2 recovery or splitting factor (*S.Fr.*) (Eq. (3)) may increase but the separation factor (S.F.) (Eq. (4)) may reduce. Reduced rates of hydrate growth and initial gas uptake also have been reported (Adeyemo et al., 2010; Daraboina et al., 2013). As THF molecules occupy the large $5^{12}6^4$ cavities of S_{II} hydrates, high THF concentration also leads to reduced availability of cavities for CO_2 and other gases, therefore leading to reductions in both CO_2 recovery and separation factor. One percent mole (1 mol%) of THF has been reported to be optimal for CO_2 separation from CO_2/N_2 and CO_2/H_2 systems (Kang and Lee, 2000; Lee et al., 2010; Linga et al., 2007a). More details of THF-enhanced CO_2 separation reported by various research groups are summarised in Table 2.

2.4.2. Cyclopentane

Cyclopentane (CP) forms the S_{II} hydrate and occupies only large water cages at temperatures near 280 K and atmospheric pressure (Sloan and Koh, 2008; Sun et al., 2002). The presence of CP also reduces the equilibrium pressure and induction time. However, unlike THF, the formation of CO_2 hydrates in the presence of CP is independent of the concentration, which is likely due to the immiscibility of CP with water. Experimental results regarding CO_2 separation in the presence of CP are summarised in Table 3.

2.4.3. Propane

Like CP, propane (C_3H_8) also promotes hydrate formation at reduced equilibrium pressure (Babu et al., 2013b; Kumar et al., 2006). Propane alone forms S_{II} hydrates at 275 K and between 0.36 MPa and 0.48 MPa (Giavarini et al., 2003; Hendriks et al., 1996). It induces the formation of S_{II} hydrates when it competes with CO_2 for occupancy of large cages (Adisasmito and Sloan, 1992). A study has shown that 57% of large cages are occupied by CO_2 when 2.5 mol% C_3H_8 was added to the system (Kumar et al., 2009a). In most studies, the S_{II} hydrate form of CO_2 hydrates was observed. The formation of S_I hydrates also was observed when a gas mixture of 80.0% CO_2, 18.8 mol% H_2 and 1.2% C_3H_8 was used, reportedly due to the low propane concentration (Babu et al., 2013b). A pressure reduction of 49% was obtained when 2.5 mol% C_3H_8 was added to the hydrate system (Kumar et al., 2009b). This is less effective than THF. Reductions in induction time and hydrate formation rate also were reported by the same group. The lower growth rate caused less CO_2 gas to be enclathrated within a given period. Therefore, gas consumption was reduced from 0.101 to 0.078 mol within 2 h. As for the CO_2 recovery and separation factor, the presence of C_3H_8 produced little effect on the former and a slight decreasing effect on the latter (Kumar et al., 2009a; Linga et al., 2007b).

2.4.4. Tetra-n-butyl ammonium bromide

Tetra-n-butyl ammonium bromide (TBAB) is widely proposed gas hydrate promoter, which consists mainly of environmentally friendly TBA^+ ionic liquid. TBAB forms semi-clathrate (SC) hydrates, which is different from the action of other promoters (Fowler et al., 1940). In the SC hydrate structure, bromide anions are bonded to water molecules and form water + bromide hosts, with the cages being occupied by cations as guests (Jeffrey and McMullan, 1967).

Table 2
The effects of THF on gas hydrate-based CO_2 capture.

Author(s)	Gas systems[a]	Findings
Adeyemo et al. (2010)	CO_2/N_2/THF CO_2/H_2/THF	• Pressure reduction: 9 MPa $\xrightarrow{\text{1 mol\% THF}}$ 5 MPa • CO_2 concentration for CO_2/N_2 system: 17 mol% $\xrightarrow{\text{Three stages, without THF}}$ 98.8 mol% • CO_2 concentration for CO_2/H_2 system: 40 mol% $\xrightarrow{\text{Three stages, without THF}}$ 92 mol%
Daraboina et al. (2013)	$CO_2/N_2/SO_2$/THF CO_2 = 17 mol%, N_2 = 82 mol%, SO_2 = 1 mol%	• Gas consumption: 0.164 mol $\xrightarrow{\text{1 mol\% THF}}$ 0.059 mol • Induction time: 10 min $\xrightarrow{\text{1 mol\% THF}}$ 6 min
Kang and Lee (2000)	CO_2/N_2/THF	• Pressure reduction: 14 MPa $\xrightarrow{\text{1 mol\% THF}}$ 1.65 MPa • CO_2 concentration: 17 mol% $\xrightarrow{\text{One stage, 1 mol\% THF}}$ 34.71 mol% 17 mol% $\xrightarrow{\text{Three stages, without THF}}$ 99.67 mol%
Kang et al. (2001)	CO_2/N_2/THF	• Pressure reduction: 8.35 MPa $\xrightarrow{\text{1 mol\% THF}}$ 0.48 MPa • CO_2 concentration: 17 mol% $\xrightarrow{\text{Two stages, without THF}}$ 96 mol%
Lee et al. (2010)	CO_2/H_2/THF CO_2 = 39.2 mol%, H_2 = 60.8 mol%	• Pressure reduction: 11 MPa $\xrightarrow{\text{1 mol\% THF}}$ 2.25 MPa • At 1.78 MPa: Gas consumption: 0.6 mol Induction time: 3.3 min • At 0.89 MPa: Gas consumption: 0.2 mol Induction time: 6.6 min
Linga et al. (2007a)	CO_2/N_2/THF CO_2 = 16.9 mol%, N_2 = 83.1 mol%	• Pressure reduction: 7.7 MPa $\xrightarrow{\text{1 mol\% THF}}$ 2.5 MPa • CO_2 concentration: 17 mol% $\xrightarrow{\text{One stage, 1 mol\% THF}}$ 36.9 mol% 17 mol% $\xrightarrow{\text{Three stages, 1 mol \% THF}}$ 94 mol%
Linga et al. (2007c)	CO_2/N_2/THF CO_2 = 16.9 mol%, N_2 = 83.1 mol%; CO_2/H_2/THF CO_2 = 39.2 mol%, N_2 = 60.8 mol%	• Induction time decreased with increasing THF concentration • The equilibrium hydrate formation conditions: CO_2/N_2 → 7.7 MPa, 273.7 K CO_2/H_2 → 5.1 MPa, 273.7 K • Pressure reduction in CO_2/N_2 mixture: 7.7 MPa $\xrightarrow{\text{1 mol\% THF}}$ 0.345 MPa • Hydrates from CO_2/H_2 mixture grew faster than those from the CO_2/N_2 mixture • Induction time for CO_2/N_2 mixture:

(*continued on next page*)

Table 2 (*continued*)

Author(s)	Gas systems[a]	Findings
		16.3 min $\xrightarrow{1\ \text{mol\% THF}}$ < 1 min
Park et al. (2013)	CO_2/H_2/THF	• 5.6 mol% THF resulted in the maximum stabilization effect • Pressure reduction: 8 MPa $\xrightarrow{5.6\ \text{mol\% THF}}$ 0.5 MPa
Tang et al. (2013)	CO_2/N_2/THF CO_2 = 59 mol%, N_2 = 41 mol%	• Optimal THF concentration: 1 mol% • CO_2 recovery: 59% CO_2 $\xrightarrow{1\ \text{mol\% THF}}$ 75% CO_2

[a] Default composition unless specified: In CO_2/N_2, CO_2 = 17 mol% and N_2 = 83 mol%; In CO_2/H_2, CO_2 = 40 mol% and H_2 = 60 mol%.

Table 3
Hydrate-based CO_2 separation in the presence of CP.

Author(s)	Gas systems[a]	Findings
Li et al. (2012a)	CO_2/H_2/CP	• CO_2 concentration: 40 mol% $\xrightarrow{5\ \text{vol\% CP}}$ 84 mol% • Gas uptake: 0.022 mol • Induction time: 15 s
Zhang and Lee (2008a)	CO_2/CP	• CO_2 hydrates growth: independent of CP volume; dependent on initial water volume and pressure • Best growth rate: at 5 vol% CP and 3.06 MPa • Induction time: <0.2 h • Complete hydrate growth time: <2 h
Zhang and Lee (2008b)	CO_2/CP H_2/CP	• CO_2/CP hydrate showed slightly higher dissociation temperature and lower pressure than both CO_2/THF and CO_2/TBAB at 0.89–3.51 MPa
Zhang et al. (2009)	CO_2/H_2/CP	• Pressure reduction: 5.3 MPa $\xrightarrow{1.5\ \text{vol\% CP}}$ 1.3 MPa • CO_2 concentration: 40 mol% $\xrightarrow{\text{Two stages, 1.5 vol\% CP}}$ 98 mol%

[a] Default composition unless specified: In CO_2/N_2, CO_2 = 17 mol% and N_2 = 83 mol%; In CO_2/H_2, CO_2 = 40 mol% and H_2 = 60 mol%.

Due to this feature, SC hydrates allow greater gas capacity in water cages and better stability at atmospheric pressure (Wataru et al., 2003). The phase boundaries of CO_2 hydrates in the presence of TBAB form at temperatures from 273.15 K to 291.15 K and pressures from 0.25 MPa to 4.09 MPa, which are much lower pressure values than for pure CO_2 hydrate formation, specifically at lower temperatures (1.15 MPa–4.33 MPa) (Fig. 3).

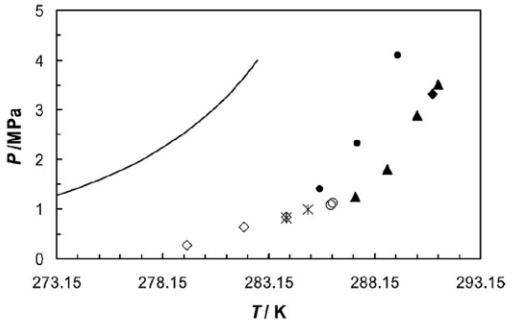

Fig. 3. CO_2/TBAB phase equilibrium data (Arjmandi et al., 2007): ●, TBAB, w = 0.10 and ▲, TBAB, w = 0.427; ◇, TBAB, w = 0.05 ○, TBAB, w = 0.10 and ◆, TBAB, w = 0.40; *, TBAB, w = 0.65; solid line, CO_2 hydrate phase boundary predicted by an in-house (HWHYD) model.

Studies on TBAB SC hydrates have demonstrated that there are two types, namely Type A and Type B, which grow simultaneously when in aqueous solution (Oyama et al., 2005). Type A has a cylindrical shape and a hydration number of 26. Type B has an irregular shape composed of thin crystals and shows a hydration number of 38. For the pure TBAB hydrate systems, when TBAB concentration is 0.014 mol%, type B is more stable than type A. Above 0.014 mol%, type A becomes more stable (Oyama et al., 2005; Wataru et al., 2003). The change of TBAB structure between these two different types in different TBAB concentrations makes the phase behaviour of SC hydrates difficult to study and complicated to analyse. Nevertheless, due to the high stability of TBAB's SC structure at low pressure, TBAB has the potential to reduce the formation pressure of CO_2 hydrate by up to over 90% at a concentration as low as 0.29 mol% (Li et al., 2010b). Increasing TBAB concentration not only reduces the equilibrium hydrate formation pressure but also increases the equilibrium hydrate forming temperature, which advances other clathrate hydrate promoters such as THF and CP (Meysel et al., 2011; Mohammadi et al., 2012). TBAB also has been found to reduce the induction time and increase the hydrate formation rate for the CO_2/N_2 mixture (Fan et al., 2009; Li et al., 2012b).

Other types of TBA^+ salts that are able to form SC hydrates also have been reported. Some examples of these additives are tetra n-butyl ammonium fluoride (TBAF), tetra n-butylphosphonium bromide (TBPB), and tetra n-butyl ammonium nitrate ($TBANO_3$). $TBANO_3$ was found to be approximately 1.5 times more effective than TBAB in reducing the pressure of the CO_2/N_2 hydrate system

Table 4
The effects of TBAB on hydrate-based CO_2 capture (weight percentage is presented as %).

Author(s)	Gas systems[a]	Findings
Babu et al. (2014a)	CO_2/H_2/TBAB TBAB = 0.3, 1.0, 1.5, 2.0, 3.0 mol%	• At TBAB = 0.3 mol%: highest gas consumption and longer induction time • At TBAB = 0.1 mol%: highest hydrate growth rate
Belandria et al. (2012a)	CO_2/N_2/TBAB CO_2 = 15.1, 39.9, 74.9 mol%, N_2 = 84.9, 60.1, 25.1 mol%, TBAB = 5, 30%	• Equilibrium hydrate formation: 275.2 K, 10.1 MPa $\xrightarrow{30\%\ \text{TBAB}}$ 285.7 K, 1.57 MPa • Increasing TBAB concentration: the dissociation pressure decreased and temperature increased • Increasing the N_2 concentration resulted in increasing hydrate formation pressure
Belandria et al. (2012b)	CO_2/N_2/TBAB CO_2 = 15.1, 39.9, 74.9 mol%, N_2 = 84.9, 60.1, 25.1 mol%, TBAB = 5, 30%	• Equilibrium pressure decreased with increasing TBAB concentration
Duc et al. (2007)	CO_2/TBAB N_2/TBAB CO_2/N_2/TBAB	• Pressure reduction at 284 K: CO_2: 14.36 MPa $\xrightarrow{0.29\ \text{mol\% TBAB}}$ 0.84 MPa N_2: 50 MPa $\xrightarrow{0.29\ \text{mol\% TBAB}}$ 29 MPa • Equilibrium pressure: CO_2 = 23.4 mol% , N_2 = 76.6 mol% $\xrightarrow{0.29\ \text{mol\% TBAB}}$ 0.5 MPa CO_2 = 48.2 mol%, N_2 = 51.8 mol% $\xrightarrow{0.29\ \text{mol\% TBAB}}$ 9 MPa
Gholinezhad et al. (2011)	CO_2/H_2/TBAB CO_2 = 40.2 mol%, H_2 = 59.8 mol%	• Gas consumption: 0.0502 mol at 5% TBAB; 0.086 mol at 10% TBAB • CO_2 recovery: 42% at 0% TBAB; 41% at 5% TBAB; 47% at 10% TBAB • Separation factor: 15.7 at 5% TBAB; 28 at 10% TBAB • CO_2 concentration at 10% TBAB: 40 mol% $\xrightarrow{\text{Two stages}}$ 96 mol%
Kim et al. (2011)	CO_2/H_2/TBAB	• Optimal TBAB concentration: 1 mol% • Gas consumption: 0.031 mol • CO_2 recovery: 24% • Separation factor: 26 • Induction time: 10.2 min
Li et al. (2009)	CO_2/N_2/TBAB CO_2 = 19.9 mol%, N_2 = 80.1 mol%, TBAB = 5%	• Induction time: 5 min • CO_2 recovery: 45% • Separation factor at 4.3 MPa: 7.3
Li et al. (2010b)	CO_2/H_2/TBAB CO_2 = 39.2 mol%, H_2 = 60.8 mol%, TBAB = 0.14–2.67 mol%	• Pressure reduction 9.84 MPa $\xrightarrow{0.29\ \text{mol\% TBAB}}$ 0.4 MPa • Higher TBAB concentration resulted in further pressure reduction
Li et al. (2010c)	CO_2/H_2/TBAB	• Optimal conditions: 2.5 MPa and 0.29 mol% TBAB • Gas Consumption: at 2.5 MPa $\longrightarrow$ 0.12 mol at 4.5 MPa $\longrightarrow$ 0.16 mol • CO_2 in residual gas: at 2.5 MPa $\longrightarrow$ 18.5 mol% at 4.5 MPa $\longrightarrow$ 22 mol%
Li et al. (2010d)	CO_2/N_2/TBAB/DTAC	• CO_2 concentration at 1.66 MPa: 17 mol% $\xrightarrow{\text{Two stages, 0.29 mol\% TBAB and 0.028 mol\% DTAC}}$ 99.2 mol% • CO_2 recovery: 54% • Induction time: 1 min • Optimal concentration of DTAC: 0.028 mol%
Li et al. (2011b)	CO_2/H_2/TBAB CO_2 = 39.2 mol%, H_2 = 60.8 mol%	• Optimal TBAB conditions: 0.29 mol% concentration and 2.5 MPa • CO_2 concentration: 39.2 mol% $\xrightarrow{0.29\ \text{mol\% TBAB}}$ 97 mol% • CO_2 recovery: 67.16% • Separation factor: 136.08
Li et al. (2012b)	CO_2/N_2/TBAB CO_2/N_2/$TBANO_3$ Co_2/N_2/TBPB	• $TBANO_3$ = 1 mol%: ➢ Highest gas uptake ➢ Gas consumption: 0.088 mol ➢ CO_2 recovery and separation factor at 3.26 MPa: 67%, 15.5 ➢ Induction time: 4.2 min ➢ CO_2 concentration:

(*continued on next page*)

Table 4 (*continued*)

Author(s)	Gas systems[a]	Findings
		17% $\xrightarrow{\text{1 mol\% TBANO}_3}$ 7%
		• TBAB = 0.65 mol%: ➢ Gas consumption: 0.056 mol ➢ CO_2 recovery and separation factor at 3.26 MPa: 46%, 12.8 ➢ Induction time: 0.1 min • TBPB = 1 mol%: • CO_2 recovery and separation factor at 3.26 MPa: 61% and 14 • Induction time: 2.7 min
Li et al. (2012a)	CO_2/H_2/TBAB/CP	• CO_2, H_2, TBAB = 0.29 mol%: ➢ Gas consumption: 0.126 mol ➢ Induction time: 2.7 min • CO_2, H_2, TBAB = 0.29 mol%, CP = 5 vol%: ➢ Gas consumption: 0.214 mol • Induction time: 0.32 min
Meysel et al. (2011)	CO_2/H_2/TBAB CO_2 = 20, 50, 75 mol%, H_2 = 80, 50, 25 mol%, TBAB = 5, 10, 2%	• Increasing TBAB concentration resulted in decreasing pressure • SC formed at a higher temperature than gas hydrates
Mohammadi et al. (2012)	CO_2/N_2/TBAB CO_2 = 15.1, 39.9 mol%, N_2 = 84.9, 60.1 mol%	• Equilibrium hydrate formation condition for CO_2 = 39.9 mol%, N_2 = 60.1 mol%: ➢ 5% TBAB: 285.6 K, 5.93 MPa ➢ 15% TBAB: 286.6 K, 2.89 MPa ➢ 30% TBAB: 286.4 K, 1.71 MPa
Mohammadi et al. (2013)	CO_2/H_2/TBAB CO_2 = 14.81, 39.52, 75.01 mol%, H_2 = 85.19, 60.48, 24.99 mol%	• Equilibrium hydrate formation condition for CO_2 = 39.52 mol%, H_2 = 60.48 mol%: 278.4 K, 10.5 MPa $\xrightarrow{\text{5\% TBAB}}$ 288.6 K, 12.17 MPa 278.4 K, 10.5 MPa $\xrightarrow{\text{30\% TBAB}}$ 288.6 K, 4.07 MPa

[a] Default composition unless specified: In CO_2/N_2, CO_2 = 17 mol% and N_2 = 83 mol%; In CO_2/H_2, CO_2 = 40 mol% and H_2 = 60 mol%.

(Li et al., 2012b). It also was found to instigate much higher gas uptake compared to TBAB at pressures between 2.5 and 4 MPa. Among the three TBA^+ salts investigated, it yielded the highest CO_2 recovery rate, 67%, and a separation factor of 15.54. The authors claimed that $TBANO_3$ and TBPB have high potential for replacing TBAB in the near future. The experimental studies of CO_2 capture by hydrates in the presence of TBAB are summarized in Table 4.

2.4.5. Surfactants and mixed chemical additives

Surfactants are a type of kinetic promoter that enhances the hydration kinetics by promoting gas solubility in water without modifying the thermodynamic equilibrium of the system. These compounds are composed of molecules that contain both a hydrophilic end and a hydrophobic end. Gas molecules form surfactant-gas associates with surfactants through strong hydrophobic interactions. Migration of the formed surfactant-gas associates to water molecules and/or structured water molecules is much easier than for pure gas molecules, due to the stronger affinity between water molecules and the hydrophilic end of the surfactant molecules. This ensures a faster formation of gas hydrates and, therefore, reduced induction time (Zhang et al., 2007). Fig. 4 is an illustration of the gas hydration process in the presence of sodium dodecyl sulphate (SDS). Surfactants have no effect on hydrate formation pressure. They can effectively improve the hydration kinetics by reducing the water surface tension.

Many surfactants have been investigated for hydrate-based CO_2 separation. Tween-80 (T-80), dodecyl-trimethyl-ammonium chloride (DTAC) and SDS are the most widely used. Among these three surfactants, SDS shows the greatest effect on hydrate promotion. This is mainly because SDS is an anionic surfactant, which is superior to both non-ionic and cationic surfactants for the same purpose (Okutani et al., 2008; Yoslim et al., 2010). Since surfactants do not partake in the enclathration process, unlike thermodynamic promoters, they do not sacrifice CO_2 recovery, separation factor or gas consumption for their enhancement of hydrate formation kinetics. Higher CO_2 recovery, reportedly, has been associated with higher SDS concentrations. However, when the SDS concentration is too high, SDS micelles may form, resulting in reduced gas and liquid contact surfaces and, therefore, lower CO_2 recovery (Tang et al., 2013).

Surfactants have been used together with THF or TBAB in order to achieve better separation of CO_2. For example, the SDS/THF additive mixture has been proven to double the gas uptake, compared with the case of using THF alone (Table 5). Addition of surfactants or light mineral oils into the hydration systems containing CP also has been found to increase the hydrate formation rate. This is due to the formation of a CP/water emulsion and the consequent increase in the CP/water interfacial area in the presence of surfactants. The presence of surfactants improves the gas diffusion through the gas/water and gas/hydrates interfaces, leading to enhanced inward and outward growth of hydrates (Fig. 5), therefore improving the hydrate formation rate. Other reported mixed chemical additives include CP/TBAB and DTAC/TBAB. The purpose of using mixed chemical additives is to reach higher CO_2 separation efficiency through the synergistic effects of the two chemical promoters. Table 5 summarises the findings by different research groups on the synergistic effects of chemical additives.

2.5. Mechanical methods

In addition to the chemical additives, investigations of various reactors and/or reaction conditions also have been carried out in order to improve the CO_2 formation efficiencies and to reduce energy consumption. In this paper, the term 'mechanical methods' is used because of its convenience. It should be noted that the discussions in previous sections were mostly of research activities that were based on laboratory experiments using a stirred tank reactor. In stirred tank reactors, the agglomeration of hydrate crystals becomes an obstacle to reducing the gas/water interface area and, consequently, the rate of hydrate formation and conversion of

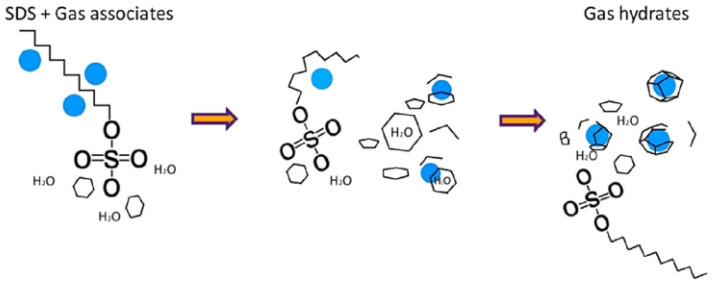

Fig. 4. Illustration of the migration of surfactants-gas associates to water molecules and/or cages.

water. The fixed bed crystalliser with porous silica gel has been widely studied in an effort to overcome this problem. The porous nature of the silica used in the fixed bed can significantly enhance the contact area between gas and water, allowing more gas to be enclathrated in a shorter time, therefore, improving the total gas uptake and induction. A study reported by Seo and Kang (2010) showed that over 93% of small cages and 100% of large cages were occupied by CO_2 when porous silica gels were used. Improved CO_2 selectivity and hydrate formation rate also have been achieved using the silica bed (Kang et al., 2013). In fact, the dispersed water in silica pores reacts readily with gas mixtures, which in turn eliminates the need for energy intensive mechanical agitation and excess water. This remains a strong economic advantage that keeps the need for research going (Adeyemo et al., 2010; Seo et al., 2005).

The silica bed can be further classified into silica gel bed and silica sand bed. Silica is very cheap and more economically desirable for large scale CO_2 separation. Babu et al. (2013a) claimed that water conversion reached up to 36% in the silica sand bed but only 13% in the silica gel bed. They also reported that the silica sand bed gave better performance for hydrate-based CO_2 capture due to higher gas uptake. A study by the same group also demonstrated that the silica sand bed provided a higher rate of hydrate formation and total gas uptake, when compared with a stirred crystalliser (Linga et al., 2012). Changing the physical properties, such as the particle and pore sizes of the porous silica gel, can further improve the kinetics of hydrate formation. Kang et al. (2008) found that pores which are too small lead to inhibition of their effect on hydrate formation due to the decreased water activity in the pores. Hydrate blockage of the pores may reduce the contact of gas and liquid, leading to incomplete migration of the solution through the hydrates (Yang et al., 2013a). Increasing pore size can overcome this problem. Larger pores and particle sizes tend to improve gas consumption, CO_2 recovery, separation factor and water conversion to hydrate, thus reducing the operating pressure (Adeyemo et al., 2010; Park et al., 2013). This is due to the lower flow resistance across a larger pore than a smaller pore. In other words, the larger exposed surface area of the silica gel significantly reduces induction time due to the better contact between gas and water within the gel (Kumar et al., 2013). A summary of the above-mentioned studies is given in Table 6.

The bubble method also has been attempted for gas hydrate-based CO_2 separation. The findings indicate that the hydrate shell formation around the bubble may hinder the further formation of hydrate within the bubble, due to isolation of the liquid from the gas (Luo et al., 2007). However, this can be improved by using a smaller bubble size. It was reported that an ideal size of gas bubbles for CO_2 separation is 50 μm (Xu et al., 2012b). Unlike stirring and the packed bed crystalliser, the bubble method requires a large bubbling column, which is not easily built and run on an experimental scale. This makes the method limited for further investigation.

More recent studies have shown that temperature fluctuation (via vibration) can be used to improve CO_2 hydrate formation (Li et al., 2011a; Liu et al., 2011; Xu et al., 2012a). This method is based on the fact that, when the temperature decreases, the solubility of CO_2 decreases in the hydrate-forming region while increasing in the non-hydrate-forming region (Kojima et al., 2002). The authors reported that, in the experiments using temperature fluctuation, the pressure drop was increased by 30%. A 30–35% increase in total gas consumption also was observed. The positive effect of the temperature fluctuation was mostly observed during the early period of hydrate growth. The method was demonstrated to be effective when the reaction scale was increased by 100-fold (Xu et al., 2012a).

3. Advantages and limitations of current HBCC technology

The cost of HBCC technology in an integrated gasification combined cycle (IGCC) plant was reported in 1999 by the US Department of Energy to be US$ 8.75 per ton of CO_2 captured, which is comparable to the cost of US$ 59 per ton of CO_2 captured using conventional amine-based absorption and US$ 64 per ton of CO_2 for adsorption by zeolite (Ho et al., 2008; Reiner et al., 1994; Tam et al., 2001). It is this remarkable value that has drawn significant attention from CO_2 capture-related industries and has resulted in the increasing number of research projects involving HBCC technology over the past decade. Other advantages of HBCC technology include: 1) its moderate operational temperature range (273–283 K), 2) its relatively low energy consumption in hydrate dissociation/regeneration and the ease of recycling of aqueous solution containing additives, and 3) its capability for continuous operation, which allows large scale treatment (with the potential to achieve 8000 ton/day CO_2) (Kang and Lee, 2000).

However, the practical application of HBCC technology is limited due to its high pressure operating condition and large footprint. A case study using HBCC technology was completed by Tajima et al., based on a 100 MW thermal power plant where the energy penalty for CO_2 capture was found to be 15.8% and the required reactor volume was 7000 m^3 (Tajima et al., 2004). This shows that HBCC is still incomparable with conventional technologies, such as amine absorption, which has a much lower energy penalty (7–10%) (Tajima et al., 2004). A comparison of different CO_2 separation technologies is summarised in Table 7.

Table 5
Synergistic effects of chemical additives (weight percentage is presented as %).

Author(s)	System[a]	Findings
Herslund et al. (2014)	CO_2/THF/SDS SDS = 0.054 mol%	• Addition of 5 mol% THF decreased hydrate equilibrium pressure by up to 20%
Li et al. (2010)	CO_2/N_2/CP CO_2 = 16.6 mol%, N_2 = 83.4 mol%; CO_2/N_2/CP/H_2O emulsion CO_2 = 16.6 mol%, N_2 = 83.4 mol%	• Higher hydrate formation rate in presence of CP/H_2O emulsion • CO_2 concentration in the presence of: ➢ CP at 2.9 MPa ⟶ 44 mol% ➢ CP/H_2O emulsion at 3.29 MPa ⟶ 35.29 mol%
Li et al. (2010d)	CO_2/N_2/TBAB/DTAC	• Higher pressure and induction time reduction, with addition of DTAC • CO_2 concentration: 17 mol% —(0.028 mol% DTAC, 0.29 mol% TBAB)→ 67 mol% 17 mol% —(Two stages, 0.028 mol% DTAC, 0.29 mol% TBAB)→ 99.4 mol%
Li et al. (2011c)	CO_2/H_2/TBAB/CP CO_2 = 38.6 mol%, H_2 = 61.4 mol%	• Optimal CP and TBAB concentrations: 5 vol% and 0.29 mol% • The addition of CP: sped up the nucleation rate and CO_2 separation • CO_2 separation: 40 mol% —(5 vol% ratio CP/0.29 mol% TBAB)→ 93 mol% • Gas consumption: 0.22 mol • CO_2 recovery: 58% • Separation factor: 31 • Decreasing induction time with increasing CP/TBAB ratio
Li et al. (2012a)	CO_2/H_2/TBAB/CP CO_2 = 38.6 mol%, H_2 = 61.4 mol%	• CO_2 concentration: 38.6 mol% —(5 vol% CP, 29 mol% TBAB)→ 91.3 mol% • Gas uptake: 0.214 mol • Both S_H and SC hydrate observed at 4 MPa and 274.65 K • The formation of S_H hydrate by CP reduced the SC hydrate induction time from over 150 s–19 s
Lirio et al. (2013)	CO_2/THF/SDS	• High reduction in reduction time in the presence of THF • Under 3 MPa, 500 ppm SDS/5 mol% THF: ➢ 91.9% yield ➢ 25 min induction time
Liu et al. (2014)	CO_2/H_2/CP/TBAB CO_2 = 46.8, 15.6 mol%, H_2 = 53.2, 84.8 mol%, CP = 30, 50 vol%	• The optimal TBAB concentration: 0.29 mol% • Separation factor increased from 37 to 99 at 0.29 mol% TBAB • TBAB is an anti-agglomerant which can improve the flow behaviour of hydrate slurry
Torré et al. (2011)	CO_2/THF/SDS	• Optimal concentrations: SDS > 1500 ppm 1% < THF <4%
Torré et al. (2012)	CO_2/THF/SDS	• Optimal concentrations: 0.3% SDS 4% THF • The combination of THF and SDS showed significant gas uptake • THF increased the hydrate temperature and decreased the hydrate pressure • SDS had no influence on equilibrium conditions
Yang et al. (2013b)	CO_2/THF/SDS	• Shortest induction time in presence of 1000 mg/L SDS and 3 mol% THF • Hydrate equilibrium temperature decreased with increasing SDS concentration
Zhang et al. (2014)	THF/SDS/CO_2/N_2	• Increasing THF concentration resulted in lower reduction in equilibrium pressure • Optimal THF concentration: 3 mol%

[a] Default composition unless specified: In CO_2/N_2, CO_2 = 17 mol% and N_2 = 83 mol%; In CO_2/H_2, CO_2 = 40 mol% and H_2 = 60 mol%.

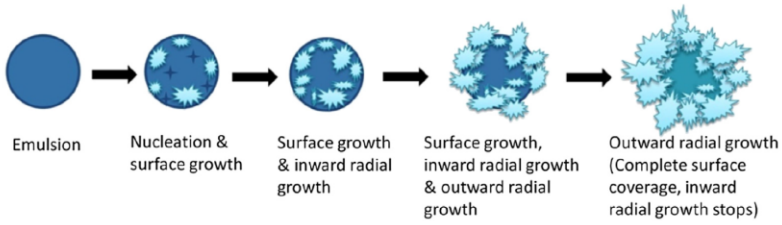

Fig. 5. Illustration of hydrate formation in an emulsion (Rework of Karanjkar et al., 2012).

Table 6
CO_2 capture in fixed bed crystallisers.

Author(s)	Gas systems[a]	Findings
Adeyemo et al. (2010)	CO_2/N_2 CO_2/H_2	• The rate of hydrate formation and hydrate yield were higher than in a stirred crystalliser • Total gas consumption, CO_2 recovery and water-to-hydrate conversion increased with larger pores and particle sizes
Babu et al. (2013a)	CO_2/H_2	• Sand bed: ➢ Water conversion: 36% ➢ Induction time: 18 min • Gel bed: ➢ Water conversion: 13% ➢ Induction time: 14 min • The performance of the sand bed was sensitive to the pressure driving force, while the gel bed was not • The sand bed is claimed to be a better porous medium
Babu et al. (2014b)	CO_2/H_2/TBAB/THF TBAB = 0.3, 1, 3 mol%, THF = 1, 5.53 mol%	• In the presence of THF, higher gas consumption and shorter induction time in the silica sand bed crystalliser • By increasing THF concentration, higher gas consumption was achieved but induction time did not change significantly • Increasing TBAB concentration resulted in lower gas consumption and significant change in induction time
Kang et al. (2008)	CO_2	• Hydrate growth was inhibited in small pores • S_I hydrate was formed in silica gel pores, similar to that in bulk water
Kang et al. (2013)	CO_2/H_2	• With 100 nm silica gel, 98.7% CO_2 in hydrate phase was achieved under 9.2 MPa • Hydrate dissociation pressure decreased with increasing CO_2 concentration in the feed
Kumar et al. (2013)	CO_2	• Larger surface area enhanced water-to-hydrate conversion and shortened induction time
Linga et al. (2012)	CO_2 $CO_2/H_2/C_3H_8$ CO_2 = 38.1 mol%, H_2 = 59.4 mol%, C_3H_8 = 2.5 mol%	• Silica sand bed crystalliser showed higher rate of hydrate formation and higher gas uptake than in a stirred vessel
Park et al. (2013)	CO_2/H_2	• 100 nm gel: ➢ Showed lowest equilibrium pressure ➢ Increased gas uptake significantly
Seo and Kang (2010)	CO_2/H_2 CO_2 = 41 mol%, H_2 = 59 mol%	• CO_2 occupied 93% of small cages and 100% of large cages of S_I hydrate formed in silica gel pores • 98.7 mol% CO_2 in hydrate phase was achieved with 100 nm silica gel

[a] Default composition unless specified: In CO_2/N_2, CO_2 = 17 mol% and N_2 = 83 mol%; In CO_2/H_2, CO_2 = 40 mol% and H_2 = 60 mol%.

4. Conclusions

In summary, we have reviewed the available methods of improving the hydrate-based CO_2 separation technology in terms of CO_2 separation efficiency, gas consumption and rate of hydrate formation, which includes chemical and mechanical approaches. The paper has focused on scholarly published research activities between 2000 and 2014. The studies performed to date show a more diverse field of research in chemical approaches, which include thermodynamic promoters (THF, TBAB, C_3H_8, CP) and kinetic promoters (surfactants). The research into mechanical methods is, however, receiving less attention. This is probably

Table 7
A comparison of different CO_2 separation technologies.

Methods	Energy consumption (MJ/kg CO_2)	Cost (USD/ton CO_2)	Advantages	Drawbacks
Absorption	4–6 (Favre, 2007)	30–60 (Yang et al., 2011)	- Well established process - Up to 95% CO_2 recovery (Olajire, 2010) - Easily incorporated into existing plant	- Energy intensive regeneration (Aaron and Tsouris, 2005) - Degradation of solvent - Sensitive to SO_x and NO_x - Corrosion issue
Adsorption	2–3 (Mondal et al., 2012)	40–63 (Yang et al., 2011)	- Simultaneous dehydration (Olajire, 2010) - Lower regeneration energy - Adsorbents are commercially available	- Low selectivity - Low capacity - Slow adsorption rate - Only suitable for CO_2 concentration between 0.04% and 1.5% (Audus, 1997)
Membrane	0.5–1 (Bounaceur et al., 2006)	50–78 (Yang et al., 2011)	- No regeneration required - Simple system - No waste streams - Membranes are commercially available	- Only suitable for CO_2 > 20% (Bounaceur et al., 2006; Favre, 2007) - Sensitive to high temperature (Spigarelli and Kawatra, 2013) - Plugged by impurities (Olajire, 2010) - Low removal efficiency, multiple stages required - Sensitive to sulphur compounds - Membrane ageing (Brunetti et al., 2010)
Hydrate-based	3 (Tajima et al., 2004)	8.75 (Tam et al., 2001)	- Moderate operational temperature range (273–283 K) - Relatively low energy consumption - Easy recycling of aqueous solution - Continuous operation allows large scale treatment (Kang and Lee, 2000)	- Immature technology - High pressure operating condition and large footprint (Tajima et al., 2004) - Large energy penalty (Tajima et al., 2004)

because the readily access to the default stirred reactor that is easier to build and run on a laboratory scale. The risk of building a different reactor for experimental purposes is not willingly undertaken, probably due to the large investment and unknown performance. However, the outcome from the review suggests that both chemical and mechanical approaches should be used, in parallel, to achieve the ultimate performance of hydrate-based technology. Also, a method should be established to ensure direct comparison of experimental results cross-batch and/or cross-laboratory. Moreover, the hydrate-based CO_2 separation method is known to be a novel technology with high potential. In order to outshine the conventional technologies, the economic aspect is a significant factor compared to performance. More detailed studies on the feasibility and economic cost must be performed in order to convince the industry with a quantitative argument and to draw more investment into hydrate-based CO_2 separation technology in the near future.

References

Aaron, D., Tsouris, C., 2005. Separation of CO_2 from flue gas: a review. Sep. Sci. Technol. 40, 321–348.

Adeyemo, A., Kumar, R., Linga, P., Ripmeester, J., Englezos, P., 2010. Capture of carbon dioxide from flue or fuel gas mixtures by clathrate crystallization in a silica gel column. Int. J. Greenh. Gas Control 4, 478–485.

Adisasmito, S., Sloan, E.D., 1992. Hydrates of hydrocarbon gases containing carbon dioxide. J. Chem. Eng. Data 37, 343–349.

Arjmandi, M., Chapoy, A., Tohidi, B., 2007. Equilibrium data of hydrogen, methane, nitrogen, carbon dioxide, and natural gas in semi-clathrate hydrates of tetra-butyl ammonium bromide. J. Chem. Eng. Data 52, 2153–2158.

Audus, H., 1997. Greenhouse gas mitigation technology: an overview of the CO_2 capture and sequestration studies and further activities of the IEA greenhouse gas R&D programme. Energy 22, 217–221.

Babu, P., Kumar, R., Linga, P., 2013a. Pre-combustion capture of carbon dioxide in a fixed bed reactor using the clathrate hydrate process. Energy 50, 364–373.

Babu, P., Yang, T., Veluswamy, H.P., Kumar, R., Linga, P., 2013b. Hydrate phase equilibrium of ternary gas mixtures containing carbon dioxide, hydrogen and propane. J. Chem. Thermodyn. 61, 58–63.

Babu, P., Chin, W.I., Kumar, R., Linga, P., 2014a. Systematic evaluation of tetra-n-butyl ammonium bromide (TBAB) for carbon dioxide capture employing the clathrate process. Ind. Eng. Chem. Res. 53, 4878–4887.

Babu, P., Ho, C.Y., Kumar, R., Linga, P., 2014b. Enhanced kinetics for the clathrate process in a fixed bed reactor in the presence of liquid promoters for pre-combustion carbon dioxide capture. Energy 70, 664–673.

Belandria, V., Mohammadi, A.H., Eslamimanesh, A., Richon, D., Sánchez-Mora, M.F., Galicia-Luna, L.A., 2012a. Phase equilibrium measurements for semi-clathrate hydrates of the (CO_2+N_2+tetra-n-butylammonium bromide) aqueous solution systems: Part 2. Fluid Phase Equilib. 322–323, 105–112.

Belandria, V., Mohammadi, A.H., Richon, D., 2012b. Compositional analysis of the gas phase for the CO_2+N_2+Tetra-n-butylammonium bromide aqueous solution systems under hydrate stability conditions. Chem. Eng. Sci. 84, 40–47.

Bounaceur, R., Lape, N., Roizard, D., Vallieres, C., Favre, E., 2006. Membrane processes for post-combustion carbon dioxide capture: a parametric study. Energy 31, 2556–2570.

Brunetti, A., Scura, F., Barbieri, G., Drioli, E., 2010. Membrane technologies for CO_2 separation. J. Membr. Sci. 359, 115–125.

Daraboina, N., Ripmeester, J., Englezos, P., 2013. The impact of SO_2 on post combustion carbon dioxide capture in bed of silica sand through hydrate formation. Int. J. Greenh. Gas Control 15, 97–103.

Davidson, D.W., Handa, Y.P., Ratcliffe, C.I., Ripmeester, J.A., Tse, J.S., Dahn, J.R., Lee, F., Calvert, L.D., 1986. Crystallographic studies of clathrate hydrates. Part I. Mol. Cryst. Liq. Cryst. 141, 141–149.

Duc, N.H., Chauvy, F., Herri, J.M., 2007. CO_2 capture by hydrate crystallization – a potential solution for gas emission of steelmaking industry. Energy Convers. Manag. 48, 1313–1322.

Dyadin, Y.A., Larionov, E.G., Manakov, A.Y., Zhurko, F.V., Aladko, E.Y., Mikina, T.V., Komarov, V.Y., 1999. Clathrate hydrates of hydrogen and neon. Mendeleev Commun. 9, 209–210.

Englezos, P., Lee, J.D., 2005. Gas hydrates: a cleaner source of energy and opportunity for innovative technologies. Korean J. Chem. Eng. 22, 671–681.

Eslamimanesh, A., Mohammadi, A.H., Richon, D., Naidoo, P., Ramjugernath, D., 2012. Application of gas hydrate formation in separation processes: a review of experimental studies. J. Chem. Thermodyn. 46, 62–71.

Fan, S., Li, S., Wang, J., Lang, X., Wang, Y., 2009. Efficient capture of CO_2 from simulated flue gas by formation of TBAB or TBAF semiclathrate hydrates. Energy Fuels 23, 4202–4208.

Favre, E., 2007. Carbon dioxide recovery from post-combustion processes: can gas permeation membranes compete with absorption? J. Membr. Sci. 294, 50–59.

Fowler, D.L., Loebenstein, W.V., Pall, D.B., Kraus, C.A., 1940. Some unusual hydrates of quaternary ammonium salts. J. Am. Chem. Soc. 62, 1140–1142.

Gholinezhad, J., Chapoy, A., Tohidi, B., 2011. Separation and capture of carbon dioxide from CO_2/H_2 syngas mixture using semi-clathrate hydrates. Chem. Eng. Res. Des. 89, 1747–1751.

Giavarini, C., Maccioni, F., Santarelli, M.L., 2003. Formation kinetics of propane hydrates. Ind. Eng. Chem. Res. 42, 1517–1521.

Hawkins, R.E., Davidson, D.W., 1966. Dielectric relaxation in the clathrate hydrates of some cyclic ethers. J. Phys. Chem. 70, 1889–1894.

Hendriks, E.M., Edmonds, B., Moorwood, R.A.S., Szczepanski, R., 1996. Hydrate structure stability in simple and mixed hydrates. Fluid Phase Equilib. 117, 193–200.

Herslund, P.J., Daraboina, N., Thomsen, K., Abildskov, J., von Solms, N., 2014. Measuring and modelling of the combined thermodynamic promoting effect of tetrahydrofuran and cyclopentane on carbon dioxide hydrates. Fluid Phase Equilib. 381, 20–27.

Herzog, H., Golomb, D., 2004. Carbon capture and storage from fossil fuel use. Encycl. Energy 1, 1–11.

Ho, M.T., Allinson, G.W., Wiley, D.E., 2008. Reducing the cost of CO_2 capture from flue gases using pressure swing adsorption. Ind. Eng. Chem. Res. 47, 4883–4890.

Jeffrey, G.A., McMullan, R.K., 1967. Clathrate hydrates. Prog. Inorg. Chem. 8, 43.

Kamath, V.A., 1984. Study of Heat Transfer Characteristics during Dissociation of Gas Hydrates in Porous Media. University of Pittsburgh (Ph.D thesis).

Kang, S., Lee, H., 2000. Recovery of CO_2 from flue gas using gas hydrate: thermodynamic verification through phase equilibrium measurements. Environ. Sci. Technol. 34, 4397–4400.

Kang, S.P., Lee, H., Lee, C.S., Sung, W.M., 2001. Hydrate phase equilibria of the guest mixtures containing CO_2, N_2 and tetrahydrofuran. Fluid Phase Equilib. 185, 101–109.

Kang, S.P., Lee, J.W., Ryu, H.J., 2008. Phase behavior of methane and carbon dioxide hydrates in meso- and macro-sized porous media. Fluid Phase Equilib. 274, 68–72.

Kang, S.P., Lee, J., Seo, Y., 2013. Pre-combustion capture of CO_2 by gas hydrate formation in silica gel pore structure. Chem. Eng. J. 218, 126–132.

Karanjkar, P.U., Lee, J.W., Morris, J.F., 2012. Calorimetric investigation of cyclopentane hydrate formation in an emulsion. Chem. Eng. Sci. 68, 481–491.

Kelland, M.A., 2006. History of the development of low dosage hydrate inhibitors. Energy Fuels 20, 825–847.

Kim, S.M., Lee, J.D., Lee, H.J., Lee, E.K., Kim, Y., 2011. Gas hydrate formation method to capture the carbon dioxide for pre-combustion process in IGCC plant. Int. J. Hydrog. Energy 36, 1115–1121.

Kojima, R., Yamane, K., Aya, I., 2002. Dual nature of CO_2 solubility in hydrate forming region. In: 4th International Conference on Gas Hydrates, Yokohama, Japan.

Kumar, R., Wu, H., Englezos, P., 2006. Incipient hydrate phase equilibrium for gas mixtures containing hydrogen, carbon dioxide and propane. Fluid Phase Equilib. 244, 167–171.

Kumar, R., Englezos, P., Moudrakovski, I., Ripmeester, J.A., 2009a. Structure and composition of CO_2/H_2 and CO_2/H_2/C_3H_8 hydrate in relation to simultaneous CO_2 capture and H_2 production. AIChE J. 55, 1584–1594.

Kumar, R., Linga, P., Ripmeester, J.A., Englezos, P., 2009b. Two-stage clathrate hydrate/membrane process for precombustion capture of carbon dioxide and hydrogen. J. Environ. Eng. (Rest. VA, U. S.) 135, 411–417.

Kumar, A., Sakpal, T., Linga, P., Kumar, R., 2013. Influence of contact medium and surfactants on carbon dioxide clathrate hydrate kinetics. Fuel 105, 664–671.

Lee, H.J., Lee, J.D., Linga, P., Englezos, P., Kim, Y.S., Lee, M.S., Kim, Y.D., 2010. Gas hydrate formation process for pre-combustion capture of carbon dioxide. Energy 35, 2729–2733.

Li, S., Fan, S., Wang, J., Lang, X., Liang, D., 2009. CO_2 capture from binary mixture via forming hydrate with the help of tetra-n-butyl ammonium bromide. J. Nat. Gas Chem. 18, 15–20.

Li, S., Fan, S., Wang, J., Lang, X., Wang, Y., 2010. Clathrate hydrate capture of CO_2 from simulated flue gas with cyclopentane/water emulsion. Chin. J. Chem. Eng. 18, 202–206.

Li, X.S., Xia, Z.M., Chen, Z.Y., Yan, K.F., Li, G., Wu, H., 2010b. Equilibrium hydrate formation conditions for the mixtures of CO_2 + H_2 + tetrabutyl ammonium bromide. J. Chem. Eng. Data 55, 2180–2184.

Li, X.S., Xia, Z.M., Chen, Z.Y., Yan, K.F., Li, G., Wu, H., 2010c. Gas hydrate formation process for capture of carbon dioxide from fuel gas mixture. Ind. Eng. Chem. Res. 49, 11614–11619.

Li, X.S., Xu, C.G., Chen, Z.Y., Wu, H., 2010d. Tetra-n-butyl ammonium bromide semi-clathrate hydrate process for post-combustion capture of carbon dioxide in the presence of dodecyl trimethyl ammonium chloride. Energy 35, 3902–3908.

Li, X., Xu, C., Chen, Z., Wu, H., Cai, J., 2011a. Effect of temperature fluctuation on hydrate-based CO_2 separation from fuel gas. J. Nat. Gas Chem. 20, 647–653.

Li, X.S., Xia, Z.M., Chen, Z.Y., Wu, H., 2011b. Precombustion capture of carbon dioxide and hydrogen with a one-stage hydrate/membrane process in the presence of tetra-n-butylammonium bromide (TBAB). Energy Fuels 25, 1302–1309.

Li, X.S., Xu, C.G., Chen, Z.Y., Wu, H., 2011c. Hydrate-based pre-combustion carbon dioxide capture process in the system with tetra-n-butyl ammonium bromide solution in the presence of cyclopentane. Energy 36, 1394–1403.

Li, X.S., Xu, C.G., Chen, Z.Y., Cai, J., 2012a. Synergic effect of cyclopentane and tetra-n-butyl ammonium bromide on hydrate-based carbon dioxide separation from fuel gas mixture by measurements of gas uptake and X-ray diffraction patterns. Int. J. Hydrog. Energy 37, 720–727.

Li, X.S., Zhan, H., Xu, C.G., Zeng, Z.Y., Lv, Q.N., Yan, K.F., 2012b. Effects of tetrabutyl-

(ammonium/phosphonium) salts on clathrate hydrate capture of CO_2 from simulated flue gas. Energy Fuels 26, 2518–2527.
Linga, P., Adeyemo, A., Englezos, P., 2007a. Medium-pressure clathrate hydrate/membrane hybrid process for postcombustion capture of carbon dioxide. Environ. Sci. Technol. 42, 315.
Linga, P., Kumar, R., Englezos, P., 2007b. The clathrate hydrate process for post and pre-combustion capture of carbon dioxide. J. Hazard. Mater. 149, 625–629.
Linga, P., Kumar, R., Englezos, P., 2007c. Gas hydrate formation from hydrogen/carbon dioxide and nitrogen/carbon dioxide gas mixtures. Chem. Eng. Sci. 62, 4268–4276.
Linga, P., Daraboina, N., Ripmeester, J.A., Englezos, P., 2012. Enhanced rate of gas hydrate formation in a fixed bed column filled with sand compared to a stirred vessel. Chem. Eng. Sci. 68, 617–623.
Lirio, C.F.S., Pessoa, F.L.P., Uller, A.M.C., 2013. Storage capacity of carbon dioxide hydrates in the presence of sodium dodecyl sulfate (SDS) and tetrahydrofuran (THF). Chem. Eng. Sci. 96, 118–123.
Liu, N., Chen, W., Liu, D., Xie, Y., 2011. Characterization of CO_2 hydrate formation by temperature vibration. Energy Convers. Manag. 52, 2351–2354.
Liu, H., Wang, J., Chen, G., Liu, B., Dandekar, A., Wang, B., Zhang, X., Sun, C., Ma, Q., 2014. High-efficiency separation of a CO_2/H_2 mixture via hydrate formation in W/O emulsions in the presence of cyclopentane and TBAB. Int. J. Hydrog. Energy 39, 7910–7918.
Luo, Y.T., Zhu, J.H., Fan, S.S., Chen, G.J., 2007. Study on the kinetics of hydrate formation in a bubble column. Chem. Eng. Sci. 62, 1000–1009.
Meysel, P., Oellrich, L., Raj Bishnoi, P., Clarke, M.A., 2011. Experimental investigation of incipient equilibrium conditions for the formation of semi-clathrate hydrates from quaternary mixtures of (CO_2+N_2+TBAB+H_2O). J. Chem. Thermodyn. 43, 1475–1479.
Mohammadi, A.H., Eslamimanesh, A., Belandria, V., Richon, D., Naidoo, P., Ramjugernath, D., 2012. Phase equilibrium measurements for semi-clathrate hydrates of the (CO_2+N_2+tetra-n-butylammonium bromide) aqueous solution system. J. Chem. Thermodyn. 46, 57–61.
Mohammadi, A.H., Eslamimanesh, A., Richon, D., 2013. Semi-clathrate hydrate phase equilibrium measurements for the CO_2+H_2/CH_4+tetra-n-butylammonium bromide aqueous solution system. Chem. Eng. Sci. 94, 284–290.
Mondal, M.K., Balsora, H.K., Varshney, P., 2012. Progress and trends in CO_2 capture/separation technologies: a review. Energy 46, 431–441.
Okutani, K., Kuwabara, Y., Mori, Y.H., 2008. Surfactant effects on hydrate formation in an unstirred gas/liquid system: an experimental study using methane and sodium alkyl sulfates. Chem. Eng. Sci. 63, 183–194.
Olajire, A.A., 2010. CO_2 capture and separation technologies for end-of-pipe applications – a review. Energy 35, 2610–2628.
Oyama, H., Shimada, W., Ebinuma, T., Kamata, Y., Takeya, S., Uchida, T., Nagao, J., Narita, H., 2005. Phase diagram, latent heat, and specific heat of TBAB semiclathrate hydrate crystals. Fluid Phase Equilib. 234, 131–135.
Park, S., Lee, S., Lee, Y., Lee, Y., Seo, Y., 2013. Hydrate-based pre-combustion capture of carbon dioxide in the presence of a thermodynamic promoter and porous silica gels. Int. J. Greenh. Gas Control 14, 193–199.
Reiner, P., Audus, H., Smith, A.R., 1994. Carbon Dioxide Capture from Power Plants. IEA Greenhouse Gas R&D Programme, Cheltenham, UK.
Seo, Y., Kang, S.P., 2010. Enhancing CO_2 separation for pre-combustion capture with hydrate formation in silica gel pore structure. Chem. Eng. J. 161, 308–312.
Seo, Y.T., Moudrakovski, I.L., Ripmeester, J.A., Lee, J., Lee, H., 2005. Efficient recovery of CO_2 from flue gas by clathrate hydrate formation in porous silica gels. Environ. Sci. Technol. 39, 2315–2319.
Sloan, E.D., 2003. Fundamental principles and applications of natural gas hydrates. Nature 426, 353–363.
Sloan, E.D., Koh, C.A., 2008. Clathraye Hydrates of Natural Gases, third ed. Taylor & Francis Group, New York.
Spigarelli, B.P., Kawatra, S.K., 2013. Opportunities and challenges in carbon dioxide capture. J. CO_2 Util. 1, 69–87.
Strobel, T.A., Koh, C.A., Sloan, E.D., 2009. Thermodynamic predictions of various tetrahydrofuran and hydrogen clathrate hydrates. Fluid Phase Equilib. 280, 61–67.
Sun, Z.G., Fan, S.S., Guo, K.H., Shi, L., Guo, Y.K., Wang, R.Z., 2002. Gas hydrate phase equilibrium data of cyclohexane and cyclopentane. J. Chem. Eng. Data 47, 313–315.
Tajima, H., Yamasaki, A., Kiyono, F., 2004. Energy consumption estimation for greenhouse gas separation processes by clathrate hydrate formation. Energy 29, 1713–1729.
Tam, S.S., Stanton, M.E., Ghose, S., Deppe, G., Spencer, D.F., Currier, R.P., Young, J.S., Anderson, G.K., Le, L.A., Devlin, D.J., 2001. A high pressure carbon dioxide separation process for IGCC plants. In: First National Conference on Carbon Sequestration, Washington DC, USA.
Tang, J., Zeng, D., Wang, C., Chen, Y., He, L., Cai, N., 2013. Study on the influence of SDS and THF on hydrate-based gas separation performance. Chem. Eng. Res. Des. 91, 1777–1782.
Torré, J.P., Dicharry, C., Ricaurte, M., Daniel-David, D., Broseta, D., 2011. CO_2 capture by hydrate formation in quiescent conditions: in search of efficient kinetic additives. Energy Procedia 4, 621–628.
Torré, J.-P., Ricaurte, M., Dicharry, C., Broseta, D., 2012. CO_2 enclathration in the presence of water-soluble hydrate promoters: hydrate phase equilibria and kinetic studies in quiescent conditions. Chem. Eng. Sci. 82, 1–13.
Wataru, S., Takao, E., Hiroyuki, O., Yasushi, K., Satoshi, T., Tsutomu, U., Jiro, N., Hideo, N., 2003. Separation of gas molecule using tetra-n-butyl ammonium bromide semi-clathrate hydrate crystals. Jpn. J. Appl. Phys. 42, L129.
Xu, C.G., Cai, J., Li, X.S., Lv, Q.N., Chen, Z.Y., Deng, H.W., 2012a. Integrated process study on hydrate-based carbon dioxide separation from integrated gasification combined cycle (IGCC) synthesis gas in scaled-up equipment. Energy Fuels 26, 6442–6448.
Xu, C.G., Li, X.S., Lv, Q.N., Chen, Z.Y., Cai, J., 2012b. Hydrate-based CO_2 (carbon dioxide) capture from IGCC (integrated gasification combined cycle) synthesis gas using bubble method with a set of visual equipment. Energy 44, 358–366.
Yang, H., Fan, S., Lang, X., Wang, Y., Nie, J., 2011. Economic comparison of three gas separation technologies for CO_2 capture from power plant flue gas. Chin. J. Chem. Eng. 19, 615–620.
Yang, M., Song, Y., Jiang, L., Wang, X., Liu, W., Zhao, Y., Liu, Y., Wang, S., 2013a. Dynamic measurements of hydrate based gas separation in cooled silica gel. Ind. Eng. Chem. 20, 322–330.
Yang, M., Song, Y., Liu, W., Zhao, J., Ruan, X., Jiang, L., Li, Q., 2013b. Effects of additive mixtures (THF/SDS) on carbon dioxide hydrate formation and dissociation in porous media. Chem. Eng. Sci. 90, 69–76.
Yoslim, J., Linga, P., Englezos, P., 2010. Enhanced growth of methane–propane clathrate hydrate crystals with sodium dodecyl sulfate, sodium tetradecyl sulfate, and sodium hexadecyl sulfate surfactants. J. Cryst. Growth 313, 68–80.
Zhang, J., Lee, J.W., 2008a. Enhanced kinetics of CO_2 hydrate formation under static conditions. Ind. Eng. Chem. Res. 48, 5934–5942.
Zhang, J.S., Lee, J.W., 2008b. Equilibrium of hydrogen + cyclopentane and carbon dioxide + cyclopentane binary hydrates. J. Chem. Eng. Data 54, 659–661.
Zhang, J.S., Lee, S., Lee, J.W., 2007. Kinetics of methane hydrate formation from SDS solution. Ind. Eng. Chem. Res. 46, 6353–6359.
Zhang, J., Yedlapalli, P., Lee, J.W., 2009. Thermodynamic analysis of hydrate-based pre-combustion capture of CO_2. Chem. Eng. Sci. 64, 4732–4736.
Zhang, Y., Yang, M., Song, Y., Jiang, L., Li, Y., Cheng, C., 2014. Hydrate phase equilibrium measurements for (THF + SDS + CO_2 + N_2) aqueous solution systems in porous media. Fluid Phase Equilib. 370, 12–18.

Chapter 3. Energy consumption estimation: Gas Hydrate-based CO_2 Capture Processes

This chapter published as a chapter book in Energy Technology 2018, part of the Minerals, Metals & Materials Series book series (MMMS), (pp. 3-16). Springer, Cham.

Gas Hydrate-Based CO_2 Separation Process: Quantitative Assessment of the Effectiveness of Various Chemical Additives Involved in the Process

Hossein Dashti and Xia Lou

Abstract Gas hydrates technology has been considered as an alternative method for carbon dioxide (CO_2) separation. A wide range of studies have been reported in the past decade on the improvement of the separation efficiency by using chemical additives. While most of these studies have shown improved kinetics, thermodynamics and/or separation efficiency at the laboratory scale, there has been no quantitative analysis of the energy consumption for viable industrial applications. Comparison of the effectiveness of the chemical additives from separate studies or groups also is impossible. The present work is focused on the modelling of the hydrate-based CO_2 separation process and provides a quantitative approach that is new in its analysis of the effectiveness of chemical additives in relation to the energy required and the kinetic parameters involved in the process.

Keywords CO_2 capture · CO_2 hydrates · Chemical additives

Introduction

Carbon dioxide (CO_2) separation and capture is one of the most challenging issues to investigate in order to alleviate the problem of CO_2 emissions worldwide. Gas hydrate-based CO_2 capture/separation (HBCC) is a relatively new separation method for CO_2 and has attracted increasing attention in the past decade. The technology employs a unique separation mechanism that is easy to regenerate and is capable of separating various gas mixtures, which might not be achievable via conventional methods. The feasibility study of the process was first reported by Spencer [1], and later supported by Tam et al. [2] According to the authors, the cost of HBCC technology in an integrated gasification combined cycle plant was US$ 8.75 per ton of CO_2 captured. It was reportedly comparable to that of US$ 57 per

H. Dashti · X. Lou (✉)
Department of Chemical Engineering, Curtin University, Kent Street, Bentley, WA 6102, Australia
e-mail: x.lou@curtin.edu.au

Z. Sun et al. (eds.), *Energy Technology 2018*, The Minerals, Metals & Materials Series, https://doi.org/10.1007/978-3-319-72362-4_1

ton of CO_2 captured through the pressure swing adsorption (PSA) method, and that of US$ 49 per ton of CO_2 captured using the monoethanolamine (MEA) chemical absorption method [3].

CO_2 form hydrates between 1.1–4.3 MPa and 273–283 K respectively. Separating CO_2 from the other gases such as oxygen and nitrogen can be achieved by first forming a solid hydrate phase that is enriched with CO_2, followed by separation of the hydrate phase from the gaseous phase and dissociation of the hydrates, leading to the recovery of CO_2 that is much higher in concentration than in the original gas mixture. Upon dissociation, one volume of CO_2 hydrates can release 175 volumes of CO_2 gas at standard conditions [4]. However, the high operation pressures required in the HBCC process lead to the high compression costs and energy consumption. This has limited the viable industrial application of the HBCC [5]. The relatively low separation efficiency also is a challenge [6, 7]. Many chemical additives have been investigated in an attempt to lower the operation pressure, and to increase the formation rate, of CO_2 gas hydrates. Among the most commonly studied chemical additives, tetrahydrofuran (THF) and cyclopentane (CP) have been found to be useful in reducing the operating pressure and increasing the CO_2 recovery rate. Other additives, like tetra-n-butyl ammonium bromide (TBAB), dodecyl-trimethyl-ammonium chloride (DTAC) and $TBANO_3$, have been found to be useful in increasing the gas storage capacity and reducing the operating pressure. Surfactants, such as sodium dodecyl sulphate (SDS), only enhance the hydration rate of the process. Mixed chemical additives also have been studied to enhance their effects in HBCC.

Studies on chemical additives have been mostly focused on the effect of the chemical additives upon the kinetics, the operational conditions and the separation efficacy. Details of the progress in chemical additives improved HBCC can be found in a few recent review papers [6–8]. Other work on chemical additives associated HBCC includes thermodynamic modelling of the CO_2 fluid and hydrate phase behaviour. For instance, Herslund et al. [5, 9, 10] modelled the fluid phase and hydrate phase in the presence of THF, CP and the mixture of both. Verrett et al. [11] developed a thermodynamic model to simulate the HBCC process in the presence of TBAB. Another study by Shi and Liang [12] proposed a thermodynamic model to investigate the effects of TBAB, tetrabutyl ammonium fluoride (TBAF) and tetrabutyl ammonium chloride (TBAC) in HBCC process. Kinetic studies on gas hydrate formation are mostly based on the model established by Englezos et al. [13] that considers both mass transfer and crystallisation processes at the gas-liquid interface. The driving force in this model is the difference between the fugacity of the dissolved gas and the fugacity at equilibrium. However, the report on kinetic models for chemical additives enhanced HBCC process is limited. A recent study by ZareNezhad et al. [14] reported a single component gas (CO_2) hydrates kinetics in the absence and presence of SDS. In this model, the crystallization theory was coupled with the mass transfer phenomena but the gas composition difference between the liquid phase and the solid-liquid interface was considered as the driving force. Sun and Kang [15] also proposed a two-parameter kinetic model to predict the CO_2 hydrate formation rate in presence of THF. In this

work, the Gibbs free energy difference was considered as the driving force. In terms of quantitative analysis of the energy consumption associated with the HBCC, Tajima et al. [16] reported the energy consumption by a designed HBCC process for separating CO_2 from the emitted flue gases, using the thermodynamic approach. There was no chemical additive used in the design. A later report by Duc et al. [17] used the process simulator PRO II, to estimate the energy consumption involved in a multi-staged HBCC process in the presence of TBAB.

The present work is focused on the development and validation of a quantitative approach for the energy estimation of the HBCC process using the production scale reported by Tajima et al. [16]. The proposed approach will then be applied to the reported HBCC processes in the presence of THF [18, 19], TBAB [20, 21], and a mixture of TBAB with DATC [22]. The impact of the chemical additive on the energy consumption in relation to the formation pressure and temperature, and the kinetics of the CO_2 hydrates will be discussed.

Methodology

A schematic flow diagram (Fig. 1) is first established based on the reported HBCC process by Tajima et al. [16]. Two compressors and three heat exchangers are used before the flue gas enters the reactor where the flue gas mixes with water with or without chemical additives. Gas hydrates form in the reactor. The hydrates slurry is separated from the gas phase and sent to a hydrates dissociation reactor from which purified CO_2 is collected.

According to the authors: (1) the process was applied to the treatment of total emission from a 1,000 MW power plant; (2) the total flow rate of the input flue gas was $1.0 \times 10^6 \mathrm{N\,m^3.h^{-1}}$; (3) the volume of the reactor was about 7,000 $\mathrm{m^3}$; (4) the pressurisation was performed using adiabatic compressors with 80% efficiency; (5) the inlet and outlet temperatures of coolant were 253 K and 263 K, respectively; (6) the coefficient of performance (COP) in heat exchangers is assumed to be 3 and (7) the composition of CO_2 in the hydrates stream is 100%. Based on these

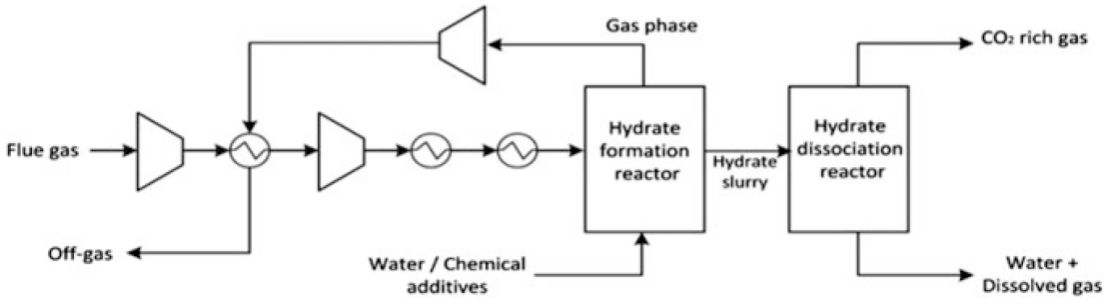

Fig. 1 A schematic flow diagram of the gas hydrate-based CO_2 separation process

assumptions, the total energy consumption involved in this process was calculated using Eq. 1:

$$E_{total} = E_{compression} + E_{cooling} + E_{hydrates} \quad (1)$$

in which $E_{compression}$ and $E_{cooling}$ represent the energy consumption during the compression and cooling stages and $E_{hydrates}$ is the energy consumption associated with hydrate formation and dissociation.

Estimation of $E_{compression}$ and $E_{cooling}$

The energy consumption values in the pressurising and cooling processes were simulated using Aspen HYSYS (V.8.6). The temperature and pressure of the input flue gas were, reportedly, 298 K and 0.1 MPa [16].

Estimation of $E_{hydrates}$

For the estimation of $E_{hydrates}$, an energy balance around the formation and dissociation reactor (Fig. 2) was first established (Eq. 2).

$$E_{hydrates} = \sum_{i=1}^{5} F_i H_i - r_f \Delta H_f + r_d \Delta H_d \quad (2)$$

where F_i is the flow rate of stream i, H_i is the enthalpy of stream i, r_f and r_d are the rates of hydrate formation and dissociation, respectively, and ΔH_f and ΔH_d are the enthalpies of hydrate formation and dissociation, respectively. Below are the details of the modelling of each of the parameters.

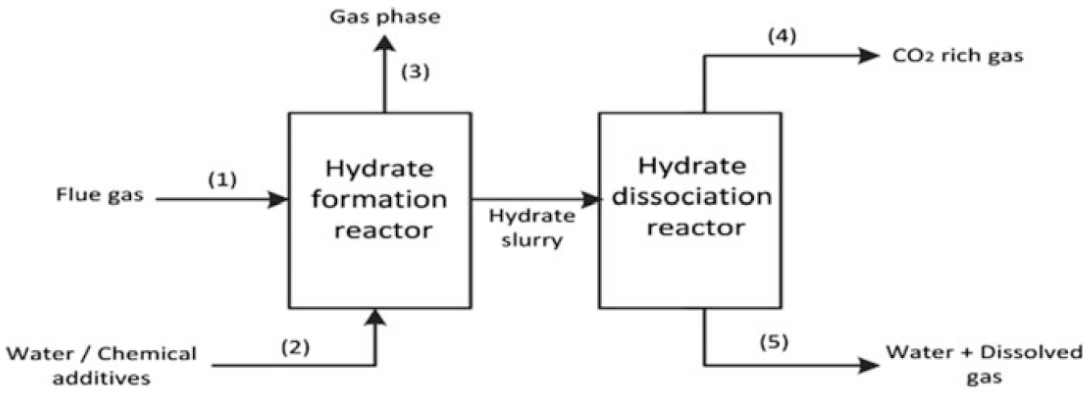

Fig. 2 CO_2 hydrates formation and dissociation unit

Enthalpy of Different Streams

The enthalpy of different streams was calculated using Eq. 3:

$$H_i = \int_0^{T_i} C_{p(mixture),i} dT_i \quad i = 1, 2, 3, 4, 5 \tag{3}$$

where i denotes a specific stream, T_i is the temperature of the stream i and $C_{p(mixture),i}$ is the specific heat capacity of the gas mixture of the stream i at pressure p, given by Eq. 4:

$$C_{p(mixture)} = \sum x_{j,i} C_{P,j} \quad \begin{matrix} j = CO_2, N_2, H_2O, O_2 \\ i = 1, 2, 3, 4, 5 \end{matrix} \tag{4}$$

in which $x_{j,i}$ is the mole fraction of component j in stream i and $C_{P,j}$ is the specific heat capacity of component j at pressure, p, which was determined using Eqs. 5–9 [23]:

$$C_{p,CO_2} = 36.11 + \left(4.23 \times 10^{-2}\right)T - \left(2.88 \times 10^{-5}\right)T^2 + \left(7.46 \times 10^{-9}\right)T^3 \tag{5}$$

$$C_{p,N_2} = 29 + \left(0.21 \times 10^{-2}\right)T + \left(0.57 \times 10^{-5}\right)T^2 - \left(2.87 \times 10^{-9}\right)T^3 \tag{6}$$

$$C_{p,O_2} = 29.10 + \left(1.15 \times 10^{-2}\right)T + \left(0.60 \times 10^{-5}\right)T^2 - \left(1.31 \times 10^{-9}\right)T^3 \tag{7}$$

$$C_{p,H_2O(g)} = 33.46 + \left(0.69 \times 10^{-2}\right)T + \left(0.80 \times 10^{-5}\right)T^2 - \left(3.60 \times 10^{-9}\right)T^3 \tag{8}$$

$$C_{p,H_2O(L)} = 75.4 \tag{9}$$

Enthalpy of Hydrate Formation

The formation of hydrates in the form of a reaction is illustrated by Eq. 10,

$$CO_2(Vapor) + nH_2O\,(Liquid) \rightarrow CO_2 hydrates(Solid) \tag{10}$$

where n is the hydration number, which is reportedly between 5.75 and 7.66 for CO_2 [4, 24]. The enthalpy of hydrate formation is calculated using Eq. 11, taken from Kamath [25],

$$\Delta H_f = C_1 + C_2 T \tag{11}$$

where ΔH_f is in cal/gmol gas and T is the temperature at which hydrates form with $C_1 = 9.290 \times 10^3$ and $C_2 = -12.93$ at-25 < T < 0 °C, and $C_1 = 19.199 \times 10^3$ and $C_2 = -14.95$ at 0 < T < 11 °C.

Enthalpy of Hydrate Dissociation

The amount of heat required to dissociate hydrate crystals is a key thermodynamic property in the hydrate formation and dissociation process. Obtaining this parameter from the numerical equations or experiments is a challenging area of research [26]. While the high-pressure differential scanning calorimeter (DSC) has been found to be useful for the measurement of the dissociation heat in the laboratory setting [27], the application of the Clausius-Clapeyron Eq. 12 has been widely used for simple hydrates systems and it has proven to be thermodynamically correct, as long as the system is univariant [4]. Recent studies by Kang et al. [28], Delahaye et al. [29], and Sabil [30] have further demonstrated the suitability of the Clausius–Clapeyron equation for the calculation of the dissociation enthalpy of single and mixed CO_2 hydrates. The equation is expressed as,

$$\frac{dlnP_{eq}}{d\left(\frac{1}{T_{eq}}\right)} = -\frac{\Delta H_d}{ZR} \tag{12}$$

where T_{eq} and P_{eq} are the absolute temperatures and pressures that were obtained from literature data, [18, 20, 22] R is the gas constant, and Z is the gas compressibility. Note that the equation was derived from the Clapeyron equation assuming that the volume of solid hydrates approximates that of water in the hydrates formation reaction therefore the changes of volume equals to the volume of gases (see Eq. 10). The value of Z was calculated using the Peng-Robinson equation of state [31] by solving Eq. 13:

$$Z^3 - (1-B)Z^2 + \left(A - 2B - 3B^2\right)Z - \left(AB - B^2 - B^3\right) = 0 \tag{13}$$

where A and B are determined by Eqs. 14–16,

$$A = 0.45724\left[1 + \kappa\left(1 - \sqrt{\frac{T}{T_c}}\right)\right]^2 \frac{P/P_c}{(T/T_c)^2} \tag{14}$$

$$B = 0.07780\frac{PT_c}{TP_c} \tag{15}$$

$$\kappa = 0.37464 + 1.54226\omega - 0.26992\omega^2 \tag{16}$$

Taking T_c = 304.2 K, P_c = 7.38 MPa and ω = 0.228 for CO_2 [23] and plotting ln P_{eq} against $\frac{1}{T_{eq}}$ results in a slope which equals $-\frac{\Delta H_d}{ZR}$.

Hydrate Formation Rate

Research into gas hydrates kinetic models has not been as prevalent as that for thermodynamic models. A recent paper by Ribeiro and Lage [32] has reviewed the kinetic models for hydrates formation. Among all models, the work by Englezos et al. [13] is most commonly quoted and applied. [33] In their model, the hydrates formation rate is expressed as a function of the fugacity difference between the operating condition and equilibrium condition, based on Eq. 17:

$$r_f = aK^*(f_g - f_{eq}) \tag{17}$$

where a is the interfacial area, f_g and f_{eq} represent the fugacity of the dissolved gas and fugacity at equilibrium, respectively, and K^* is the overall kinetic constant that is determined by Eq. 18,

$$\frac{1}{K^*} = \frac{1}{k_f} - \frac{1}{k_L} \tag{18}$$

where k_f is the crystal growth constant and k_L is the mass transfer coefficient in the liquid phase. For vigorous mixing systems, Fan et al. [21] further developed the model as described by Eq. 19:

$$r_f = \frac{V_g}{RT}\frac{(P - P_{eq})}{\Delta t} \tag{19}$$

in which P is the operating pressure and P_{eq} is equilibrium pressure, V_g is the volume of the gas phase and Δt is the time to reach equilibrium. The term P_{eq} is calculated based on the hydrate formation condition inside the reactor, for which Chen-Guo's model [34] was used. It assumes that the fugacity in vapour, f_i^v, equals that in the hydrate phase, f_i^H, at equilibrium condition. Using the equations displayed in Table 1, in which θ is the fraction of linked cavities occupied by gas molecules, c is the Langmuir constant, f_T^0 is an Antoine-like function, f^0 is a function of pressure and temperature, α_w is the activity of water and α is the value dependant on the type of hydrate structure, the value of P_{eq} was computed iteratively via the contracting Newton method until it satisfied $f_i^v = f_i^H$.

Hydrate Dissociation Rate

For hydrates dissociation, a published work on methane hydrates [35] was adapted by this study. The rate of hydrate dissociation, r_d, is calculated using Eq. 20:

Table 1 Governing equations and constants for the determination of P_{eq} [34]

Equations	Constants for CO_2 gas species
$f_i^v = 10^{(Z-1)-\ln(Z-B)-\frac{A}{2\sqrt{2}B}\ln\left(\frac{Z+(\sqrt{2}+1)B}{Z-(\sqrt{2}+1)B}\right)} + P_{eq}$	Z, A and B are calculated by Eqs. 13–15
$\theta = \frac{cf_i^v}{1+cf_i^v}$	
$c = X\,exp\left(\frac{Y}{T-z}\right)$	$X = 1.6464 \times 10^{-17} MPa,\ Y = 2799.66\,K,\ z = 15.90\,K$
$f_T^0 = A\,exp(\frac{B}{T-C})$	$A = 963.72 \times 10^9 MPa,\ B = -6444.50\,K,\ C = 36.67\,K$
$f^0 = f_T^0 exp\left(\frac{\beta P_{eq}}{T}\right)\alpha_w^{-1/\lambda}$	$\beta = 4.242\frac{K}{MPa},\ \lambda = 3/23,\ \alpha_w = 1$
$f_i^H = f^0(1-\theta)^\alpha$	$\alpha = 1/3$

$$r_d = k_d A_s \left(f_{eq} - f_g\right) \tag{20}$$

where K_d is the dissociation rate constant and is determined using Eq. 21,

$$k_d = k_d^0 e^{-\Delta E/RT} \tag{21}$$

where $k_d^0 = 1.83 \times 10^{14} \frac{mol}{m^2 MPas}$ is the intrinsic rate constant of CO_2 hydrates dissociation, and $\Delta E = 102.88 \frac{\text{kJ}}{\text{mol}}$ is CO_2 activation energy [36]. A_s in Eq. 22 is determined using:

$$A_s = \left[\frac{6}{\psi \rho_H D_0}\right] n_0^{1/3} n_H^{1/3} \tag{22}$$

where ψ is the sphericity factor and the shape of the CO_2 hydrates is assumed to be spherical, $\psi = 1$, ρ_H is the superficial density of CO_2 (25,431.42 mol/m^3) [37], D_0 is the CO_2 hydrate diameter (5.12×10^{-10} m) and n_0 and n_H are the numbers of moles at t = 0 and time of hydrate formation, respectively. Assuming that the pressure difference is the driving force, the rate of dissociation can be obtained by Eq. 23, as a result of substituting k_d and A_s into Eq. 20.

$$r_d = \left[\frac{1.09 \times 10^9}{\varphi \rho_H D_0}\right] e^{-102880/RT}\left(P_{eq} - P\right) n_0^{1/3} n_H^{2/3} \tag{23}$$

Energy Consumption Calculations

The above model was first applied to the process reported by Tajima et al. [16], assuming that both N_2 and CO_2 form hydrates at the operating conditions. The model was further applied to three cases, assuming the same production scale, in which the chemical additives THF, TBAB, and TBAB + DTAC were used,

Table 2 Operational parameters for energy consumption calculations

Case	Chemical additives	Operating Conditions: (T [K], P [MPa])/(x_{CO_2}, x_{N_2})/Molar flow rate × 10^7 mol/h			References
		Stream 1	Stream 3	Stream 4	
I	None	(274, 14)/(0.10, 0.79)[a]/4.46	(274, 14)/(0.005, 0.87)[b]/4.03	(274, 0.10)/(1, 0)/42.3	[16]
II	THF (1 mol%)	(274, 0.35)/(0.17, 0.83)/4.46	(274, 0.35)/(0.10, 0.90)/3.32	(274, 0.10)/(0.37, 0.63)/1.13	[18, 19]
III	TBAB (5 wt%)	(283, 3.16)/(0.17, 0.83)/4.46	(283, 3.16)/(0.05, 0.95)/2.48	(283, 0.10)/(0.32, 0.68)/1.98	[20, 21]
IV	TBAB (0.29 mol %) + DTAC (0.028 mol%)	(275, 1.66)/(0.17, 0.83)/4.46	(275, 1.66)/(0.05, 0.95)/3.57	(275, 0.10)/(0.65, 0.35)/0.9	[22]

[a]The remaining fraction is 0.04 of O_2 and 0.07 of H_2O [b]The remaining fraction is 0.04 of O_2 and 0.08 of H_2O

respectively. It is noteworthy that only the optimal chemical loadings that have produced the maximum CO_2 separation efficiency have been selected for this study. More details are given in Table 2.

Results and Discussion

For Case I, the computed energy consumption by the compressors and heat exchangers, as well as that associated with the hydrates formation and dissociation, are listed in Table 3. The reported data [16] also are tabulated for comparison. It can be seen that the computed values of $E_{compression}$ and $E_{hydrates}$ are in good agreement with the reported data. It should be noted that the $E_{hydrates}$ reported by Tajima is a sum of the energies associated with the removal of the heat of hydrates formation (29.5 MW), the supply of the sea water for hydrates dissociation

Table 3 Computed energy consumption for Case I. Data in brackets are taken from Tajima's work [16]

Item	Energy consumption, MW
$E_{compression}$	234.5(240.1)
$E_{cooling}$	36.4(15.3)
$E_{hydrates} = \sum_{i=1}^{5} F_i H_i - r_f \Delta H_f + r_d \Delta H_d$	−16.5(29.5 + 0.85 + 0.40)
$E_{recovery}$	−113.7(−127.7)
E_{total}	140.8(158.4)

(0.85 MW) and the water supply for hydrates formation (0.40 MW). There is no provision of the computational details by the authors. The reported recovery energy ($E_{recovery}$) was −127.7 MW from the off-gas stream which was used to cool the feed gas. Our estimation is −113.7 MW, which is slightly lower than the reported data. However, the energy involved in the precooling stage was estimated to be 36.4 MW, which is higher than that of the reported data, 15.3 MW. Taking the differences in the recovered energy from the off-gas stream into consideration, this result also is acceptable. It should be noted that, while Tajima et al. [16] have reported the inclusion of a brine stream to maintain the temperature of the hydrate formation reactor at 274 K, there was no indication of how this has contributed to the cooling energy. Regardless, the computed total energy consumption, using Eq. 1, is 136.4 MW, while the reported value was 158.4 MW, indicating an effective approach for the energy estimation of other cases.

Using the same model, energy consumption values in the presence of different chemical additives also were calculated. The results are summarised in Table 4. In this table, E_m is energy per unit mass of captured CO_2 and $E_{Recovery}$ is recovery energy. In comparison with Case I, reduced compression energy was seen in all cases where chemical additives were used in the HBCC process, mostly due to the reduced operating pressures in the presence of chemical additives [7]. The lowest $E_{compression}$ was seen in Case II, when THF was used due to the significant pressure reduction from 14 to 0.35 MPa. The presence of TBAB also reduced the hydrates-forming pressure, but by a lesser degree. That is, the compression energy

Table 4 Energy consumption involved in four different case studies

Energy value (MW)			Case I	Case II	Case III	Case IV
$E_{compression}$			**234.5**	**52.5**	**195.4**	**139.1**
$E_{cooling}$			**36.4**	**10.8**	**8.7**	**6.8**
$E_{hydrates}$	Hydrate formation	$r_f \times 10^6$(mol/h)	1.2	0.8	1.4	0.8
		$\Delta H_f \times 10^4$ (J/mol)	6.3[a] (5.0)[b]	6.3[a] (12.0)[b]	6.3[a] (16.0)[**]	6.3[a] (12.0)[b]
	Hydrate dissociation	$r_d \times 10^4$ (mol/h)	6.9	1.7	55.0	5.9
		$\Delta H_d \times 10^4$ (J/mol)	5.0	12.0	16.0	12.0
	Energy of streams, $\sum_{i=1}^{5} F_i H_i$		−0.3	2.3	2.4	1.8
	$\sum_{i=1}^{5} F_i H_i - r_f \Delta H_f + r_d \Delta H_d$		**−16.5**	**−23.1**	**−33.7**	**−22.5**
$E_{recovery}$			**−113.7**	**−28.6**	**−89.7**	**−47.6**
E_{total}			**140.8**	**11.6**	**80.7**	**75.9**
E_m (MJ/Kg CO_2)			**2.7**	**0.2**	**1**	**1.1**

[a] and [b] denoting that data were obtained from Eqs. (11) and (12) respectively. The latter was used for $E_{hydrates}$ calculation

was reduced in comparison with Case I, however, the reduction was not as much as that seen in Case II. Using mixed chemical additives (TBAB + DTAC), a more effective reduction in compression energy was observed, due to the resultant lower hydrates formation pressure than when TBAB alone was used [22]. Similarly, the cooling energy was lowered when chemical additives were added to the HBCC process. A greater than 70% reduction was seen in all cases. The results indicate that the influence upon the cooling energy by chemical additives is strongest in the presence of TBAB + DTAC, followed by TBAB alone then THF, in comparison with Case I.

The calculated enthalpy of hydrate formation, ΔH_f, is of a similar value in all cases by using Eq. 11. This is understandable because ΔH_f is a rather weak function of the temperature in this equation. The addition of chemical additives has resulted in some changes in the rate of hydrates formation, as shown in Table 4. The slightly lower rates in Cases II and IV are probably due to the lower operating pressures and, therefore, the lower driving forces for hydrates to form. The enthalpy value of hydrate dissociation,ΔH_d, obtained from the Clausius-Clapeyron Eq. 12, indicated more significant changes upon the addition of chemicals. This is due to the more sensitive nature of the approach, being a function of both the temperature and the pressure. The computed values of ΔH_d for Cases I and II are 5×10^4 J/mol and 12×10^4 J/mol, respectively, which are in agreement with the reported values of 5.7×10^4 J/mol by Yoon et al. [38], and 10.9×10^4 J/mol by Kang et al. [28]. For Cases III and IV, the calculated dissociation enthalpies are 16×10^4 J/mol and 12×10^4 J/mol, respectively, and, to the best of our knowledge, no reported data is available in the open literature. The values of ΔH_d in Cases II, III and IV are greater than that of Case I. Pure CO_2 forms Structure I hydrates. However, in the presence of chemical additives, it forms Structure II and/or semi-clathrate hydrates, which are more stable or contain higher numbers of CO_2 molecules in the cavities, resulting in higher values for the enthalpy of dissociation [30]. There also was a significant increase in the hydrates dissociation rate,r_d, when TBAB was used. This is likely to be due to the higher operating temperature. The lowest dissociation rate was found when THF was used, resulting from the lowest operating temperature. The higher rate and enthalpy of hydrates formation/dissociation in the presence of TBAB has led to its highest absolute value of $E_{hydrates}$ which was followed by Case II (THF) and Case IV (TBAB + DTAC), and Case I (no chemical additive). These results demonstrate that the presence of chemical additives can also reduce the energy consumption associated with CO_2 hydration.

The energy distribution in each case is displayed in Fig. 3. A significant reduction in all categories was well demonstrated in all cases where chemical additives were used. The presence of THF has resulted in the lowest total energy consumption among the four cases (Table 4). The significant impact of THF on the overall energy consumption profile is a result of both the drastic reduction in the hydrates formation pressure and the improved hydrates formation/dissociation kinetics. It is well known that the use of THF as a thermodynamic chemical additive encourages structure II hydrates to form, which allows CO_2 to occupy both small

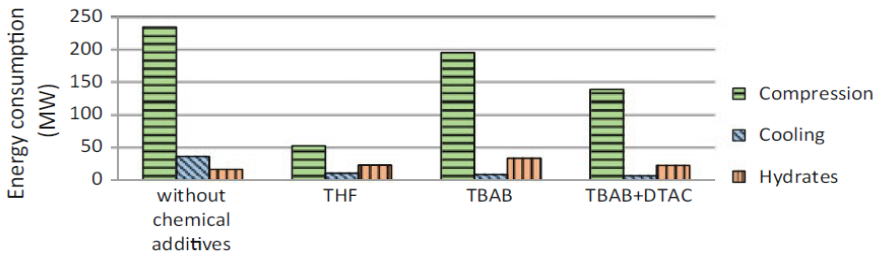

Fig. 3 The energy distribution (For better illustration, the absolute values of $E_{hydrates}$ are shown in this figure)

and large water cages at lower pressure [7, 39]. It is interesting to note that the total energy consumption in the presence of TBAB is not much lower than for Case I, although the lowest $E_{hydrates}$ is associated with the presence of TBAB. This is due to the fact that the changes in the hydrates-forming pressure and temperature are not sufficiently significant in Case III, therefore, the reduction in both compression and cooling is not apparent, although TBAB allows greater gas capacity and consequently higher conversion rates. On the other hand, using a mixture of TBAB and DTAC has produced a greater degree of energy reduction, since DTAC lowers the equilibrium pressure of CO_2 hydrates [22]. In general, energy consumption values in both the hydrate formation and dissociation stages are much lower than that during the cooling and compression processes.

When the total energy was converted into the energy demand per unit mass of captured CO_2, E_M, the results further confirmed that the addition of suitable chemicals can reduce the total energy associated with the HBCC processes. This, in turn, would lead to a reduction in the economic costs of HBCC. The economic impact of the chemical additives to the HBCC processes is currently under investigation.

Conclusions

In summary, a model has been developed to estimate the energy required at various stages during a hydrate-based CO_2 separation process. Application of the established energy analysis to the HBCC process in the presence of chemical additives has demonstrated that the chemical additives reduced the total energy consumed, through their impact on the pressures and temperatures at which CO_2 hydrates form and dissociate, and on the CO_2 hydration kinetics. Among the chemical additives investigated, THF has shown a significant reduction in the energy required in all stages, including the cooling, the compression, the formation and the dissociation of CO_2 hydrates. The quantitative analysis was proved to be effective in the comparison of the effectiveness of different chemical additives reported by various groups. The results also indicated that the chemical additives being able to reduce the operation pressure will bring more benefit to the ultimate application of the HBCC process.

Acknowledgment The authors wish to thank the Australia-China Natural Gas Technology Partnership Fund for financial assistance to this work.

References

1. Spencer DF (1999) Integration of an advanced CO_2 separation process with methods for disposing of CO_2 in oceans and terrestrial deep aquifers. In: Eliasson B, Riemer P, Wokaun A (eds) Greenhouse gas control technologies. Elsevier p. 89–94
2. Tam S et al (2001) A high pressure carbon dioxide separation process for IGCC plants. Paper presented at First National Conference on Carbon Sequestration, Washington DC, USA, 14–17 May 2001
3. Ho MT, Allinson GW, Wiley DE (2008) Reducing the cost of CO_2 capture from flue gases using pressure swing adsorption. Ind Eng Chem Res 47:4883–4890
4. Sloan ED, Koh CA (2008) Clathraye hydrates of natural gases. Taylor & Francis, New York
5. Herslund PJ, Daraboina N, Thomsen K, Abildskov J, Solms NV (2014) Measuring and modelling of the combined thermodynamic promoting effect of tetrahydrofuran and cyclopentane on carbon dioxide hydrates. Fluid Phase Equilib 381:20–27
6. Babu P, Linga P, Kumar R, Englezos P (2015) A review of the hydrate based gas separation (HBGS) process for carbon dioxide pre-combustion capture. Energy 85:261–279
7. Dashti H, Yew LZ, Lou X (2015) Recent advances in gas hydrate-based CO_2 capture. J Nat Gas Sci Eng 23:195–207
8. Xu CG, Li XS (2014) Research progress of hydrate-based CO_2 separation and capture from gas mixtures. RSC Adv 4:18301–18316
9. Herslund PJ, Thomsen K, Abildskov J, Solms NV (2013) Application of the cubic-plus-association (CPA) equation of state to model the fluid phase behaviour of binary mixtures of water and tetrahydrofuran. Fluid Phase Equilib 356:209–222
10. Herslund PJ, Thomsen K, Abildskov J, Solms NV (2014) Modelling of cyclopentane promoted gas hydrate systems for carbon dioxide capture processes. Fluid Phase Equilib 375:89–103
11. Verrett J, Renault-Crispo JS, Servio P (2015) Phase equilibria, solubility and modeling study of CO_2/CH_4 + tetra-n-butylammonium bromide aqueous semi-clathrate systems. Fluid Phase Equilib 388:160–168
12. Shi LL, Liang DQ (2015) Thermodynamic model of phase equilibria of tetrabutyl ammonium halide (fluoride, chloride, or bromide) plus methane or carbon dioxide semiclathrate hydrates. Fluid Phase Equilib 386:149–154
13. Englezos P, Kalogerakis N, Dholabhai PD, Bishnoi PR (1987) Kinetics of formation of methane and ethane gas hydrates. Chem Eng Sci 42:2647–2658
14. ZareNezhad B, Mottahedin M, Varaminian F (2015) A new approach for determination of single component gas hydrate formation kinetics in the absence or presence of kinetic promoters. Chem Eng Sci 137:447–457
15. Sun Q, Kang YT (2015) Experimental correlation for the formation rate of CO_2 hydrate with THF (tetrahydrofuran) for cooling application. Energy 91:712–719
16. Tajima H, Yamasaki A, Kiyono F (2004) Energy consumption estimation for greenhouse gas separation processes by clathrate hydrate formation. Energy 29:1713–1729
17. Duc NH, Chauvy F, Herri JM (2007) CO_2 capture by hydrate crystallization —A potential solution for gas emission of steelmaking industry. Energy Convers Manag 48:1313–1322
18. Kang SP, Lee H (2000) Recovery of CO_2 from flue gas using gas hydrate: thermodynamic verification through phase equilibrium measurements. Environ Sci Technol 34:4397–4400
19. Linga P, Adeyemo A, Englezos P (2008) Medium-pressure clathrate hydrate/membrane hybrid process for postcombustion capture of carbon dioxide. Environ Sci Technol 42:315–320

Chapter 4. Kinetic modelling of the gas hydrate-based CO_2 processes: Variations of the shrinking core model

This chapter is accepted in the 29th European Symposium on Computer Aided Process Engineering to be published as a book chapter in Computer Aided Chemical Engineering (Elsevier). This work is exactly as the accepted version of the manuscript however we added Supplementary appendix and Nomenclature at the end of this chapter.

Anton A. Kiss, Edwin Zondervan, Richard Lakerveld, Leyla Özkan (Eds.)
Proceedings of the 29th European Symposium on Computer Aided Process Engineering
June 16th to 19th, 2019, Eindhoven, The Netherlands.

Variations of the shrinking core model for effective kinetics modeling of the gas hydrate-based CO_2 capture process

Hossein Dashti,[a] Daniel Thomas,[b] Amirpiran Amiri,[b,*] Xia Lou [a]

[a]*Department of Chemical Engineering, WA School of Mines: Minerals, Energy and Chemical Engineering, Curtin University, Kent Street, Bentley WA 6102, Australia*

[b]*European Bioenergy Research Institute (EBRI), School of Engineering and Applied Science, Aston University, Birmingham, B4 7ET, United Kingdom*

a.p.amiri@aston.ac.uk

Abstract

The hydrate-based carbon dioxide (CO_2) capture (HBCC) process has been widely studied for CO_2 separation and sequestration. This paper aims to conduct a model-based investigation of the kinetics of the HBCC process. A variation of the shrinking core model (SCM) was developed for the analysis of this heterogeneous system under varying boundary conditions. The results revealed that while CO_2 diffusion through the hydrate layer is the dominant controlling mechanism, for a realistic scenario in which a time-dependent bulk gas concentration exists, the model results would better match the experimental data if the effects of the reaction rate were incorporated into the diffusion-based model. Sensitivity analysis showed that increasing the diffusivity through the hydrate layer significantly decreases the full conversion time of the water. Moreover, the effect of temperature change was investigated, and it was found that lower temperatures slow the hydrate growth rate. The model was demonstrated to be a computationally effective and time-efficient predictive tool that does not require high-speed computers for large-scale (reactor) applications.

Keywords: gas hydrate, CO_2 capture, shrinking core model

1. Introduction

Gas hydrates are solid clathrates comprising gas molecules (guests) such as CO_2, nitrogen (N_2), hydrogen (H_2), methane (CH_4) encased in a cage of water molecules (H_2O) connected to each other by hydrogen bonds. Hydrates form under specific thermodynamic conditions, including low temperature and high pressure. The small and nonpolar CO_2 gas forms hydrate structure I at temperatures lower than 283 K and pressures lower than 4.5 MPa (Sloan and Koh, 2008). CO_2 hydration under 203 K and 0.08 MPa has also been reported (Falabella, 1975). The potential of gas hydrate technology to capture CO_2 from flue gases has sparked research interest in investigating different aspects of this novel technology (Dashti and Lou, 2018; Dashti et al., 2015). Early research mostly focused on the experimental investigation of CO_2 hydrate formation and methods to improve the hydration kinetics and separation efficiency. In recent years, studies focused on understanding gas hydrate formation kinetics have increased (Yin et al., 2018). Many of these studies have been based on the methane hydrate formation process, and the kinetic model reported by Englezos et al. (1987) has been frequently used (Englezos et al., 1987).

This model follows the modeling approach for crystal growth from solution (Karpiński, 1980) and divides hydrate particle growth into two steps: 1) diffusion of the dissolved gas from the bulk solution to the hydrate-liquid interface and 2) the hydrate formation reaction at the interface. According to Lederhos et al. (1996), gas hydrate formation is similar to the crystallization process, which is governed by nucleation followed by the rapid growth of hydrates; both are controlled by kinetics and mass and heat transfer phenomena (Lederhos et al., 1996).

The unreacted shrinking core model (SCM) has been widely used for solid reactions in which the intrinsic reaction rate is much higher than the mass transfer rate (Amiri et al., 2013; Amiri et al., 2015). This paper applies a modified SCM to model the CO_2 hydrate formation process assuming a single mechanism for a better understanding of gas hydrate formation kinetics.

2. Modeling methodology

2.1. Base model with a constant boundary condition

A variation of SCM with the steady boundary condition was applied to the CO_2 hydrate formation case study. In a batch reactor, however, the composition of the bulk gas surrounding the reactive particle is significantly dynamic, which conflicts with the boundary condition assumption in a mechanistic model.

In the typical SCM paradigm, the gas-solid reaction initiates at the outer surface of a solid particle and then moves towards the particle core, leaving a product layer behind. The unreacted core radius shrinks with time until full conversion of the solid particles to products, as shown in Figure 1. The model can be adopted to describe the CO_2 hydrate formation process, which includes three steps. Assuming effective agitation leading to the formation of water droplets that interact with CO_2 to form gas hydrates, the whole process involves (i) CO_2 diffusion through the gas film surrounding the hydrate particle to reach the particle's surface; (ii) CO_2 diffusion through the hydrate shell to reach the unreacted core (water) surface; and (iii) reaction of CO_2 with water (Eq. (1)) at the hydrate–liquid interface or unreacted core surface. The overall reaction can be expressed using Eq. (1):

$$CO_2 + nH_2O \leftrightarrow CO_2 \cdot nH_2O \qquad r_h = kC_{CO_2} \qquad (1)$$

where n is the hydrate number, 5.75 (Sun and Kang, 2016); r_h represents the overall hydrate formation rate; C_{CO_2} is the CO_2 concentration at the water-hydrate interface; and k is the reaction rate constant for reaction (1).

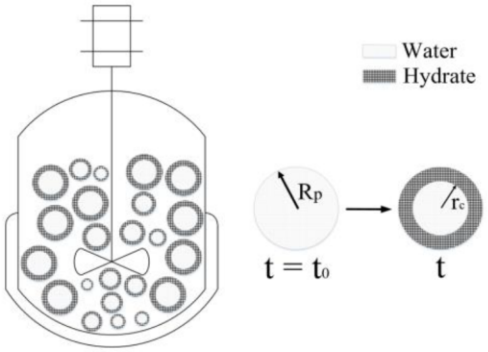

Figure 1: Schematic diagram of the CO_2 hydrate formation in a well-mixed batch reactor (Left) and a shrinking core hydrate particle (Right)

To build a comprehensive model, the system is first analyzed step by step, assuming that the analyzed step is rate limiting. The results are then compared with the experimental data. According to Eq. (1) and Figure 1 (right), for a liquid droplet with a spherical geometry, water conversion (X_{H_2O}) and the unreacted water core radius (r_c) can be correlated as follows:

$$X_{H_2O} = 1 - \left(\frac{r_c}{R_p} \right)^3 \tag{2}$$

where R_p is the particle radius. Assuming a rigid hydrate shell and constant R_p, step (ii) and step (iii) occur instantaneously. There is a linear relationship between the conversion rate and time (Eq. (3)).

$$t = \frac{\rho_{H_2O} R_p}{3 n k_g C^b_{CO_2}} X_{H_2O} \tag{3}$$

where ρ_{H_2O} is the molar density of water and k_g and $C^b_{CO_2}$ are the mass transfer coefficient of CO_2 through the gas layer surrounding the hydrate particle and the molar concentration of CO_2 in the gas bulk, respectively. Similarly, the conversion rate and rate relationship for step (ii) rate limiting and step (iii) rate limiting can be expressed by Eqs. (4) and (5), respectively.

$$t = \frac{\rho_{H_2O} R_p^2}{6 n D_e C^b_{CO_2}} [1 - 3\left(1 - X_{H_2O}\right)^{\frac{2}{3}} + 2\left(1 - X_{H_2O}\right)] \tag{4}$$

$$t = \frac{\rho_{H_2O} R_p}{n k C^b_{CO_2}} [1 - \left(1 - X_{H_2O}\right)^{\frac{1}{3}}] \tag{5}$$

where D_e is the CO_2 diffusion coefficient in the hydrate layer.

2.2. Base model with a varying boundary condition

The base model presented earlier is based on the constant partial pressure of CO_2 in the bulk gas, $p^b_{CO_2}$. However in a closed system, when CO_2 capture in the hydrate cages is exceedingly fast, $p^b_{CO_2}$ declines with time. Given that the partial pressure of CO_2 in the bulk gas is the boundary condition in solving the mass transfer differential equations, the CO_2 concentration profile inside the particle, C_{CO_2}, might be influenced by the transient CO_2 partial pressure in the batch reactor. The base model for the hydrate layer diffusion-dominated case, step (ii), is extended. Eq. (6) defines the rate of CO_2 capture:

$$\frac{dN_{CO_2}}{dt} = -4\pi r^2 D_e \frac{dC_{CO_2}}{dr} \tag{6}$$

in which N_{CO_2} is the number of moles of CO_2. The steady-state assumption and integration yield Eq. (7) and Eq. (8):

$$\frac{dN_{CO_2}}{dt} \int_{r_c}^{R_p} \frac{dr}{r^2} = -4\pi D_e \int_0^{C^b_{CO_2}} dC_{CO_2} \tag{7}$$

$$\frac{dN_{CO_2}}{dt} \left(\frac{1}{r_c} - \frac{1}{r_p} \right) = -4\pi D_e C^b_{CO_2}(t) \tag{8}$$

Instant N_{CO_2} can be presented as a function of $r(t)$ according to Eq. (9):

$$\frac{1}{n} dN_{CO_2} = 4\pi \rho_{H_2O} r_c^2 dr_c \tag{9}$$

CO_2 concentration in bulk gas is the boundary condition for Eq. (6) and is related to the CO_2 partial pressure in the reactor by Eq. (10):

$$C^b_{CO_2}(t) = \frac{p^b_{CO_2}(t)}{RT} \tag{10}$$

Eq. (9) and (10) are substituted in Eq. (8) and integrated across the hydrate layer, resulting in Eq. (11):

$$\frac{R_p^2 \rho_{H_2O} RT}{6nD_e}\left[1-3\left(1-X_{H_2O}\right)^{\frac{2}{3}}+2\left(1-X_{H_2O}\right)\right] = \int_0^t p_{CO_2}(t)\,dt \tag{11}$$

which describes the correlation between water conversion and CO_2 partial pressure changes and allows monitoring of the time-dependent mass diffusion resistance based on the reactor pressure readings. Similarly, the governing equations for the reaction control case with a varying boundary condition have been derived and are given below:

$$\frac{R_p \rho_{H_2O} RT}{nk}\left(1-\left(1-X_{H_2O}\right)^{\frac{1}{3}}\right) = \int_0^t p_{CO_2}(t)\,dt \tag{12}$$

Combining Eq. (11) with Eq. (12), a model considering both the diffusion step (ii) and the reaction step (iii) is produced according to Eq. (13):

$$\frac{R_p \rho_{H_2O} RT}{n}\left[\frac{R_p}{6D_e}\left[1-3\left(1-X_{H_2O}\right)^{\frac{2}{3}}+2\left(1-X_{H_2O}\right)\right]+\frac{1-\left(1-X_{H_2O}\right)^{\frac{1}{3}}}{k}\right] = \int_0^t p(t)dt \tag{13}$$

The right-hand side of Eq. (13) presents the measured time-dependent CO_2 partial pressure inside the reactor. This must be provided practically, making the presented model a semi-empirical model.

3. Results and Discussion

3.1. Controlling mechanism identification

The models derived based on the individual mechanisms (Eqs. 3, 4, 5) were compared against a set of experimental data obtained from batch reaction vessel experiments at 203 K and 0.08 MPa (Falabella, 1975). As shown in Figure 2(A), for the model based on step (ii), diffusion through the hydrate layer best fits the data. The model developed based on gas film control (step (i)) predicts a linear relationship between conversion and time that departs greatly from the experimental data. This is not surprising and is consistent with the assumptions of Englezos et al. (1987) (Englezos et al., 1987). Judgments about the dominant mechanism become critically challenging when comparing the modeling results based on the intrinsic reaction with those based on the diffusion controlling model. While both models follow the practically observed non-linear clathrate conversion trend, the diffusion-dominated model seems more appropriate. This is more obvious at the early stages of the process, from zero to 55% conversion, because the reaction on the water-hydrate interface occurs after gas diffusion through the hydrate layer. At higher conversion ranges, above 55%, both models reasonably predict the experimental data. It can be concluded that while diffusion through the formed hydrate predominantly controls the hydration progress rate, the inherent reaction kinetic role is not negligible. The former becomes more significant when considering the depleting CO_2 partial pressure in the bulk gas surrounding the particle that occurs in a batch reactor.

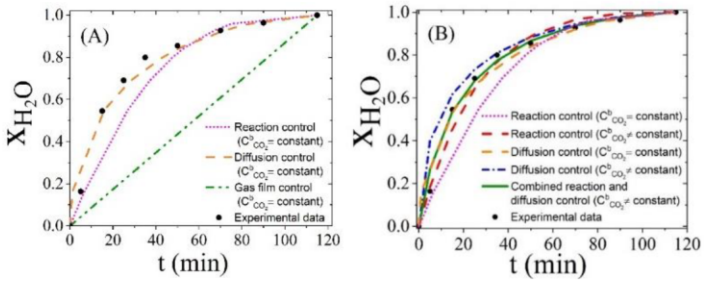

Figure 2: Comparisons of (A) the single-mechanism model prediction with the experimental data for constant bulk concentration and (B) the single- and combined-mechanism model predictions against the experimental data for constant ($C^b_{CO_2}$ = constant) and varying bulk concentration ($C^b_{CO_2}$ ≠ constant)

The assumptions, including the single mechanism control and constant CO_2 partial pressure in bulk gas, used in the base model derivation may be responsible for the observed deviation between the modeled and experimental results in Figure 2(A). The model was improved by accounting for combined mass transfer and reaction kinetics rates, both of which are influenced by the depleting CO_2 fraction in the surrounding gas. Figure 2(B) presents the prediction results for (i) the hydrate diffusion control model with varying CO_2 concentration in the bulk gas (Eq. (11)), (ii) the intrinsic reaction control model with varying CO_2 concentration in the bulk gas (Eq. (12)), and (iii) the combined model under a transient CO_2 concentration (Eq. (13)) and compares these results with the experimental data (Falabella, 1975). The results of the combined model fall between the hydrate layer diffusivity and reaction control results, thus improving the prediction results compared with the experimental data.

3.2. Model analysis

Due to the role of the diffusion rate demonstrated earlier, the accuracy of the diffusion coefficient estimation is of critical importance for model fidelity. The diffusivity of CO_2 in hydrates has been reported to be in the range of 1×10^{-16} m^2/s to 2×10^{-14} m^2/s (Liang et al., 2016). The effect of CO_2 diffusivity on the CO_2 hydrate conversion time was investigated as shown in Figure 3(A). The total conversion time increases dramatically with decreasing diffusivity because at lower diffusivity values, the diffusion of the gas into the inner layer of the gas hydrate shell is slower. As a result, it takes longer to form the gas hydrate particle and consequently reach the end of the conversion time.

In further analysis of the model, the effects of the gas hydrate formation temperature on the completion time were investigated. As shown in Figure 3(B), the effect of the temperature changes on the completion time is not as significant as the effects of the diffusivity on the completion time. At lower temperatures, CO_2 hydrate formation is faster. For example, at 250 K and 298 K, the completion times are approximately 107 min and 130 min, respectively.

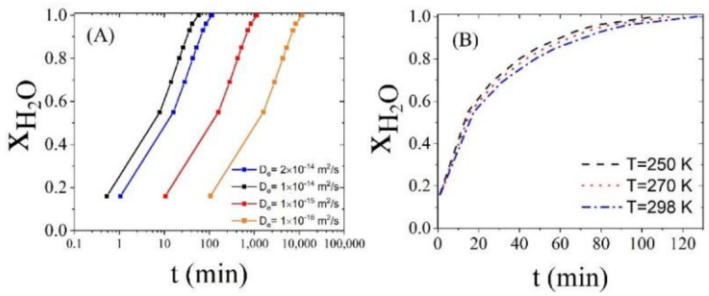

Figure 3: Effects of (A) CO_2 diffusivity and (B) hydrate formation temperature change on the conversion time

4. Conclusions

The purpose of the present study was to determine the dominant controlling mechanism during gas hydrate formation using a novel variation of SCM. The primary model was proposed based on a constant concentration of CO_2 in the bulk gas. The model was further improved by considering the transient CO_2 concentration in the bulk gas, which is a more realistic case. While the diffusion-based model reasonably predicts the CO_2 hydration rate under a constant bulk gas concentration condition, for the realistic scenario in which the bulk gas varies with time, the model must consider the reaction control role as well. The proposed model was successfully used to quantify the effects of the CO_2 diffusivity and the operating temperature on conversion.

References

A. Amiri, A.V. Bekker, G.D. Ingram, I. Livk, N.E. Maynard, 2013, A 1-D non-isothermal dynamic model for the thermal decomposition of a gibbsite particle, Chemical Engineering Research and Design, 91, 485-496.

A. Amiri, G.D. Ingram, N.E. Maynard, I. Livk, A.V. Bekker , 2015, An unreacted shrinking core model for calcination and similar solid-to-gas reactions, Chemical Engineering Communications, 202, 1161-1175.

H. Dashti, X. Lou, 2018, Gas hydrate-based CO_2 separation process: Quantitative assessment of the effectiveness of various chemical additives involved in the process, Springer International Publishing, Cham, pp. 3-16.

H. Dashti, , L. Zhehao Yew, X. Lou, , 2015, Recent advances in gas hydrate-based CO_2 capture, Journal of Natural Gas Science and Engineering, 23, 195-207.

P. Englezos, N. Kalogerakis, P.D. Dholabhai, P.R. Bishnoi, 1987, Kinetics of formation of methane and ethane gas hydrates, Chemical Engineering Science, 42, 2647-2658.

B.J. Falabella, 1975, A Study of Natural Gas Hydrates, University of Massachusetts Amherst, Ann Arbor, p. 180.

P.H. Karpiński, 1980, Crystallization as a mass transfer phenomenon, Chemical Engineering Science, 35, 2321-2324.

J.P. Lederhos, J.P. Long, A. Sum, R.L. Christiansen, E.D. Sloan, 1996, Effective kinetic inhibitors for natural gas hydrates, Chemical Engineering Science, 51, 1221-1229.

S. Liang, D. Liang, N. Wu, L. Yi, G. Hu, 2016, Molecular mechanisms of gas diffusion in CO_2 hydrates, The Journal of Physical Chemistry C, 120, 16298-16304.

E.D. Sloan, , C.A. Koh, 2008, Clathraye Hydrates of Natural Gases, third ed., Taylor & Francis Group, New York.

Q. Sun, Y.T. Kang, 2016, Review on CO_2 hydrate formation/dissociation and its cold energy application, Renewable and Sustainable Energy Reviews, 62, 478-494.

Z. Yin, M. Khurana, H.K. Tan, P. Linga, 2018, A review of gas hydrate growth kinetic models, Chemical Engineering Journal 342, 9-29.

Nomenclature

C_{CO_2}	CO_2 concertation inside the particle (mol/m^3)
$C_{CO_2}^b$	concentration of CO_2 in gas bulk (mol/m^3)
CO_2	carbon dioxide
D_e	effective CO_2 diffusivity coefficient (m^2/s)
h	heat transfer coefficient (kW/m^2K)
H_2O	water
k_g	mass transfer coefficient of CO_2 gas (m/s)
n	hydration number
N	moles
r	radius (m)
r_h	rate of water conversion to hydrate (kg/m^2s)
r_N	rate of nucleate conversion to hydrate (kg/m^2s)
r_W	rate of the water conversion to nucleate (kg/m^2s)
R_p	particle radius (m)
t	time (min)
X_{H_2O}	water conversion

Greek Letters

ρ	density (kg/m^3)

Sub-/Superscripts

b	gas bulk
CO_2	carbon dioxide
g	gaseous phase
H	hydrate
H_2O	water
p	particle
s	solid phase
W	water

Appendix A. Governing equations

Diffusion through gas film control:

Rate of reaction in terms of size R_p of shrinking unreacted particle is given by:

$$-\frac{1}{4\pi R_p^2}\frac{dN_{H_2O}}{dt} = -\frac{n}{4\pi R_p^2}\frac{dN_{CO_2}}{dt} = nk_g C_{CO_2}^b \quad \text{(A.4.1)}$$

The disappearance of the dN_{H_2O} is then given by:

$$-dN_{H_2O} = \rho_{H_2O}dV = -4\pi\rho_{H_2O}r_c^2 dr_c \quad \text{(A.4.2)}$$

Replacing (A2) in (A1):

$$-\frac{1}{4\pi R_p^2}\frac{dN_{H_2O}}{dt} = \frac{\rho_{H_2O}r_c^2}{R_p^2}\frac{dr_c}{dt} = nk_g C_{CO_2}^b \quad \text{(A.4.3)}$$

After integration:

$$t = \frac{\rho_{H_2O}R_p}{3nk_g C_{CO_2}^b}\left[1 - \left(\frac{r_c}{R_p}\right)^3\right] \quad \text{(A.4.4)}$$

or

$$t = \frac{\rho_{H_2O}R_p}{3nk_g C_{CO_2}^b}X_{H_2O} \quad \text{(A.4.5)}$$

Diffusion through hydrate layer control:

The rate of the reaction is given by:

$$-\frac{dN_{CO_2}}{dt} = 4\pi r^2 D_e \frac{dc_{CO_2}}{dr} \quad \text{(A.4.6)}$$

Integrating across the hydrate layer from R_p to r_c, we obtain:

$$-\frac{dN_{CO_2}}{dt}\left(\frac{1}{r_c} - \frac{1}{R_p}\right) = 4\pi D_e C_{CO_2}^b \quad \text{(A.4.7)}$$

Integration of Eq. (A7) with respect to time:

$$t = \frac{\rho_{H_2O}R_p^2}{6nD_e C_{CO_2}^b}\left[1 - 3\left(\frac{r_c}{R_p}\right)^2 + 2\left(\frac{r_c}{R_p}\right)^3\right] \quad \text{(A.4.8)}$$

or

$$t = \frac{\rho_{H_2O} R_p^2}{6nD_e C_{CO_2}^b}\left[1 - 3\left(1 - X_{H_2O}\right)^{\frac{2}{3}} + 2(1 - X_{H_2O})\right] \quad \text{(A.4.9)}$$

Reaction control:

The rate of the reaction is:

$$-\frac{1}{4\pi r_c^2}\frac{dN_{CO_2}}{dt} = -\frac{n}{4\pi r_c^2}\frac{dN_{CO_2}}{dt} = nkC_{CO_2}^b \quad \text{(A.4.10)}$$

Writing N_{H_2O} in terms of the shrinking radius, we obtain:

$$-\frac{1}{4\pi r_c^2}\rho_{H_2O} 4\pi r_c^2 \frac{dr_{CO_2}}{dt} = -\rho_{H_2O}\frac{dr_{CO_2}}{dt} = nkC_{CO_2}^b \quad \text{(A.4.11)}$$

After integration:

$$t = \frac{\rho_{H_2O}(R_p - r_c)}{nkC_{CO_2}^b} \quad \text{(A.4.12)}$$

or

$$t = \frac{\rho_{H_2O} R_p}{nkC_{CO_2}^b}\left[1 - \left(1 - X_{H_2O}\right)^{\frac{1}{3}}\right] \quad \text{(A.4.13)}$$

Chapter 5. Kinetic modelling of the gas hydrate-based CO_2 processes: a multistage shrinking core model

This chapter is published in the Journal of Cleaner Production.

5.1. Introduction

Clathrate gas hydrates are small, solid crystalline, ice-like structures formed at high-pressure and low-temperature conditions via van der Waals interactions of water molecules in the hydrate lattice and gas molecules (Peter Englezos, 1993). Many gases such as methane (CH_4), carbon dioxide (CO_2), ethane (C_2H_6), nitrogen (N_2) and hydrogen sulfide (H_2S) are capable of forming gas hydrates. Applications of hydrate technology in the separation and storage of gases such as CH_4 and CO_2 and desalination have been reported in the literature (Dashti & Lou, 2018; Dashti, Zhehao Yew, & Lou, 2015; Sloan & Koh, 2008). Under appropriate thermodynamic conditions, the amount of gas inside the hydrated crystals can reach up to 170 times more than that feasible under standard thermodynamic conditions (Selim & Sloan, 1989). At a pressure higher than 4.5 MPa and a temperature lower than 283 K, CO_2 forms a hydrate structure, $CO_2 \cdot nH_2O$, where n=5.75 assuming full occupancy of the water cages (Sloan & Koh, 2008; Sun & Kang, 2016). Under these conditions, the solubility of CO_2 in water is approximately 0.031 mole CO_2/mole H_2O (Diamond & Akinfiev, 2003). Feasible CO_2 capture in water may increase by fivefold through hydration. Unique features such as the moderate operational temperature range, low energy consumption and capability for continuous operation have made gas hydrate technology one of the promising approaches for CO_2 capture and separation (Dashti et al., 2015). Extensive research has focused on the thermodynamics of the gas hydrate formation process (Eslamimanesh, Mohammadi, Richon, Naidoo, & Ramjugernath, 2012). Experimental investigations of CO_2 hydrate formation mechanisms have also been widely reported (Clarke & Bishnoi, 2005; Dashti & Lou, 2018; Teng, Kinoshita, & Masutani, 1995; Uchida, Ebinuma, Kawabata, & Narita, 1999; Yang, Le, Martinez, Currier, & Spencer, 2011; Yin, Khurana, Tan, & Linga, 2018). However, an insightful understanding of the complex fundamentals of the process, such as nucleation, is still needed for the gas hydrate-based CO_2 capture (HBCC) process to become technically and economically viable at large scales.

The process of gas hydrate formation includes two main steps: hydrate nucleation and growth. Based on concepts of crystallization, the availability of a supersaturated condition does not necessarily guarantee the initiation of the crystallization process; solid nucleate particles must exist in the solution (Mullin, 2001). Sloan and Koh defined the “nucleation” stage as the process in which small cluster particles of the gas

and water molecules initiate, grow and dissolve in order to reach a critical cluster size (Sloan & Koh, 2008). Khurana et al. reported that the classical nucleation approach is insufficient to reveal the exact pathway of the nucleation process as well as the hydrate structures (Khurana, Yin, & Linga, 2017).

Measurement of nucleation phase behavior through experimental investigations is very difficult and complicated due to the stochastic and sudden appearance of this phase (Ripmeester & Alavi, 2016). The nucleation stage is followed by the so-called "growth" stage in which a considerable increase in gas uptake occurs, and gas hydrate formation can be controlled by pseudo-reaction intrinsic kinetics, heat or mass transfer phenomena or a combination thereof (Sloan & Koh, 2008). The roles played by these phenomena might be greatly affected by the nucleation process and variations in nucleate phase properties. Experimentally, it is challenging to capture the time-dependent variations of the nucleation process, which emphasizes the importance of numerical simulation as an alternative to further understanding this intermediate stage.

Current models for the gas hydration and nucleation processes are mostly based on thermodynamic concepts. Chemical potential (Skovborg, Ng, Rasmussen, & Mohn, 1993), fugacity (Natarajan, Bishnoi, & Kalogerakis, 1994), and temperature (Vysniauskas & Bishnoi, 1983) variations are key variables used in hydrate modeling in the literature as driving forces to explain hydrate behavior. The modeling scale and methodology vary depending on the modeling target. The molecular simulation approach, for instance, is widely used in the literature to investigate gas hydrates at the nanoscale (English & MacElroy, 2015). Molecular simulations describe the nucleation process as a two-step process in which disordered crystal-like structures form and then are converted to more detectable crystalline forms of particles (Jacobson, Hujo, & Molinero, 2010a). A critical challenge associated with molecular-level simulations is the time-consuming computations because of the slow processes, which include gas diffusion into the liquid phase and heat transfer during the formation of nucleate particles (English & MacElroy, 2015). To avoid large simulation timescales in the nucleation process, most studies have attempted to use a high driving force, which is not representative of the real experimental and industrial settings of the nucleation process (Walsh et al., 2011). Similar challenges and pitfalls are present when modeling of the gas hydrate growth phase is attempted (Ribeiro Jr & Lage, 2008).

Solid-fluid models are another approach to model the process of gas hydrate formation. The unreacted shrinking core model (SCM), in particular, has been commonly used for solid reactions in which the intrinsic reaction rate is much greater than the mass transfer rate (Amiri, Ingram, Maynard, Livk, & Bekker, 2015). In SCM, the initial reaction occurs at the outer radius of the solid particle, and then the zone of the reaction moves into the core. As conversion proceeds, the size of the unreacted core decreases. Shi et al. proposed a variation of SCM to simulate gas hydrate growth in the presence of condensate oil in the flow loop (Shi et al., 2011) that incorporated the kinetic model developed by Englezos et al. (P. Englezos, Kalogerakis, Dholabhai, & Bishnoi, 1987) The authors used experimental data to optimize the kinetic controlling parameters (gas diffusivity, porous property, and mass transfer efficiency). This model was further developed to study the growth kinetics of the methane hydrates in the presence of dry water and porous hydrogel particles (Shi, Fan, & Lou, 2014; Shi, Yang, Fan, & Lou, 2017). Falenty et al. supported the applicability of SCM for CO_2 hydrate formation from ice powders using cryo-scanning electron microscopy images (Falenty, Salamatin, & Kuhs, 2013). While all of these studies have demonstrated the effectiveness of SCM for the prediction of CO_2 hydrate growth, none have investigated aspects of hydrate nucleation.

The Englezos model integrates the crystallization and mass transfer theories to describe hydrate crystal growth (P. Englezos et al., 1987). According to this model, hydrate particle growth involves two sequential steps: (1) diffusion of gas molecules from the bulk solution of gas to the hydrate-water interface and (2) hydration reactions at the interface. The second step is an adsorption process involving the incorporation of gas molecules into water molecules and subsequent stabilization of the structured water. The driving force in this model is the difference between the fugacity of the dissolved gas and the three-phase equilibrium fugacity. The hydrate nucleation stage significantly affects the hydration history profiles, gas concentration, and temperature profiles, based on numerous experimental studies (Khurana et al., 2017; Mullin, 2001; Natarajan et al., 1994; Vatamanu & Kusalik, 2010). It is evident that an understanding of nucleation phase behavior and induction time variations requires nucleation experiments with a complex design. Numerical studies can provide invaluable insights on this stage of the process. Previous modeling studies have mostly focused on either the CO_2 hydrate growth phase (Yin et al., 2018) or the microscale phenomena of CO_2

nucleation formation conditions at microsecond timescales via molecular simulation (He, Linga, & Jiang, 2017; Khurana et al., 2017). From the reactor design and optimization perspective, however, a mesoscale model must be integrated with a macroscale (reactor) model that considers mass and heat transport barriers.

In this paper, a new variation of the SCM with modifications to the reported work by Amiri et al. (Amiri, Ingram, Bekker, Livk, & Maynard, 2013) is developed to describe gas hydrate formation. The model captures both the mass transfer and heat transfer involved in the hydrate formation process and provides a simulated temperature profile and gas consumption profile that are similar to the reported experimental results. The new model consists of two stages to simulate both the nucleation and growth of the gas hydrates. The most significant contribution of the current work is to propose and demonstrate an efficient and fast predictive tool for the nucleation process as part of a whole CO_2 hydration process. Moreover, a model-based estimation of the induction time, as a critical parameter in CO_2 hydrate rate estimation and control, is presented. Table 5.1 provides a comparison of recent CO_2 hydrate modeling studies in the open literature with the present work.

Table 5.1. Comparison of recent CO_2 hydrate modeling studies and the current study.

Features	**Contributions**				
	(Falenty et al., 2013; Henning, Schultz, Thieu, & Halpern, 2000; Staykova, Kuhs, Salamatin, & Hansen, 2003)	(Mochizuki & Mori, 2006; Mori, 2001; Uchida et al., 1999; Uddin, Coombe, Law, & Gunter, 2008)	(Kvamme et al., 2004; Radhakrishnan & Trout, 2002)	(Bai, Chen, Zhang, & Wang, 2011, 2012)	This work
Application of SCM in CO_2 hydrates	*	–	–	–	*
Model-based induction time prediction	–	–	–	*	*
Modeling of the nucleation stage	–	–	*	*	*
Non-isothermal modeling	–	*	–	–	*

Notations: Considered (*), Not considered (–)

5.2. Multi-stage SCM development

A multi-stage SCM (MSSCM) is proposed and used in this study to capture the features relevant to the nucleation and growth stages, especially the effects of transient control factors. The model is established based on work by Amiri et al. on the simulation of the calcination process in which the gas product inhibits the reaction and

a solid intermediate product also forms (Amiri, Bekker, Ingram, Livk, & Maynard, 2013; Amiri et al., 2015). In an effectively agitated reactor with a constant supply of CO_2 gas molecules, as reported by Linga et al. (Linga, Kumar, & Englezos, 2007), hydrate formation is considered to occur in individual water droplets, and therefore the MSSCM encompassing both the nucleation and growth steps can be schematically illustrated as shown in Figure 5.1. Nucleation occurs at Stage 1, and there is no hydrate formation/growth during this stage. Further progress of the process in Stage 2 results in the initial growth of gas hydrates, with the formation of the first layer of hydrates. At this stage, nucleation continues while growth of hydrates also occurs. At the end of Stage 2, the fresh water is fully consumed, leaving either nucleate or hydrate behind. At Stage 3, rapid hydrate growth occurs and converts all nucleates to the CO_2 hydrate. There is no new nucleate formation at Stage 3. The following assumptions have been applied in the current model:

1. The water droplet is initially pure and spherical with a constant radius throughout the process.
2. When the process starts, the reactor pressure and temperature are 3.25 MP and 270 K, respectively. At this time, CO_2 dissolution begins.
3. CO_2 dissolution was assumed to be included in the nucleation processes. Therefore, the induction time refers to the time needed to allow CO_2 accumulation – via dissolution and nucleation – to reach a critical level sufficient for hydrate formation. The contribution of the dissolution term in overall model performance was examined as presented in the model analysis part.

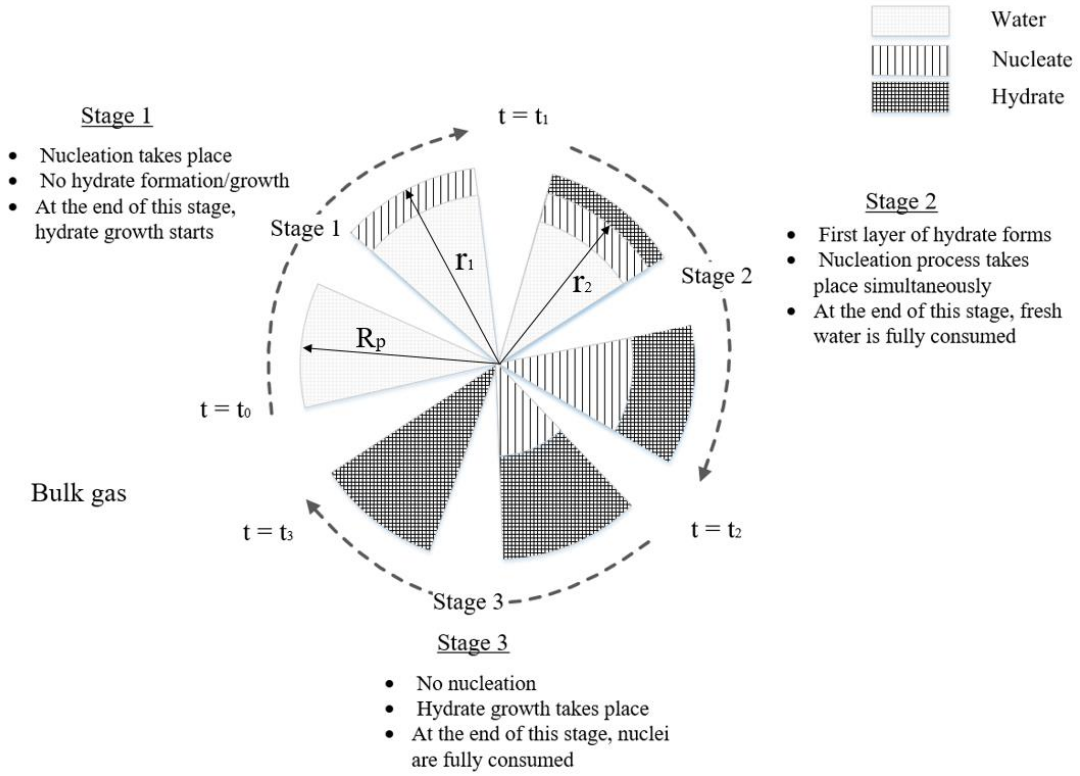

Figure 5.1. Schematic of the multi-stage-multi-reaction model for the CO_2 hydration process with spherical geometry ($r_1 = r^{W.N}, r_2 = r^{N.H}$)

For the formation of CO_2 hydrates, the overall reaction is expressed by Eq. (5.1).

$$CO_2 + nH_2O \overset{k_1}{\rightarrow} CO_2 \cdot nH_2O \qquad r_h = k_1 C_{CO_2} \qquad (5.1)$$

in which C_{CO_2} is the CO_2 local concentration and k_1 is the reaction rate constant.

In this model, an intermediate nucleate (N or $CO_2 \cdot mH_2O$) stage is considered over the pathway to CO_2 hydrate (H or $CO_2 \cdot nH_2O$) product, expressed as the following:

$$mH_2O_{(aq)} + CO_{2\,(aq)} \overset{k_2}{\rightarrow} N_{(s)} \qquad r_W = k_2 C_{CO_2}^{W.N} \qquad (5.2)$$

$$N_{(s)} + \alpha CO_{2(aq)} \overset{k_3}{\rightarrow} (\alpha + 1)H_{(s)} \qquad r_N = k_3 C_{CO_2}^{N.H} \qquad (5.3)$$

where k_2 and k_3 are the reaction rate constants in Eq. (5.2) and Eq (5.3) and $m = (1 + \alpha)n$. $C_{CO_2}^{W.N}$ and $C_{CO_2}^{N.H}$ are the CO_2 concentrations at the water/nucleate ($W.N$) and nucleate/hydrate ($N.H$) interfaces, respectively. The multi-stage hydration model governing equations and their derivation details are presented in Table 5.2 and the Appendix A, respectively. The initial and boundary conditions are the variables' values at the stages' interface (variables subscripted with 12 and 23 for stage 1 to 2

and 2 to 3 exchanges, respectively). As the two subsequent stages provide the same concentration and temperature at the interface, the stage exchange time is estimated by equating the stages in the models.

Table 5.2. Model equations for the multi-stage gas hydrate nucleation and growth stages

Stage	Equations	Initial conditions
1	$1-\frac{C_{CO_2}^{W.N}}{C_{CO_2}^{b}}\left(1+\frac{\vartheta_1 k_2 R_p}{D_{e,1}}\left(\frac{r_1}{R_p}\right)^2\left(\frac{1}{\left(\frac{r_1}{R_p}\right)}-1\right)\right)=0$	
	$\frac{dr_1}{dt}=-\frac{MW_{H_2O}}{\rho_{H_2O}}k_2 C_{CO_2}^{W.N}$	$r_1=R_p$ at $t=t_0$
	$\frac{dT}{dt}=\frac{h(T_b-T)-\left(\frac{r_1}{R_p}\right)^2 k_2\Delta H_2 C_{CO_2}^{W.N}}{\frac{R_p\rho_{H_2O}}{3MW_{H_2O}}C_{p,1}}$	$T=T_b$ at $t=t_0$
2	$\frac{C_{CO_2}^{N.H}}{C_{CO_2}^{b}}-\frac{C_{CO_2}^{W.N}}{C_{CO_2}^{b}}\left(1+\frac{\vartheta_1 k_2 R_p}{D_{e,2}}\left(\frac{r_1}{R_p}\right)^2\left(\frac{1}{\left(\frac{r_1}{R_p}\right)}-\frac{1}{\left(\frac{r_2}{R_p}\right)}\right)\right)=0$	
	$1-\frac{C_{CO_2}^{N.H}}{C_{CO_2}^{b}}-\left(\frac{\vartheta_1 k_2 R_p}{D_{e,2}}\frac{C_{CO_2}^{W.N}}{C_{CO_2}^{b}}\left(\frac{r_1}{R_p}\right)^2+\frac{\vartheta_2 k_3 R_p}{D_{e,2}}\frac{C_{CO_2}^{N.H}}{C_{CO_2}^{b}}\left(\frac{r_2}{R_p}\right)^2\right)\left(\frac{1}{\left(\frac{r_2}{R_p}\right)}-1\right)=0$	
	$\frac{dr_1}{dt}=-\frac{MW_{H_2O}}{\rho_{H_2O}}k_2 C_{CO_2}^{W.N}$	$r_1=r_{12}$ at $t=t_1$
	$\frac{dr_2}{dt}=-\frac{MW_N}{\rho_N}k_3 C_{CO_2}^{N.H}$	$r_2=R_p$ at $t=t_1$
	$\frac{dT}{dt}=\frac{h(T_b-T)-\left(\frac{r_1}{R_p}\right)^2 k_2\Delta H_2 C_{CO_2}^{W.N}-\left(\frac{r_2}{R_p}\right)^2 k_3\Delta H_3 C_{CO_2}^{N.H}}{\frac{R\rho_{avg,2}}{3MW_{avg,2}}C_{p,2}}$	$T=T_{12}$ at $t=t_1$
3	$1-\frac{C_{CO_2}^{N.H}}{C_{CO_2}^{b}}\left(1+\frac{\vartheta_2 k_3 R_p}{D_{e,3}}\left(\frac{r_2}{R_p}\right)^2\left(\frac{1}{\left(\frac{r_2}{R_p}\right)}-1\right)\right)=0$	

$\frac{dr_2}{dt} = -\frac{MW_N}{\rho_N} k_3 C_{CO_2}^{N.H}$	$r_2 = r_{23}$ at $t = t_2$
$\frac{dT}{dt} = \frac{h(T_b - T) - \left(\frac{r_2}{R_p}\right)^2 k_3 \Delta H_3 C_{CO_2}^{N.H}}{\frac{R_p \rho_{avg,3}}{3MW_{avg,3}} C_{p,3}}$	$T = T_{23}$ at $t = t_2$

5.3. Model solution and validation

The Matlab *ode23* solver tool was used to numerically solve the set of ordinary differential equations in Table 5.2. Due to the complex nature of the nucleation phase, the uncertainty in its physical parameters is a real challenge. For the numerical solution (Table 5.3), the nucleate parameters were assumed based on the fact that the nucleation stage is a precursor stage to the hydration stage and is comprised of cages not fully occupied by the CO_2 molecules or semi-formed cages. Therefore, average values of water and hydrates were initially assumed for the nucleate physical properties. For instance, the molecular weight (MW_N) and the density (ρ_N) of nucleates were assumed to be the average value between the molecular weight and density of water and the CO_2 hydrates. The nucleation number (m) was assumed as 10, and different values of the nucleation number were used in the model parametric analysis. The CO_2 concentration in the bulk gas ($C_{CO_2}^b$) was estimated using the Peng-Robinson equation of state (Robinson & Peng, 1978) at a temperature of 270 K (Liang, Liang, Wu, Yi, & Hu, 2016) and pressure of 3.25 MPa.

The effective diffusivities (D_e) was estimated as the phase portion-based average value of the diffusivity of the hydrate and nucleate phases. For example, the effective diffusivity in the first stage ($D_{e,1}$) is the average of the diffusivity of the nucleate and the water and changes with the change in the thickness of the nucleated layer with time. The effective CO_2 diffusivity coefficient values in gas hydrates were selected based on the reported values in the literature, which range from 1.0×10^{-14} m^2/s to 2.0×10^{-16} m^2/s (Liang et al., 2016).

The reaction rate coefficient *k* values are reportedly affected by the hydrate surface areas measured in the experiments (Yin et al., 2018). Values on the order of 10^{-5} to 10^{-8} are reported in different studies (Bergeron & Servio, 2008; Hashemi, Macchi, & Servio, 2007; Ou, Lu, Qu, Geng, & Chou, 2016). In this study, however, we observed

that *k* values in this range result in a very small Thiele modulus (<<1) indicating that there is almost no role for the reaction rate in controlling the process. This observation is not consistent with previous studies reporting the intrinsic reaction rate as the second controlling mechanism. We therefore used *k* values on the order of 10^{-2} to conduct a meaningful parametric study, while more precise measurements, particularly for the nucleation reaction, are needed through experimental studies and parameter tuning optimization.

Table 5.3. Parameters used for MSSCM solution for the CO_2 hydration process

Parameter	**Value**
$C^b_{CO_2}, mol/m^3$	2063.1
$D_{e,1}, m^2/s$	8.00×10^{-14}
$D_{e,2}, m^2/s$	4.04×10^{-14}
$D_{e,3}, m^2/s$	7.80×10^{-16}
$k_2, m/s$	9.0×10^{-2}
$k_3, m/s$	1.5×10^{-3}
$\Delta H_2, KJ/kg$	– 20.61 (Lirio & Pessoa, 2013)
$\Delta H_3, KJ/kg$	– 40 (Lirio & Pessoa, 2013)
$MW_{H_2O}, g/mol$	18
$MW_N, g/mol$	404
n	5.75 (Sun & Kang, 2016)
R_p, m	8.29×10^{-7}
$\vartheta_1\ (=m)$	10
$\vartheta_2\ (=n/(m-n))$	1.35
$\rho_{H_2O}, kg/m^3$	1000
$\rho_N, kg/m^3$	1050

For the estimation of the stage change characteristics, such as time for induction, the fact that the model variables including r, C_{CO_2} and T remain the same in both phases (stages) is considered. The same approach was used to identify the time when Stage 2 shifts to 3.

The model-based time-dependent mass fraction profiles of water, nucleate, hydrate, and experimentally measured gas uptake data (Linga et al., 2007) are presented in Figure 5.2. It is impossible to obtain internal particle insights experimentally to validate the particle composition. However, the trajectory of the particle gas uptake behavior achieved via the model agrees well with the experimental trend, thus validating the modeling strategy. The experimentally reported CO_2 uptake is based on

the bulk gas concertation change over time and provides no insight on the amount of water consumed. This explains the observed deviation between the absolute values of CO_2 uptake in the model and experiment (Figure 5.2).

The results in Figure 5.2(A) show that at the first stage (t_0/t_{max}=0 to t_1/t_{max}=0.18), the nucleation process consumes water and produces nucleate without hydrate formation. This corresponds to the time period in which slow gas uptake is frequently observed in the experimental graphs (Figure 5.2(B)). At the end of this stage, the nucleate fraction reaches the maximum value. A decline starts due to the commencement of hydrate growth from critically sized nucleates, indicating the beginning of Stage 2, at t_1/t_{max}=0.18. This stage involves both nucleation and initial rapid growth of hydrates, resulting in the formation of the hydrate shell. The rapid CO_2 hydrate growth is indicated by the increase in the hydrate mass fraction. This stage corresponds to the gas uptake observed in the experimental results (t_1/t_{max}=0.18 to t_2/t_{max} =0.72). Stage 2 finishes at t_2/t_{max}=0.72, which is estimated using the point at which fresh water is fully consumed. During Stage 3, the remaining nucleate is converted to the hydrate. The rate of mass fraction changes during this stage is slow compared to the other stages, principally due to the mass transfer and heat transfer limitation, and the slow driving force will result in slow hydrate formation. Finally, at the end of this stage, the mass fraction rate of the hydrate approaches 1.

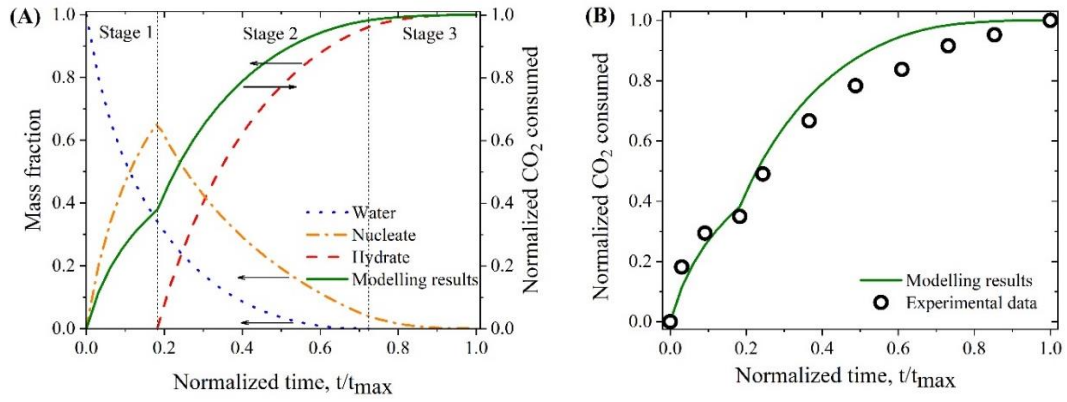

Figure 5.2. Results of multi-stage gas hydrate nucleation and growth for the basis case simulation: (A) stages, phases distribution, and gas uptake; (B) comparing modeling results with experimental gas uptake data for the CO_2/N_2 system from Linga et al. (Linga et al., 2007).

The nucleation and the growth stage results have been validated against the experimental data using the practically observed trends. The current model prediction compares reasonably with the principal gas consumption trends presented in the literature. The gas consumption and water conversion trends are exchangeable using the hydration number. The experimental data were taken from Linga et al., who reported a series of experimental works on CO_2/N_2 hydrate formation (Linga et al., 2007). The operating pressure in the study was much lower than that thermodynamically needed for N_2 hydrate formation. Although N_2 hydrates may form during the separation cycle, the model has assumed the interference of the free nitrogen and the nitrogen hydrates formation is negligible. Since model results are based on a single particle and experimental results are based on an unknown number of particles, we have considered a dimensionless (normalized) gas uptake term for comparison purpose. Assuming all particles perform similarly in the reactor, particles number has no role in the dimensionless gas uptake defined as amount of CO_2 consumed at any time over the overall CO_2 consumed over process course. As shown in Figure 2(B), the modeling result for gas consumption reveals a two-stage process that is similar to that observed experimentally. Moreover, the gas uptake history is in a good agreement with the experimentally measured values.

Furthermore, Lederhos et al. (Lederhos, Long, Sum, Christiansen, & Sloan, 1996) conducted an experimental study in a batch reactor to investigate the effects of the kinetic inhibitors on hydrate inhibition, as evaluated by measuring the gas consumption versus time. The process history graph clearly shows the hydrate nucleation and growth processes that are captured in the current model. They schematically illustrated the nucleation stage (or induction time) as the time elapsed before the first detectable gas consumption (growth stage). Yin et al. reported a similar gas uptake trend for CH_4 hydrate formation in a batch stirred reactor based on the results of Englezos et al. (P. Englezos et al., 1987; Yin et al., 2018). They considered the first stage as the gas dissolution and induction period, and at this stage, the amount of gas consumption is very small due to the dissolution of the gas molecules in the liquid phase. These practical observations corroborate the presented multi-stage model as a consistent paradigm for the hydration process. He et al. investigated the nucleation of the CO_2 hydrate using molecular simulation, and a small CO_2 mass fraction during the nucleation stage was observed (He et al., 2017). The same trend in the results using

molecular simulation was reported by Bi et al. (Bi, Porras, & Li, 2016). Jacobson et al. simulated the mechanism of the nucleation process using molecular simulation by showing the number of occupied cages versus time. They showed that at the nucleation stage, the cages are not occupied by the CO_2 molecules, and as hydrate growth starts, the cages are occupied by the CO_2 molecules (Jacobson, Hujo, & Molinero, 2010b). All of these studies support the history trends presented in Figure 5.2, confirming the validity of the modeling framework.

5.4. Non-isothermal behavior

To capture the thermal history of the reacting particles, integration of the heat transfer and kinetics of gas hydrate formation was implemented. Accordingly, energy conservation and constitutive equations were added to the primary multi-stage model and solved simultaneously (Table 5.2). The particle temperature profile resulting from the thermal profiles of the individual stages is presented in Figure 5.3. Regarding the gas hydration temperature profile, an initial rise followed by a decline and final settling at approximately 273.5 K for the CO_2 hydration case has been reported in many experimental studies. This profile can be explained based on the release of heat due to the initial nucleation and hydration. Sloan and Koh highlighted that the rapid increase in temperature indicates hydrate formation in a high-pressure cell with constant volume (Sloan & Koh, 2008). The temperature of the cell/particle subsequently gradually decreases due to nucleation rate mitigation and heat transfer to the surrounding particles. The temperature settlement at the final value can be observed in Stage 3, as shown by theoretical (this work) results. The thermal capability is an applied added value of the current model that has not been taken into account in previous models (Bollavaram, Devarakonda, Selim, & Sloan, 2000; Shi et al., 2011). While the proposed model importantly allows the prediction of the thermal trends of the particle and the reactor, parameter tuning must be conducted for any specific case study using the experimental data under relevant conditions. The model-based temperature profile, Figure 5.3, well simulates the temperature history trends observed in the experimental works including the temperature peak and settlement.

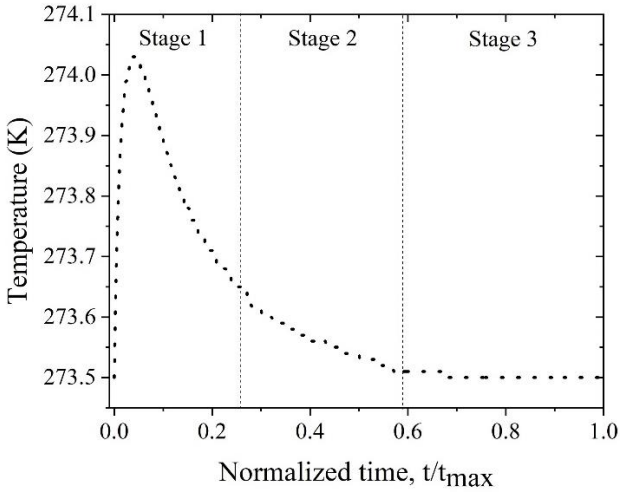

Figure 5.3. Temperature profile of the CO_2 hydration process comprising three stages of the thermal history achieved via MSSCM simulating experimentally seen temperature peak and settlement.

5.5. Model analysis

5.5.1. Sensitivity analysis of the reaction constant rates

Several studies have investigated the CO_2 hydration reaction rate during gas hydrate formation (Bergeron & Servio, 2008; Chun & Lee, 1996; Malegaonkar, Dholabhai, & Bishnoi, 1997; Ou et al., 2016; Verrett & Servio, 2016). A sensitivity analysis of the competing reactions using the rates constants k_2 and k_3 was carried out to investigate the species distribution and steps/phases lifetime and induction time.

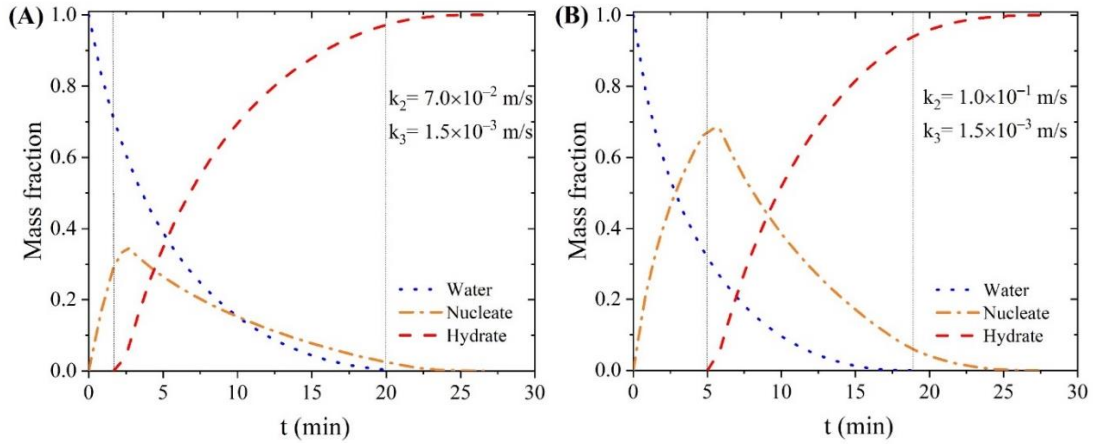

Figure 5.4. Results of the multi-stage nucleation and growth model for the mass fractions of water, nucleate and hydrate versus time for (A) k_2=7.0×10^{-2} m/s and (B) k_2=1.0×10^{-1} m/s. The black dotted lines separate the three stages in MSSCM.

Figure 5.4 indicates the phases' distributions inside the particle, the duration of the individual stages and the whole process for the two nucleation rate constants (k_2) and the hydration rate constant $k_3=1.5\times10^{-3}$ m/s. The faster nucleation process results in higher nucleate accumulation inside the particle, and the nucleate shows a stronger peak by k_2, whereas the hydration rate is slow and controlling. A greater amount of CO_2 penetrating into the water droplet would be consumed for the nucleation process, resulting in a longer induction time due to the lack of CO_2 for growth. This behavior is consistent with the mathematical estimation of the induction time in which the CO_2 profiles in Stage 1 and 2 play a crucial role. A delay in hydration process initiation leads to a longer process completion time, i.e., from 26.6 min for $k_2=1.0\times10^{-1}$ m/s to 28.4 min for $k_2=7.0\times10^{-2}$ m/s. The induction time increases, and the nucleate shows a stronger peak by k_2. For small k_2 values, the CO_2 capture process proceeds mainly through Stage 2 (lasting for 18 min, ~67% of the overall time), in which all three phases exist, while for $k_2=1.0\times10^{-1}$ m/s, Stage 2 lasts for 12.5 min, ~44% of the overall time.

In the second sensitivity analysis, the effects of varying k_3 were examined while k_2 was considered to be a constant parameter in MSSCM for comparison. Figure 5 illustrates the results for $k_3=1.3\times10^{-3}$ m/s and $k_3=1.5\times10^{-3}$ m/s at $k_2=9.0\times10^{-2}$ m/s. As shown in Figure 5.5, as the k_3 value increases, the time required for total depletion of the nucleate core decreases, which results in higher impacts on Stages 2 and 3 compared to Stage 1. The induction is shorter at higher k_3 values, and the process period mainly consists of Stages 2 and 3. Combining both individual analyses, it can be concluded that the k_2k_3 product is a reasonable measure for explaining the process behavior. A smaller k_2k_3 would lead to a longer induction time, larger nucleate fraction peak, and longer completion time.

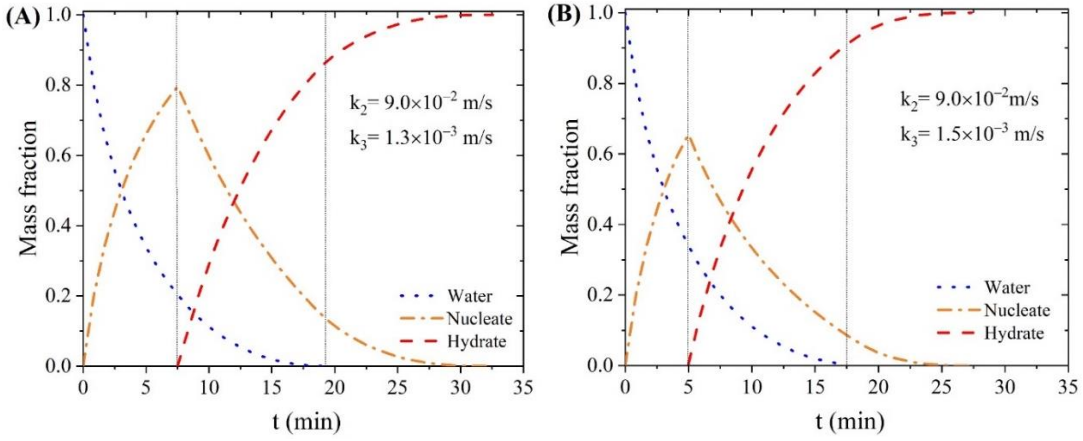

Figure 5.5. Results of the multi-stage nucleation and growth model for the mass fractions of water, nucleate and hydrate versus time for (A) k_3=1.3×10^{-3} m/s and (B) k_3=1.5×10^{-3} m/s. The black dotted lines separate the stages in MSSCM.

5.5.2. Effects of the CO_2 solubility in MSSCM

An analysis of the effects of the solubility on the CO_2 consumed using the experimental CO_2 solubility in water at 3.25 MPa and 270 K (Diamond & Akinfiev, 2003) has been investigated in this study. CO_2 dissolution in water under 3.25 MPa and 270 K is approximately 0.0325 mole CO_2 / mole H_2O (Diamond & Akinfiev, 2003), which is not enough to fully form the hydrate ($CO_2 \cdot 5.75H_2O$) or even nucleate ($CO_2 \cdot mH_2O$, m > 5.75). For hydrate formation, a solid solution of 0.174 (mole CO_2 / mole H_2O) must be achieved. Accordingly, it was assumed that the CO_2 needed for this process is mainly provided externally through diffusion. Figure 5.6 illustrated the effects of the CO_2 solubility on the CO_2 consumption in MSSCM. It can be seen from Figure 5.6 that the CO_2 solubility does not have significant effects on the amount of CO_2 consumption during CO_2 hydrate nucleation and growth.

The CO_2 solubility in water may raise concerns about the applicability of SCM for the current case study. Since the CO_2 diffusion rate decreases drastically upon formation of the hydrate layer, the overall process is controlled by the CO_2 mass transfer rate, which allows a minor amount of CO_2 to reach the interior and, in particular, the central parts of the water droplet. This behavior reasonably justifies the applicability of SCM, as demonstrated by its successful use in the literature (Falenty et al., 2013; Henning et al., 2000; Staykova et al., 2003). For the gas uptake underestimation, one may combine the gas consumed through the dissolution and nucleation mechanisms. In other words, the gas consumed for nucleation might be fitted to be representative of both dissolution

and nucleation gas consumption, where individual portions can be estimated through thermodynamic estimations. Given the significantly higher gas consumption in the growth stage compared to the dissolution and nucleation stages, this simplification would not result in significant errors as shown in Figure 5.6.

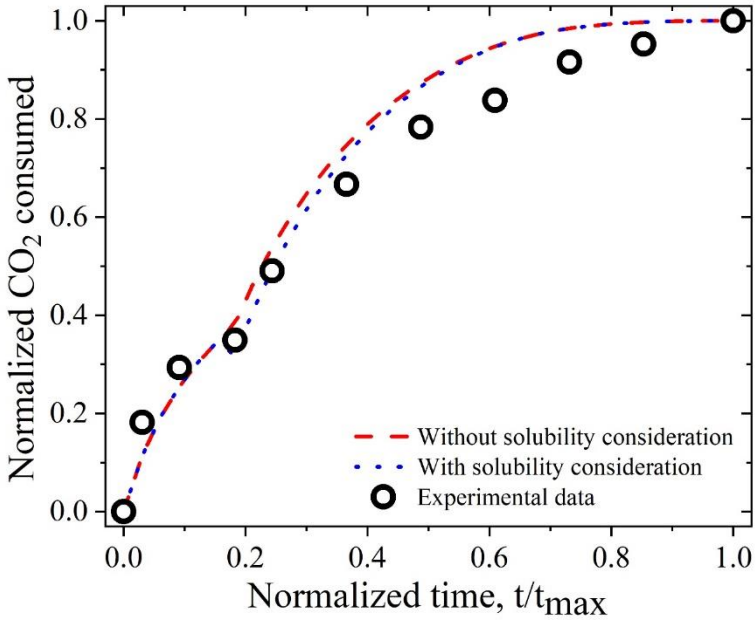

Figure 5.6. Effects of the CO_2 solubility on the CO_2 consumption estimated in MSSCM

5.5.3. Internal CO_2 concentration

As a mass transfer-controlled process, the intensification and control of CO_2 hydration might benefit significantly from insights on the distributed and time-dependent concentration profiles inside the reacting element. The proposed model readily offers such insightful data, in contrast to the challenges in achieving such data from practical measurements. The concentration difference across the phases' layers ($\Delta C/\Delta r$) was estimated for the hydrate, $(C_{CO_2}^{b} - C_{CO_2}^{N.H})/(R_p - r_2)$, and nucleate, $(C_{CO_2}^{N.H} - C_{CO_2}^{W.N})/(r_2 - r_1)$, layers during Stage 2 as presented in Figure 5.7. Water conversion, as an indicator of reaction progress, is also depicted. The concentration gradient across the nucleate layer is higher than that in the hydrate layer at any time during the second stage.

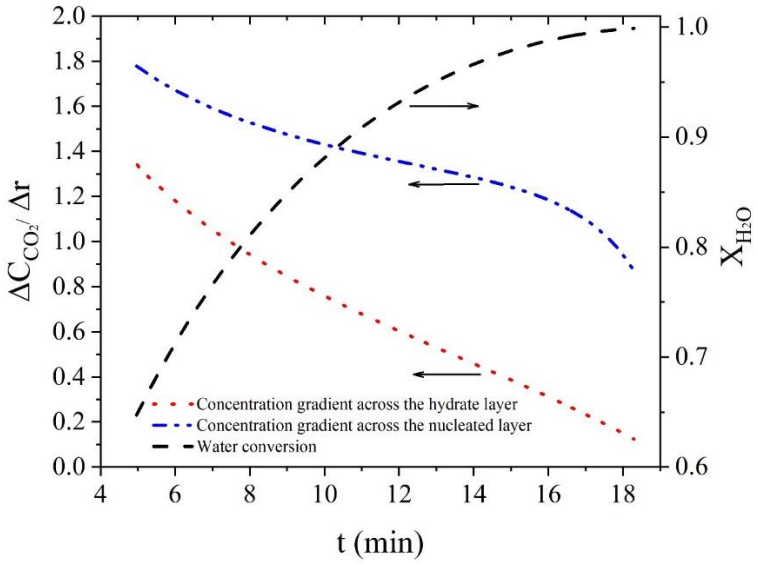

Figure 5.7. Concentration difference across the hydrate and nucleate layers and water conversion profile in Stage 2.

As the diffusivity (D_e) is supposed to be higher in the nucleate than in the hydrate, mass transfer in the hydrate is predominant in controlling the conversion rate compared to the nucleate. However, the share of the nucleate that is mass transfer resistant cannot be ignored. From this viewpoint, a detailed quantitative evaluation of each phase share is feasible through MSSCM.

5.5.4. Model-based nucleate structure identification

The nucleate configuration can be presented as $CO_2.mH_2O$ with a considerable uncertainty associated with the nucleation number value, *m*, in contrast to the hydration number, *n*, for which we use a value of 5.75 from the literature (Sun & Kang, 2016). Different nucleation numbers (m=7, 10, 15, 20) were tested in this analysis. As shown in Figure 5.8, the proposed model enables an understanding/explanation of the differences in the hydration and nucleation numbers and hence the variations in physical properties. For $m>>n$, the induction time and the nucleation stages are expected to be more distinguishable in the gas uptake profile. For $m\sim n$, the nucleation and hydration stages behave similarly in the gas consumption history, thus requiring the use of the phase distribution profiles to detect the stages and the induction time. Since all of the profile trends shown in Figure 5.8 have been observed in practical experiments, the proposed model provides judgment criteria for assessing how the formed nucleate phase deviates from the hydrate phase under the experimental condition of interest.

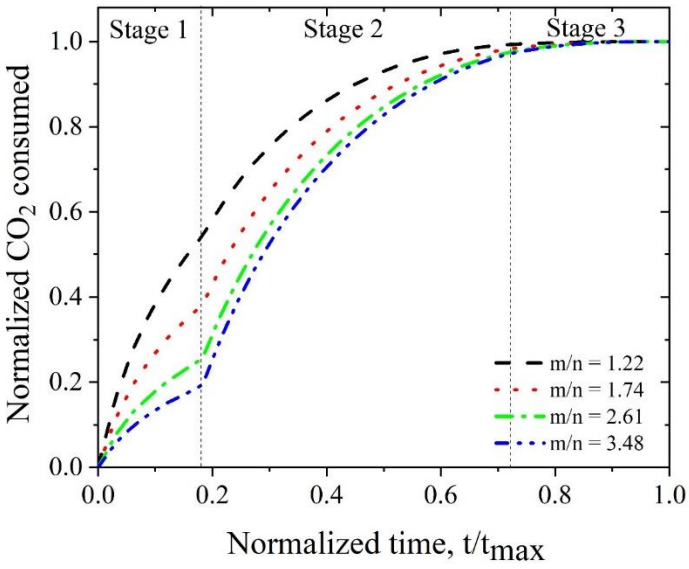

Figure 5.8. Model-based gas uptake profile for different nucleation numbers. All types of the trends shown have been observed in the experimental literature, thus indicating the diversity of possible nucleation numbers.

5.6. Conclusions

A multi-stage-multi-reaction modeling framework was proposed and successfully used for the CO_2 hydration case. Although this paper focuses on CO_2 hydrate formation, the concept is generic enough to be applied to other hydration processes, such as CH_4 hydration, with minor changes. Moreover, the model was presented for a spherical geometry but can potentially be adapted for other geometrical domains, such as slab and cylindrical geometries, depending on the reactor, pipeline, hydrodynamics regime, etc. The proposed model was capable of not only capturing the CO_2 hydration progress but also predicting nucleate phase formation and depletion. The former, in particular, is of crucial importance and enables a numerical estimation of the induction time. The induction time has been frequently observed in experimental tests. However, this study is the first to propose a model-based estimation method to predict the nucleation stage. Moreover, the model's capability in capturing the dynamic thermal behavior of the CO_2 hydration reaction was demonstrated. Based on the temperature profile, the hydration start time and progress pattern are detectable. A model-based criterion was proposed to use the experimentally measured gas uptake profiles to estimate the nucleation number, i.e., m in $CO_2 \cdot mH_2O$. The numerical estimation of the internal concentration profiles for a hydrating particle was demonstrated. The

presented model requires a minor computation time (less than a minute) using MATLAB for a single particle simulation and thus is computationally suitable for use at the reactor scale, in which enormous particles are present. The present study, therefore, provides a foundation for future research towards enhancing our understanding of gas nucleation and hydration process behavior based on predictive models at various spatiotemporal scales.

5.7. Nomenclature

C_{CO_2}	CO_2 concertation inside the particle (mol/m^3)
$C_{CO_2}^{b}$	concentration of CO_2 in gas bulk (mol/m^3)
$C_{CO_2}^{W.H}$	CO_2 concentration at the water/hydrate interface (mol/m^3)
$C_{CO_2}^{W.N}$	CO_2 concentration at the water/nucleate interface (mol/m^3)
CO_2	carbon dioxide
$C_{p,1}$	specific heat capacity in Stage 1 (kJ/kgK)
$C_{p,2}$	specific heat capacity in Stage 2 (kJ/kgK)
$C_{p,3}$	specific heat capacity in Stage 3 (kJ/kgK)
D_e	effective CO_2 diffusivity coefficient (m^2/s)
$D_{e,1}$	effective CO_2 diffusivity coefficient in Stage 1 (m^2/s)
$D_{e,2}$	effective CO_2 diffusivity coefficient in Stage 2 (m^2/s)
$D_{e,3}$	effective CO_2 diffusivity coefficient in Stage 3 (m^2/s)
h	heat transfer coefficient (kW/m^2K)
H_2O	water
k_2	reaction rate constant for Eq. (5.1) (m/s)
k_3	reaction rate constant for Eq. (5.2) (m/s)
m	nucleation number
$MW_{avg,2}$	average molecular weight in Stage 2 (g/mol)
$MW_{avg,3}$	average molecular weight in Stage 3 (g/mol)
MW_{H_2O}	molecular weight of water (g/mol)
MW_N	molecular weight of nucleate (g/mol)
n	hydration number
m	nucleation number
r	radius (m)

$r_1, r^{W.N}$	radius at water/nucleate interface (m)
$r_2, r^{N.H}$	radius at nucleate/hydrate interface (m)
r_h	rate of water conversion to hydrate (kg/m^2s)
r_N	rate of nucleate conversion to hydrate (kg/m^2s)
r_W	rate of the water conversion to nucleate (kg/m^2s)
R_p	particle radius (m)
t	time (min)
t_0	initial time (min)
t_1	time when hydrate growth starts (min)
t_2	time when fresh water is fully consumed (min)
t_3	time when nucleate is fully consumed (min)
T	temperature (K)
T_1	temperature at water/nucleate interface (K)
T_2	temperature at nucleate/hydrate interface (K)
T_b	temperature at bulk gas (K)
X_{H_2O}	water conversion

Greek Letters

ρ	density (kg/m^3)
$\rho_{avg,2}$	average density at Stage 2 (kg/m^3)
$\rho_{avg,3}$	average density at Stage 3 (kg/m^3)
ρ_N	density of nucleate (kg/m^3)
ϑ_1, ϑ_2	stoichiometry coefficient ratios
ΔH_2	reaction enthalpy in Eq. (5.2) (kJ/kg)
ΔH_3	reaction enthalpy in Eq. (5.3) (kJ/kg)

Sub-/Superscripts

b	gas bulk
CO_2	carbon dioxide
g	gaseous phase
H	hydrate
H_2O	water
N	nucleate

$N.H$	nucleate/hydrate interface
p	particle
s	solid phase
W	water
$W.N$	water/nucleate interface

5.8. References

Amiri, A., Bekker, A. V., Ingram, G. D., Livk, I., & Maynard, N. E. (2013). A 1-D non-isothermal dynamic model for the thermal decomposition of a gibbsite particle. *Chemical Engineering Research and Design, 91*(3), 485-496. doi:https://doi.org/10.1016/j.cherd.2012.10.002

Amiri, A., Ingram, G. D., Bekker, A. V., Livk, I., & Maynard, N. E. (2013). A multi-stage, multi-reaction shrinking core model for self-inhibiting gas–solid reactions. *Advanced Powder Technology, 24*(4), 728-736. doi:https://doi.org/10.1016/j.apt.2013.01.016

Amiri, A., Ingram, G. D., Maynard, N. E., Livk, I., & Bekker, A. V. (2015). An unreacted shrinking core model for calcination and similar solid-to-gas reactions. *Chemical Engineering Communications, 202*(9), 1161-1175. doi:10.1080/00986445.2014.910771

Bai, D., Chen, G., Zhang, X., & Wang, W. (2011). Microsecond molecular dynamics simulations of the kinetic pathways of gas hydrate formation from solid surfaces. *Langmuir, 27*(10), 5961-5967. doi:10.1021/la105088b

Bai, D., Chen, G., Zhang, X., & Wang, W. (2012). Nucleation of the CO_2 hydrate from three-phase contact lines. *Langmuir, 28*(20), 7730-7736. doi:10.1021/la300647s

Bergeron, S., & Servio, P. (2008). Reaction rate constant of CO_2 hydrate formation and verification of old premises pertaining to hydrate growth kinetics. *AIChE Journal, 54*(11), 2964-2970. doi:10.1002/aic.11601

Bi, Y., Porras, A., & Li, T. (2016). Free energy landscape and molecular pathways of gas hydrate nucleation. *J Chem Phys, 145*(21), 211909. doi:10.1063/1.4961241

Bollavaram, P., Devarakonda, S., Selim, M. S., & Sloan, E. D. (2000). Growth kinetics of single crystal sII hydrates: Elimination of mass and heat transfer effects. *Annals of the New York Academy of Sciences, 912*(1), 533-543. doi:10.1111/j.1749-6632.2000.tb06808.x

Chun, M.-K., & Lee, H. (1996). Kinetics of formation of carbon dioxide clathrate hydrates. *Korean Journal of Chemical Engineering, 13*(6), 620-626. doi:10.1007/bf02706029

Clarke, M. A., & Bishnoi, P. R. (2005). Determination of the intrinsic kinetics of of CO_2 gas hydrate decomposition using in-situ particle size analysis. *Chemical Engineering Science, 60*(3), 695-709. doi:10.1016/j.ces.2004.08.040

Dashti, H., & Lou, X. (2018). *Gas hydrate-based CO_2 separation process: Quantitative assessment of the effectiveness of various chemical additives involved in the process*, Cham.

Dashti, H., Zhehao Yew, L., & Lou, X. (2015). Recent advances in gas hydrate-based CO_2 capture. *Journal of Natural Gas Science and Engineering, 23*, 195-207. doi:http://dx.doi.org/10.1016/j.jngse.2015.01.033

Diamond, L. W., & Akinfiev, N. N. (2003). Solubility of CO_2 in water from −1.5 to 100 °C and from 0.1 to 100 MPa: evaluation of literature data and thermodynamic modelling. *Fluid Phase Equilibria, 208*(1), 265-290. doi:https://doi.org/10.1016/S0378-3812(03)00041-4

Englezos, P. (1993). Clathrate hydrates. *Industrial & Engineering Chemistry Research, 32*(7), 1251-1274. doi:10.1021/ie00019a001

Englezos, P., Kalogerakis, N., Dholabhai, P. D., & Bishnoi, P. R. (1987). Kinetics of formation of methane and ethane gas hydrates. *Chemical Engineering Science, 42*(11), 2647-2658. doi:http://dx.doi.org/10.1016/0009-2509(87)87015-X

English, N. J., & MacElroy, J. M. D. (2015). Perspectives on molecular simulation of clathrate hydrates: Progress, prospects and challenges. *Chemical Engineering Science, 121*, 133-156. doi:10.1016/j.ces.2014.07.047

Eslamimanesh, A., Mohammadi, A. H., Richon, D., Naidoo, P., & Ramjugernath, D. (2012). Application of gas hydrate formation in separation processes: A review of experimental studies. *The Journal of Chemical Thermodynamics, 46*, 62-71. doi:http://dx.doi.org/10.1016/j.jct.2011.10.006

Falenty, A., Salamatin, A. N., & Kuhs, W. F. (2013). Kinetics of CO_2-hydrate formation from ice powders: Data summary and modeling extended to low temperatures. *The Journal of Physical Chemistry C, 117*(16), 8443-8457. doi:10.1021/jp310972b

Hashemi, S., Macchi, A., & Servio, P. (2007). Gas hydrate growth model in a semibatch stirred tank reactor. *Industrial & Engineering Chemistry Research, 46*(18), 5907-5912. doi:10.1021/ie061048+

He, Z., Linga, P., & Jiang, J. (2017). What are the key factors governing the nucleation of CO_2 hydrate? *Phys Chem Chem Phys, 19*(24), 15657-15661. doi:10.1039/c7cp01350g

Henning, R. W., Schultz, A. J., Thieu, V., & Halpern, Y. (2000). Neutron diffraction studies of CO_2 clathrate hydrate: Formation from deuterated ice. *The Journal of Physical Chemistry A, 104*(21), 5066-5071. doi:10.1021/jp0001642

Jacobson, L. C., Hujo, W., & Molinero, V. (2010a). Amorphous precursors in the nucleation of clathrate hydrates. *Journal of the American Chemical Society, 132*(33), 11806-11811. doi:10.1021/ja1051445

Jacobson, L. C., Hujo, W., & Molinero, V. (2010b). Nucleation pathways of clathrate hydrates: Effect of guest size and solubility. *The Journal of Physical Chemistry B, 114*(43), 13796-13807. doi:10.1021/jp107269q

Khurana, M., Yin, Z., & Linga, P. (2017). A review of clathrate hydrate nucleation. *ACS Sustainable Chemistry & Engineering*. doi:10.1021/acssuschemeng.7b03238

Kvamme, B., Graue, A., Aspenes, E., Kuznetsova, T., Granasy, L., Toth, G., . . . Tegze, G. (2004). Kinetics of solid hydrate formation by carbon dioxide: Phase field

theory of hydrate nucleation and magnetic resonance imaging. *Physical Chemistry Chemical Physics, 6*(9), 2327-2334. doi:10.1039/B311202K

Lederhos, J. P., Long, J. P., Sum, A., Christiansen, R. L., & Sloan, E. D. (1996). Effective kinetic inhibitors for natural gas hydrates. *Chemical Engineering Science, 51*(8), 1221-1229. doi:https://doi.org/10.1016/0009-2509(95)00370-3

Liang, S., Liang, D., Wu, N., Yi, L., & Hu, G. (2016). Molecular Mechanisms of Gas Diffusion in CO_2 Hydrates. *The Journal of Physical Chemistry C, 120*(30), 16298-16304. doi:10.1021/acs.jpcc.6b03111

Linga, P., Kumar, R., & Englezos, P. (2007). Gas hydrate formation from hydrogen/carbon dioxide and nitrogen/carbon dioxide gas mixtures. *Chemical Engineering Science, 62*(16), 4268-4276. doi:10.1016/j.ces.2007.04.033

Lirio, C., & Pessoa, F. (2013). Enthalpy of dissociation of simple and mixed carbon dioxide clathrate hydrate. *Chemical Engineering Transactions, 32*.

Malegaonkar, M. B., Dholabhai, P. D., & Bishnoi, P. R. (1997). Kinetics of carbon dioxide and methane hydrate formation. *The Canadian Journal of Chemical Engineering, 75*(6), 1090-1099. doi:10.1002/cjce.5450750612

Mochizuki, T., & Mori, Y. H. (2006). Clathrate-hydrate film growth along water/hydrate-former phase boundaries—numerical heat-transfer study. *Journal of Crystal Growth, 290*(2), 642-652. doi:http://dx.doi.org/10.1016/j.jcrysgro.2006.01.036

Mori, Y. H. (2001). Estimating the thickness of hydrate films from their lateral growth rates: application of a simplified heat transfer model. *Journal of Crystal Growth, 223*(1), 206-212. doi:https://doi.org/10.1016/S0022-0248(01)00614-5

Mullin, J. W. (2001). Nucleation. In *Crystallization* (Fourth Edition ed., pp. 181-215). Oxford: Butterworth-Heinemann.

Natarajan, V., Bishnoi, P. R., & Kalogerakis, N. (1994). Induction phenomena in gas hydrate nucleation. *Chemical Engineering Science, 49*(13), 2075-2087. doi:https://doi.org/10.1016/0009-2509(94)E0026-M

Ou, W., Lu, W., Qu, K., Geng, L., & Chou, I. M. (2016). In situ Raman spectroscopic investigation of flux-controlled crystal growth under high pressure: A case study of carbon dioxide hydrate growth in aqueous solution. *International Journal of Heat and Mass Transfer, 101*, 834-843. doi:10.1016/j.ijheatmasstransfer.2016.05.082

Radhakrishnan, R., & Trout, B. L. (2002). A new approach for studying nucleation phenomena using molecular simulations: Application to CO_2 hydrate clathrates. *The Journal of Chemical Physics, 117*(4), 1786-1796. doi:10.1063/1.1485962

Ribeiro Jr, C. P., & Lage, P. L. C. (2008). Modelling of hydrate formation kinetics: State-of-the-art and future directions. *Chemical Engineering Science, 63*(8), 2007-2034. doi:http://dx.doi.org/10.1016/j.ces.2008.01.014

Ripmeester, J. A., & Alavi, S. (2016). Some current challenges in clathrate hydrate science: Nucleation, decomposition and the memory effect. *Current Opinion in Solid State and Materials Science, 20*(6), 344-351. doi:10.1016/j.cossms.2016.03.005

Robinson, D. B., & Peng, D.-Y. (1978). *The characterization of the heptanes and heavier fractions for the GPA Peng-Robinson programs*. Tulsa, Okla.: Gas Processors Association.

Selim, M. S., & Sloan, E. D. (1989). Heat and mass transfer during the dissociation of hydrates in porous media. *AIChE Journal, 35*(6), 1049-1052. doi:10.1002/aic.690350620

Shi, B.-H., Fan, S.-S., & Lou, X. (2014). Application of the shrinking-core model to the kinetics of repeated formation of methane hydrates in a system of mixed dry-water and porous hydrogel particulates. *Chemical Engineering Science, 109*, 315-325. doi:http://dx.doi.org/10.1016/j.ces.2014.01.035

Shi, B.-H., Gong, J., Sun, C.-Y., Zhao, J.-K., Ding, Y., & Chen, G.-J. (2011). An inward and outward natural gas hydrates growth shell model considering intrinsic kinetics, mass and heat transfer. *Chemical Engineering Journal, 171*(3), 1308-1316. doi:http://dx.doi.org/10.1016/j.cej.2011.05.029

Shi, B.-H., Yang, L., Fan, S.-S., & Lou, X. (2017). An investigation on repeated methane hydrates formation in porous hydrogel particles. *Fuel, 194*, 395-405. doi:10.1016/j.fuel.2017.01.037

Skovborg, P., Ng, H. J., Rasmussen, P., & Mohn, U. (1993). Measurement of induction times for the formation of methane and ethane gas hydrates. *Chemical Engineering Science, 48*(3), 445-453. doi:https://doi.org/10.1016/0009-2509(93)80299-6

Sloan, E. D., & Koh, C. A. (2008). *Clathraye Hydrates of Natural Gases* (third ed. Vol. 119). New York: Taylor & Francis Group.

Staykova, D. K., Kuhs, W. F., Salamatin, A. N., & Hansen, T. (2003). Formation of porous gas hydrates from ice powders: Diffraction experiments and multistage model. *The Journal of Physical Chemistry B, 107*(37), 10299-10311. doi:10.1021/jp027787v

Sun, Q., & Kang, Y. T. (2016). Review on CO_2 hydrate formation/dissociation and its cold energy application. *Renewable and Sustainable Energy Reviews, 62*, 478-494. doi:10.1016/j.rser.2016.04.062

Teng, H., Kinoshita, C. M., & Masutani, S. M. (1995). Hydrate formation on the surface of a CO_2 droplet in high-pressure, low-temperature water. *Chemical Engineering Science, 50*(4), 559-564. doi:https://doi.org/10.1016/0009-2509(94)00438-W

Uchida, T., Ebinuma, T., Kawabata, J. i., & Narita, H. (1999). Microscopic observations of formation processes of clathrate-hydrate films at an interface between water and carbon dioxide. *Journal of Crystal Growth, 204*(3), 348-356. doi:http://dx.doi.org/10.1016/S0022-0248(99)00178-5

Uddin, M., Coombe, D., Law, D., & Gunter, B. (2008). Numerical studies of gas hydrate formation and decomposition in a geological reservoir. *Journal of Energy Resources Technology, 130*(3), 032501-032501-032514. doi:10.1115/1.2956978

Vatamanu, J., & Kusalik, P. G. (2010). Observation of two-step nucleation in methane hydrates. *Phys Chem Chem Phys, 12*(45), 15065-15072. doi:10.1039/c0cp00551g

Verrett, J., & Servio, P. (2016). Reaction rate constant of CO_2-Tetra-n-butylammounium bromide semi-clathrate formation. *The Canadian Journal of Chemical Engineering, 94*(11), 2138-2144. doi:10.1002/cjce.22612

Vysniauskas, A., & Bishnoi, P. R. (1983). A kinetic study of methane hydrate formation. *Chemical Engineering Science, 38*(7), 1061-1072. doi:https://doi.org/10.1016/0009-2509(83)80027-X

Walsh, M. R., Beckham, G. T., Koh, C. A., Sloan, E. D., Wu, D. T., & Sum, A. K. (2011). Methane hydrate nucleation rates from molecular dynamics simulations: Effects of aqueous methane concentration, interfacial curvature, and system size. *The Journal of Physical Chemistry C, 115*(43), 21241-21248. doi:10.1021/jp206483q

Yang, D., Le, L. A., Martinez, R. J., Currier, R. P., & Spencer, D. F. (2011). Kinetics of CO_2 hydrate formation in a continuous flow reactor. *Chemical Engineering Journal, 172*(1), 144-157. doi:10.1016/j.cej.2011.05.082

Yin, Z., Khurana, M., Tan, H. K., & Linga, P. (2018). A review of gas hydrate growth kinetic models. *Chemical Engineering Journal, 342*, 9-29. doi:10.1016/j.cej.2018.01.120

Appendix A. Model derivation

Stage 1:

The CO_2 molar rate due to the reaction in the nucleate-hydrate interface is:

$$M_{r,1} = 4\pi {r_1}^2 \vartheta_1 k_2 C_{CO_2}^{W.N} \quad (A.5.1)$$

in which $M_{r,1}$ is the CO_2 molar reaction rate at Stage 1. Using Fick's law, the rate of the CO_2 diffusion is given by:

$$M_{d,1} = 4\pi r^2 D_{e,1} \frac{dC_{CO_2}^{W.N}}{dr} \quad (A.5.2)$$

where $M_{d,1}$ is the CO_2 diffusion rate at Stage 1. Integrating from r_1 to R_p and $C_{CO_2}^{W.N}$ to $C_{CO_2}^{b}$:

$$M_{d,1} \int_{r_1}^{R_p} \frac{1}{r^2}\, dr = -4\pi D_{e,1} \int_{C_{CO_2}^{W.N}}^{C_{CO_2}^{b}} dC_{CO_2} \quad (A.5.3)$$

or

$$M_{d,1} \left(\frac{1}{R_p} - \frac{1}{r_1}\right) = 4\pi D_{e,1} (C_{CO_2}^{b} - C_{CO_2}^{W.N}) \quad (A.5.4)$$

or

$$M_{d,1} = 4\pi D_{e,1} \frac{(C_{CO_2}^{b} - C_{CO_2}^{W.N})}{\frac{1}{r_1} - \frac{1}{R_p}} \quad (A.5.5)$$

Diffusion of CO_2 through the nucleate layer is equal to the CO_2 reaction in the water/nucleate interface:

$$M_{r,1} = M_{d,1} \quad (A.5.6)$$

or

$$4\pi {r_1}^2 \vartheta_1 k_2 C_{CO_2}^{W.N} = 4\pi D_{e,1} \frac{(C_{CO_2}^{b} - C_{CO_2}^{W.N})}{\frac{1}{r_1} - \frac{1}{R_p}} \quad (A.5.7)$$

or

$$C_{CO_2}^{b} - C_{CO_2}^{W.N} - \frac{{r_1}^2 \vartheta_1 k_2 C_{CO_2}^{W.N} \left(\frac{1}{r_1} - \frac{1}{R_p}\right)}{D_{e,1}} = 0 \quad (A.5.8)$$

or

$$C_{CO_2}^{b}\text{-}C_{CO_2}^{W.N}\left(1+\frac{{r_1}^2\vartheta_1 k_2\left(\frac{1}{r_1}\text{-}\frac{1}{R_p}\right)}{D_{e,1}}\right)=0 \qquad \text{(A.5.9)}$$

or

$$1\text{-}\frac{C_{CO_2}^{W.N}}{C_{CO_2}^{b}}\left(1+\frac{{r_1}^2\vartheta_1 k_2\left(\frac{1}{r_1}\text{-}\frac{1}{R_p}\right)}{D_{e,1}}\right)=0 \qquad \text{(A.5.10)}$$

or

$$1\text{-}\frac{C_{CO_2}^{W.N}}{C_{CO_2}^{b}}\left(1+\frac{\vartheta_1 k_2 R_p}{D_{e,1}}\left(\frac{r_1}{R_p}\right)^2\left(\frac{1}{\left(\frac{r_1}{R_p}\right)}\text{-}1\right)\right)=0 \qquad \text{(A.5.11)}$$

Water consumption rate is given by:

$$N_{H_2O}=\text{-}\frac{d}{dt}\left(\frac{4}{3}\frac{\pi r_1^3\rho_{H_2O}}{MW_{H_2O}}\right) \qquad \text{(A.5.12)}$$

in which N_{H_2O} is the water consumption rate. The relation between the water conversion and molar rate due to the reaction is:

$$N_{H_2O}=\frac{1}{\vartheta_1}M_{r,1} \qquad \text{(A.5.13)}$$

Combining eq (A12 and A13) results in:

$$\frac{dr_1}{dt}=\text{-}\frac{MW_{H_2O}}{\rho_{H_2O}}k_2 C_{CO_2}^{W.N} \qquad \text{(A.5.14)}$$

Non-isothermal equations in Stage 1:

Non-isothermal equations are based on the energy balance around the particle at each stage:

$$\frac{4}{3}\frac{\pi R_p^3\rho_{H_2O}}{MW_{H_2O}}C_{p,1}\frac{dT}{dt}=4\pi R_p^2 h(T_b\text{-}T)\text{-}4\pi r_1^2 k_2 C_{CO_2}^{W.N}\Delta H_2 \qquad \text{(A.5.15)}$$

or

$$\frac{dT}{dt}=\frac{h(T_b\text{-}T)\text{-}\left(\frac{r_1}{R_p}\right)^2 k_2\Delta H_2 C_{CO_2}^{W.N}}{\frac{R_p\rho_{H_2O}}{3MW_{H_2O}}C_{p,1}} \qquad \text{(A.5.16)}$$

Stage 2:

CO_2 reaction rate at the water-nucleate interface is:

$$M_{r,2} = 4\pi r_1^2 \vartheta_1 k_2 C_{CO_2}^{W.N} \quad \text{(A.5.17)}$$

where $M_{r,2}$ is the CO_2 reaction rate at the water-nucleate interface at Stage 2. CO_2 diffusion rate at the water-nucleate interface is given by:

$$M_{d,2} = -4\pi r_1^2 D_{e,2} \frac{dC_{CO_2}^{W.N}}{dr} \quad \text{(A.5.18)}$$

in which $M_{d,2}$ is the CO_2 diffusion rate between the water-nucleate interface and nucleate-hydrate interface at Stage 2. Or:

$$M_{d,2} = 4\pi D_{e,2} \frac{(C_{CO_2}^{N.H} - C_{CO_2}^{W.N})}{\frac{1}{r_1} - \frac{1}{r_2}} \quad \text{(A.5.19)}$$

CO_2 diffusion rate is equal to CO_2 reaction rate:

$$M_{r,2} = M_{d,2} \quad \text{(A.5.20)}$$

or

$$C_{CO_2}^{N.H} - C_{CO_2}^{W.N} - \frac{r_1^2 \vartheta_1 k_2 C_{CO_2}^{W.N}}{D_{e,2}} \left(\frac{1}{r_1} - \frac{1}{r_2}\right) \quad \text{(A.5.21)}$$

or

$$\frac{C_{CO_2}^{N.H}}{C_{CO_2}^{b}} - \frac{C_{CO_2}^{W.N}}{C_{CO_2}^{b}} \left(1 + \frac{\vartheta_1 k_2 R_p}{D_{e,2}} \left(\frac{r_1}{R_p}\right)^2 \left(\frac{1}{\left(\frac{r_1}{R_p}\right)} - \frac{1}{\left(\frac{r_2}{R_p}\right)}\right)\right) = 0 \quad \text{(A.5.22)}$$

Water consumtion is given by:

$$N'_{H_2O} = -\frac{d}{dt}\left(\frac{4}{3}\frac{\pi r_1^3 \rho_{H_2O}}{MW_{H_2O}}\right) \quad \text{(A.5.23)}$$

in which N'_{H_2O} is water consumption at Stage 2. The relation between the water conversion and molar rate due to the reaction is:

$$N'_{H_2O} = \frac{1}{\vartheta_1} M_{r,2} \quad \text{(A.5.24)}$$

or

$$\frac{dr_1}{dt} = -\frac{MW_{H_2O}}{\rho_{H_2O}} k_2 C_{CO_2}^{W.N} \quad \text{(A.5.25)}$$

CO_2 Diffusion rate through the nucleate layer is given by:

$$M'_{d,2} = 4\pi D_{e,2} \frac{\left(C_{CO_2}^{b} - C_{CO_2}^{N.H}\right)}{\frac{1}{r_2} - \frac{1}{R_p}} \quad \text{(A.5.26)}$$

where $M'_{d,2}$ is the CO_2 diffusion rate between bulk CO_2 and nucleate-hydrate layer. CO_2 reaction rate at the nucleate-hydrate interface is:

$$M_N = 4\pi r_2^2 \vartheta_2 k_3 C_{CO_2}^{N.H} \quad \text{(A.5.27)}$$

in which M_N is the CO_2 reaction rate at the nucleate-hydrate interface. Mass balance around the particle at Stage 2 is:

$$M'_{d,2} = M_{r,2} + M_N \quad \text{(A.5.28)}$$

or

$$C_{CO_2}^{b} - C_{CO_2}^{N.H} - \frac{r_1{}^2 \vartheta_1 k_2 C_{CO_2}^{W.N} + r_2^2 \vartheta_2 k_3 C_{CO_2}^{N.H}}{D_{e,2}} \left(\frac{1}{r_2} - \frac{1}{R_p}\right) = 0 \quad \text{(A.5.29)}$$

or

$$1 - \frac{C_{CO_2}^{N.H}}{C_{CO_2}^{b}} - \left(\frac{\vartheta_1 k_2 R_p}{D_{e,2}} \frac{C_{CO_2}^{W.N}}{C_{CO_2}^{b}} \left(\frac{r_1}{R_p}\right)^2 + \frac{\vartheta_2 k_3 R_p}{D_{e,2}} \frac{C_{CO_2}^{N.H}}{C_{CO_2}^{b}} \left(\frac{r_2}{R_p}\right)^2\right) \left(\frac{1}{\left(\frac{r_2}{R_p}\right)} - 1\right) = 0 \quad \text{(A.5.30)}$$

The rate of nucleate consumption is given by:

$$N_N = -\frac{d}{dt}\left(\frac{4}{3}\frac{\pi r_2^3 \rho_N}{MW_N}\right) \quad \text{(A.5.31)}$$

in which N_N is the rate of nucleate consumption. The relation between the rate of nucleate consumption and reaction at the nucleate-hydrate interface is:

$$N_N = \frac{1}{\vartheta_2} M_N \quad \text{(A.5.32)}$$

or

$$\frac{dr_2}{dt} = -\frac{MW_N}{\rho_N} k_3 C_{CO_2}^{b} \frac{C_{CO_2}^{N.H}}{C_{CO_2}^{b}} \quad \text{(A.5.33)}$$

Non-isothermal equations in Stage 2:

An energy balance around the particle at Stage 2 is given by:

$$\frac{4}{3}\frac{\pi R_p^3 \rho_{avg,2}}{MW_{avg,2}} C_{p,2} \frac{dT}{dt} = 4\pi R_p^2 h(T_b\text{-}T) - 4\pi r_1^2 k_2 C_{CO_2}^{W.N} \Delta H_2 - 4\pi r_2^2 k_3 C_{CO_2}^{N.H} \Delta H_3 \quad (A.5.34)$$

or

$$\frac{dT}{dt} = \frac{h(T_b\text{-}T) - \left(\frac{r_1}{R_p}\right)^2 k_2 \Delta H_2 C_{CO_2}^{W.N} - \left(\frac{r_2}{R_p}\right)^2 k_3 \Delta H_3 C_{CO_2}^{N.H}}{\frac{R\rho_{avg,2}}{3MW_{avg,2}} C_{p,2}} \quad (A.5.35)$$

Stage 3:

CO_2 reaction rate at the nucleate-hydrate interface is:

$$M_{r,3} = 4\pi {r_2}^2 \vartheta_2 k_3 C_{CO_2}^{N.H} \quad (A.5.36)$$

where $M_{r,3}$ is the CO_2 reaction rate at the nucleate-hydrate interface at Stage 3. CO_2 diffusion rate at Stage 3 is given by:

$$M_{d,3} = 4\pi D_{e,3} \frac{(C_{CO_2}^{b} - C_{CO_2}^{N.H})}{\frac{1}{r_2} - \frac{1}{R_p}} \quad (A.5.37)$$

in which $M_{d,3}$ is the CO_2 diffusion rate between bulk CO_2 and nucleate-hydrate interface. CO_2 rate of the reaction is equal to the rate of the diffusion:

$$M_{r,3} = M_{d,3} \quad (A.5.38)$$

or

$$C_{CO_2}^{b} - C_{CO_2}^{N.H} - \frac{{r_2}^2 \vartheta_2 k_3 C_{CO_2}^{W.N} \left(\frac{1}{r_2} - \frac{1}{R_p}\right)}{D_{e,3}} = 0 \quad (A.5.39)$$

or

$$1 - \frac{C_{CO_2}^{N.H}}{C_{CO_2}^{b}} \left(1 + \frac{\vartheta_2 k_3 R_p}{D_{e,3}} \left(\frac{r_2}{R_p}\right)^2 \left(\frac{1}{\left(\frac{r_2}{R_p}\right)} - 1\right)\right) = 0 \quad (A.5.40)$$

The rate of nucleate consumption is given by:

$$N_N^{'} = -\frac{d}{dt}\left(\frac{4}{3}\frac{\pi r_2^3 \rho_N}{MW_N}\right) \quad (A.5.41)$$

where $N_N^{'}$ is the rate of nucleate consumption at Stage 3. The relation between nucleate consumption and reaction rate in Stage 3 is:

$$N_N^{'} = \frac{1}{\vartheta_2} M_{r,3} \tag{A.5.42}$$

or

$$\frac{dr_2}{dt} = -\frac{MW_N}{\rho_N} k_3 C_{CO_2}^b \frac{C_{CO_2}^{N.H}}{C_{CO_2}^b} \tag{A.5.43}$$

Non-isothermal equations in Stage 3:

An energy balance around the particle at stage 3 is given by:

$$\frac{4}{3}\frac{\pi R_p^3 \rho_{avg,3}}{MW_{avg,3}} C_{p,3} \frac{dT}{dt} = 4\pi R_p^2 h(T_b - T) - 4\pi r_2^2 k_3 C_{CO_2}^{N.H} \Delta H_2 \tag{A.5.44}$$

or

$$\frac{dT}{dt} = \frac{h(T_b - T) - \left(\frac{r_2}{R_p}\right)^2 k_3 \Delta H_3 C_{CO_2}^{N.H}}{\frac{R_p \rho_{avg,3}}{3 MW_{avg,3}} C_{p,3}} \tag{A.5.45}$$

Chapter 6. Overall conclusions and future works

Kinetics modeling of gas hydrate formation for CO_2 hydrates has been studied in this thesis.

First, a conceptual framework for modeling and evaluating the process level of the HBCC was proposed and developed. The model estimated the required energy at various stages of the HBCC process, including cooling, compression, formation and dissociation. The application of the model in the presence of chemical additives was examined. The results provide a new quantitative method for analyzing the effectiveness of various chemical additives in relation to the energy consumption of the HBCC process, as well as kinetic parameters such as the rates of formation and dissociation. Among chemical additives, THF enabled the most significant reduction of energy consumption in all stages. Furthermore, the compression energy has the most significant effects on the total energy required for the HBCC process.

Second, this research provided particle-level modeling of the HBCC process using an effective predictive kinetics model. The dominant controlling mechanism during gas hydrate formation was determined using a novel variation of SCM. The proposed model was improved by considering the transient CO_2 concentration in the bulk gas. While the diffusion-based model reasonably predicts the CO_2 hydration rate under a constant bulk gas concentration condition, for the realistic scenario in which the bulk gas varies with time, the model must consider the reaction control role as well.

Finally, using a multi-stage-multi-reaction modeling approach, the HBCC process was modeled and validated with a greater emphasis on the nucleation and growth stages. This analysis is the first to use a model-based method to estimate both the nucleation and growth stages. The capability of the model to capture the dynamic thermal behavior of the hydration reaction was illustrated. Furthermore, a non-isothermal model of gas hydrate formation was developed, and the results of the temperature profile estimation showed the same pattern observed in experimental studies. In further analysis of the model, a model-based criterion was proposed for the first time to use the experimentally measured gas uptake profiles to estimate the nucleation number, i.e., m in $CO_2 \cdot mH_2O$. Furthermore, the numerical estimation of the internal concentration profiles for a hydrating particle was proposed and demonstrated.

This thesis lays the foundation for a range of future research studies that may be of interest to the scientific community:

- To make the technology more economically feasible at the industrial scale, the design of chemical additives should focus on those that can significantly reduce the operating pressure and, therefore, decrease the compression energy and the operation cost. Therefore, further research on the design of chemical additives with these capabilities is essential.
- Although this thesis has focused on CO_2 hydrate formation, the concept is generic enough to be applied to other hydration processes, such as CH_4, subject to minor changes. Moreover, the model presented for a spherical geometry can potentially be adapted for other geometrical domains, such as slab and cylindrical geometries, depending on the hydrodynamic regime of the reactor.
- Further optimization methods are required to find optimal physicochemical properties, such as the effective diffusivity coefficient and reaction constant rate, in the multi-stage kinetics model for different gas hydrates.
- In the multistage model, some assumptions have been applied in the model that can be improved in further research:
    - The droplets are initially considered to be spherical with a constant radius, which can be improved by using different radii in future studies.
    - In this model, it is assumed that all water molecules are ideally converted into the hydrates, which is an ideal situation and needs to be adapted with real experiments.
    - The particle model should be integrated with the reactor.
    - Further experimental studies focused on the nucleation process are needed to train the model for more precise induction times and nucleation behavior estimations.
    - The experimental research work has been a continuing topic in the group. The study on the low characteristic of the hydrates slurry is indeed important for the future application of the HBCC.

Statement of contribution

Paper #1: Recent advances in gas hydrate-based CO_2 capture. Journal of Natural Gas Science and Engineering. 2015 Mar 1; 23:195-207.

Co-author	Conception & design	Acquisition of data & method	Analysis & statistical method	Interpretation & discussion	Final approval
Leonel Zhehao Yew	×	×	×	×	×
I acknowledge that these represent my contribution to the above research output. 					
Xia Lou (Supervisor)	×	×	×	×	×
I acknowledge that these represent my contribution to the above research output.					

Paper #2: Gas Hydrate-Based CO_2 Separation Process: Quantitative Assessment of the Effectiveness of Various Chemical Additives Involved in the Process. In Energy Technology 2018, Carbon Dioxide Management and Other Technologies, 3-16, Springer.

Co-author	Conception & design	Acquisition of data & method	Analysis & statistical method	Interpretation & discussion	Final approval
Xia Lou (Supervisor)	×	×	×	×	×
I acknowledge that these represent my contribution to the above research output.					

Paper #3: Variations to the shrinking core model for effective kinetics modelling of the gas hydrate-based CO_2 process. Computer Aided Chemical Engineering. 2019, Elsevier.

Co-author	Conception & design	Acquisition of data & method	Analysis & statistical method	Interpretation & discussion	Final approval
Daniel Thomas	×	×	×		
I acknowledge that these represent my contribution to the above research output. 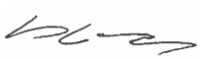					
Amirpiran Amiri	×	×	×	×	×
I acknowledge that these represent my contribution to the above research output. 					
Xia Lou (Supervisor)			×	×	×
I acknowledge that these represent my contribution to the above research output.					

Paper #4: Modeling and analysis of hydrate-based CO_2 capture with nucleation stage prediction capability, The Journal of Cleaner Production. 2019; 231: 805-816, Elsevier.

Co-author	Conception & design	Acquisition of data & method	Analysis & statistical method	Interpretation & discussion	Final approval
Daniel Thomas	×	×	×		
I acknowledge that these represent my contribution to the above research output. 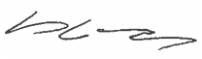					
Amirpiran Amiri	×	×	×	×	×
I acknowledge that these represent my contribution to the above research output. 					

Copyright permission

The following pages contain the right granted by Elsevier to the first author of the publication (Chapter 2 and 5) to represent the contribution in this thesis as well as right granted by Springer to the first author of the publication (Chapter 3).

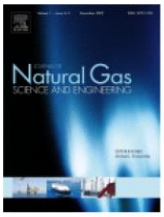

Title: Recent advances in gas hydrate-based CO2 capture

Author: Hossein Dashti,Leonel Zhehao Yew,Xia Lou

Publication: Journal of Natural Gas Science and Engineering

Publisher: Elsevier

Date: March 2015

SPRINGER NATURE LICENSE TERMS AND CONDITIONS

Dec 05, 2018

This Agreement between Mr. Hossein Dashti ("You") and Springer Nature ("Springer Nature") consists of your license details and the terms and conditions provided by Springer Nature and Copyright Clearance Center.

License Number	4482351342107
License date	Dec 05, 2018
Licensed Content Publisher	Springer Nature
Licensed Content Publication	Springer eBook
Licensed Content Title	Gas Hydrate-Based CO2 Separation Process: Quantitative Assessment of the Effectiveness of Various Chemical Additives Involved in the Process
Licensed Content Author	Hossein Dashti, Xia Lou
Licensed Content Date	Jan 1, 2018
Type of Use	Thesis/Dissertation
Requestor type	academic/university or research institute
Format	electronic
Portion	full article/chapter
Will you be translating?	no
Circulation/distribution	<501
Author of this Springer Nature content	yes
Title	CO2 Capture using Gas hydrates Technology
Institution name	Curtin University
Expected presentation date	Jan 2019
Requestor Location	Mr. Hossein Dashti Curtin University Perth, 6102 Australia Attn: Mr. Hossein Dashti
Billing Type	Invoice
Billing Address	Mr. Hossein Dashti Curtin University Perth, Australia 6102 Attn: Mr. Hossein Dashti
Total	0.00 AUD
Terms and Conditions	

Springer Nature Terms and Conditions for RightsLink Permissions

Springer Nature Customer Service Centre GmbH (the Licensor) hereby grants you a non-exclusive, world-wide licence to reproduce the material and for the purpose and requirements specified in the attached copy of your order form, and for no other use, subject to the conditions below:

1. The Licensor warrants that it has, to the best of its knowledge, the rights to license reuse of this material. However, you should ensure that the material you are requesting is original to the Licensor and does not carry the copyright of another entity (as credited in the published version).

   If the credit line on any part of the material you have requested indicates that it was reprinted or adapted with permission from another source, then you should also seek permission from that source to reuse the material.

2. Where **print only** permission has been granted for a fee, separate permission must be obtained for any additional electronic re-use.

3. Permission granted **free of charge** for material in print is also usually granted for any electronic version of that work, provided that the material is incidental to your work as a whole and that the electronic version is essentially equivalent to, or substitutes for, the print version.

4. A licence for 'post on a website' is valid for 12 months from the licence date. This licence does not cover use of full text articles on websites.

5. Where **'reuse in a dissertation/thesis'** has been selected the following terms apply: Print rights of the final author's accepted manuscript (for clarity, NOT the published version) for up to 100 copies, electronic rights for use only on a personal website or institutional repository as defined by the Sherpa guideline (www.sherpa.ac.uk/romeo/).

6. Permission granted for books and journals is granted for the lifetime of the first edition and does not apply to second and subsequent editions (except where the first edition permission was granted free of charge or for signatories to the STM Permissions Guidelines http://www.stm-assoc.org/copyright-legal-affairs/permissions/permissions-guidelines/), and does not apply for editions in other languages unless additional translation rights have been granted separately in the licence.

7. Rights for additional components such as custom editions and derivatives require additional permission and may be subject to an additional fee. Please apply to Journalpermissions@springernature.com/bookpermissions@springernature.com for these rights.

8. The Licensor's permission must be acknowledged next to the licensed material in print. In electronic form, this acknowledgement must be visible at the same time as the figures/tables/illustrations or abstract, and must be hyperlinked to the journal/book's homepage. Our required acknowledgement format is in the Appendix below.

9. Use of the material for incidental promotional use, minor editing privileges (this does not include cropping, adapting, omitting material or any other changes that affect the meaning, intention or moral rights of the author) and copies for the disabled are permitted under this licence.

10. Minor adaptations of single figures (changes of format, colour and style) do not require the Licensor's approval. However, the adaptation should be credited as shown in Appendix below.

Appendix — Acknowledgements:

For Journal Content:
Reprinted by permission from [**the Licensor**]: [**Journal Publisher** (e.g. Nature/Springer/Palgrave)] [**JOURNAL NAME**] [**REFERENCE CITATION** (Article name, Author(s) Name), [**COPYRIGHT**] (year of publication)

For **Advance Online Publication papers:**
Reprinted by permission from [**the Licensor**]: [**Journal Publisher** (e.g. Nature/Springer/Palgrave)] [**JOURNAL NAME**] [**REFERENCE CITATION** (Article name, Author(s) Name), [**COPYRIGHT**] (year of publication), advance online publication, day month year (doi: 10.1038/sj.[JOURNAL ACRONYM].)

For Adaptations/Translations:
Adapted/Translated by permission from [**the Licensor**]: [**Journal Publisher** (e.g. Nature/Springer/Palgrave)] [**JOURNAL NAME**] [**REFERENCE CITATION** (Article name, Author(s) Name), [**COPYRIGHT**] (year of publication)

Note: For any republication from the British Journal of Cancer, the following credit line style applies:

Reprinted/adapted/translated by permission from [**the Licensor**]: on behalf of Cancer Research UK: : [**Journal Publisher** (e.g. Nature/Springer/Palgrave)] [**JOURNAL NAME**] [**REFERENCE CITATION** (Article name, Author(s) Name), [**COPYRIGHT**] (year of publication)

For **Advance Online Publication** papers:
Reprinted by permission from The [**the Licensor**]: on behalf of Cancer Research UK: [**Journal Publisher** (e.g. Nature/Springer/Palgrave)] [**JOURNAL NAME**] [**REFERENCE CITATION** (Article name, Author(s) Name), [**COPYRIGHT**] (year of publication), advance online publication, day month year (doi: 10.1038/sj. [JOURNAL ACRONYM])

For Book content:
Reprinted/adapted by permission from [**the Licensor**]: [**Book Publisher** (e.g. Palgrave Macmillan, Springer etc) [**Book Title**] by [**Book author**(s)] [**COPYRIGHT**] (year of publication)

Other Conditions:

Version 1.1

Questions? customercare@copyright.com or +1-855-239-3415 (toll free in the US) or +1-978-646-2777.

Bibliography

Aaron, D., & Tsouris, C. (2005). Separation of CO_2 from Flue Gas: A Review. Separation Science and Technology, 40(1-3), 321-348. doi: 10.1081/ss-200042244

Amiri, A., Bekker, A. V., Ingram, G. D., Livk, I., & Maynard, N. E. (2013). A 1-D non-isothermal dynamic model for the thermal decomposition of a gibbsite particle. Chemical Engineering Research and Design, 91(3), 485-496. doi:https://doi.org/10.1016/j.cherd.2012.10.002

Amiri, A., Ingram, G. D., Bekker, A. V., Livk, I., & Maynard, N. E. (2013). A multi-stage, multi-reaction shrinking core model for self-inhibiting gas–solid reactions. Advanced Powder Technology, 24(4), 728-736. doi:https://doi.org/10.1016/j.apt.2013.01.016

Amiri, A., Ingram, G. D., Maynard, N. E., Livk, I., & Bekker, A. V. (2015). An unreacted shrinking core model for calcination and similar solid-to-gas reactions. Chemical Engineering Communications, 202(9), 1161-1175. doi:10.1080/00986445.2014.910771

Adeyemo, A., Kumar, R., Linga, P., Ripmeester, J., & Englezos, P. (2010). Capture of carbon dioxide from flue or fuel gas mixtures by clathrate crystallization in a silica gel column. International Journal of Greenhouse Gas Control, 4(3), 478-485. doi: http://dx.doi.org/10.1016/j.ijggc.2009.11.011

Adisasmito, S., & Sloan, E. D. (1992). Hydrates of hydrocarbon gases containing carbon dioxide. Journal of Chemical & Engineering Data, 37(3), 343-349. doi: 10.1021/je00007a020

Arjmandi, M., Chapoy, A., & Tohidi, B. (2007). Equilibrium Data of Hydrogen, Methane, Nitrogen, Carbon Dioxide, and Natural Gas in Semi-Clathrate Hydrates of Tetrabutyl Ammonium Bromide. Journal of Chemical & Engineering Data, 52(6), 2153-2158. doi: 10.1021/je700144p

Audus, H. (1997). Greenhouse gas mitigation technology: An overview of the CO_2 capture and sequestration studies and further activities of the IEA Greenhouse Gas R&D Programme. Energy, 22(2–3), 217-221. doi: http://dx.doi.org/10.1016/S0360-5442(96)00107-7

Babu, P., Kumar, R., & Linga, P. (2013). Pre-combustion capture of carbon dioxide in a fixed bed reactor using the clathrate hydrate process. Energy, 50, 364-373. doi: 10.1016/j.energy.2012.10.046

Babu, P., Yang, T., Veluswamy, H. P., Kumar, R., & Linga, P. (2013). Hydrate phase equilibrium of ternary gas mixtures containing carbon dioxide, hydrogen and propane. The Journal of Chemical Thermodynamics, 61, 58-63. doi: 10.1016/j.jct.2013.02.003

Bai, D., Chen, G., Zhang, X., & Wang, W. (2011). Microsecond molecular dynamics simulations of the kinetic pathways of gas hydrate formation from solid surfaces. Langmuir, 27(10), 5961-5967. doi:10.1021/la105088b

Bai, D., Chen, G., Zhang, X., & Wang, W. (2012). Nucleation of the CO_2 hydrate from three-phase contact lines. Langmuir, 28(20), 7730-7736. doi:10.1021/la300647s

Belandria, V., Mohammadi, A. H., Eslamimanesh, A., Richon, D., Sánchez-Mora, M. F., & Galicia-Luna, L. A. (2012). Phase equilibrium measurements for semi-

clathrate hydrates of the (CO_2+N_2+tetra-n-butylammonium bromide) aqueous solution systems: Part 2. Fluid Phase Equilibria, 322-323, 105-112. doi: 10.1016/j.fluid.2012.02.020

Belandria, V., Mohammadi, A. H., & Richon, D. (2012). Compositional analysis of the gas phase for the CO_2+N_2+tetra-n-butylammonium bromide aqueous solution systems under hydrate stability conditions. Chemical Engineering Science, 84, 40-47. doi: 10.1016/j.ces.2012.07.027

Ben-Mansour, R., Habib, M.A., Bamidele, O.E., Basha, M., Qasem, N.A.A., Peedikakkal, A., Laoui, T., Ali, M. (2016). Carbon capture by physical adsorption: Materials, experimental investigations and numerical modeling and simulations–A review. Appl. Energy 161, 225-255.

Bert Metz, Davidson, O., Heleen de Coninck, Manuela Loos, & Meyer, L. (2005). Carbon Dioxide Capture and Storage.

Bounaceur, R., Lape, N., Roizard, D., Vallieres, C., & Favre, E. (2006). Membrane processes for post-combustion carbon dioxide capture: A parametric study. Energy, 31(14), 2556-2570. doi: 10.1016/j.energy.2005.10.038

Bergeron, S., & Servio, P. (2008). Reaction rate constant of CO_2 hydrate formation and verification of old premises pertaining to hydrate growth kinetics. AIChE Journal, 54(11), 2964-2970. doi:10.1002/aic.11601

Bi, Y., Porras, A., & Li, T. (2016). Free energy landscape and molecular pathways of gas hydrate nucleation. J Chem Phys, 145(21), 211909. doi:10.1063/1.4961241

Bollavaram, P., Devarakonda, S., Selim, M. S., & Sloan, E. D. (2000). Growth Kinetics of Single Crystal sII Hydrates: Elimination of Mass and Heat Transfer Effects. Annals of the New York Academy of Sciences, 912(1), 533-543. doi:10.1111/j.1749-6632.2000.tb06808.x

Brunetti, A., Scura, F., Barbieri, G., & Drioli, E. (2010). Membrane technologies for CO_2 separation. Journal of Membrane Science, 359(1-2), 115-125. doi: 10.1016/j.memsci.2009.11.040

Cady, G. H. (1983). Composition of clathrate gas hydrates of hydrogen sulfide, xenon, sulfur dioxide, chlorine, chloromethane, bromomethane, difluorochloromethane, difluorodichloromethane, and propane. The Journal of Physical Chemistry, 87(22), 4437-4441. doi: 10.1021/j100245a023

Cheltenham. (1998). Carbon Dioxide Capture from Power Stations.

Chen, G.-J., Guo, T.-M. (1996). Thermodynamic modeling of hydrate formation based on new concepts. Fluid Phase Equilib. 122, 43-65.

Chun, M.-K., & Lee, H. (1996). Kinetics of formation of carbon dioxide clathrate hydrates. Korean Journal of Chemical Engineering, 13(6), 620-626. doi:10.1007/bf02706029

Clarke, M. A., & Bishnoi, P. R. (2005). Determination of the intrinsic kinetics of of CO_2 gas hydrate decomposition using in-situ particle size analysis. Chemical Engineering Science, 60(3), 695-709. doi:10.1016/j.ces.2004.08.040

Choi, S., Drese, J. H., & Jones, C. W. (2009). Adsorbent Materials for Carbon Dioxide Capture from Large Anthropogenic Point Sources. ChemSusChem, 2(9), 796-854. doi: 10.1002/cssc.200900036

Choi, W.-J., Seo, J.-B., Jang, S.-Y., Jung, J.-H., & Oh, K.-J. (2009). Removal characteristics of CO_2 using aqueous MEA/AMP solutions in the absorption

and regeneration process. Journal of Environmental Sciences, 21(7), 907-913. doi: http://dx.doi.org/10.1016/S1001-0742(08)62360-8

Damen, K., Troost, M. v., Faaij, A., & Turkenburg, W. (2006). A comparison of electricity and hydrogen production systems with CO_2 capture and storage. Part A: Review and selection of promising conversion and capture technologies. Progress in Energy and Combustion Science, 32(2), 215-246. doi: http://dx.doi.org/10.1016/j.pecs.2005.11.005

Daraboina, N., Ripmeester, J., & Englezos, P. (2013). The impact of SO_2 on post combustion carbon dioxide capture in bed of silica sand through hydrate formation. International Journal of Greenhouse Gas Control, 15, 97-103. doi: 10.1016/j.ijggc.2013.02.008

Dashti, H., & Lou, X. (2018). Gas hydrate-based CO_2 separation process: Quantitative assessment of the effectiveness of various chemical additives involved in the process, Cham.

Dashti, H., Zhehao Yew, L., & Lou, X. (2015). Recent advances in gas hydrate-based CO_2 capture. Journal of Natural Gas Science and Engineering, 23, 195-207. doi:http://dx.doi.org/10.1016/j.jngse.2015.01.033

Delahaye, A., Fournaison, L., Marinhas, S., Chatti, I., Petitet, J.P., Dalmazzone, D., Fürst, W. (2006). Effect of THF on equilibrium pressure and dissociation enthalpy of CO_2 hydrates applied to secondary refrigeration. Ind. Eng. Chem. Res. 45, 391-397.

Diamond, L. W., & Akinfiev, N. N. (2003). Solubility of CO_2 in water from −1.5 to 100 °C and from 0.1 to 100 MPa: evaluation of literature data and thermodynamic modelling. Fluid Phase Equilibria, 208(1), 265-290. doi:https://doi.org/10.1016/S0378-3812(03)00041-4

Doman, L. E., Arora, V., Metelitsa, A., Leahy, M., Barden, J. L., Ford, M., . . . Lindstrom, P. (2013). International Energy Outlook 2013. Washington, DC: US Energy Information Administration.

Duc, N. H., Chauvy, F., & Herri, J.-M. (2007). CO_2 capture by hydrate crystallization – A potential solution for gas emission of steelmaking industry. Energy Conversion and Management, 48(4), 1313-1322. doi: http://dx.doi.org/10.1016/j.enconman.2006.09.024

Dyadin, Y. A., Larionov, E. G., Manakov, A. Y., Zhurko, F. V., Aladko, E. Y., Mikina, T. V., & Komarov, V. Y. (1999). Clathrate hydrates of hydrogen and neon. Mendeleev Communications, 9(5), 209-210. doi: http://dx.doi.org/10.1070/MC1999v009n05ABEH001104

Englezos, P. (1993). Clathrate hydrates. Industrial & Engineering Chemistry Research, 32(7), 1251-1274. doi:10.1021/ie00019a001

Englezos, P., Kalogerakis, N., Dholabhai, P. D., & Bishnoi, P. R. (1987). Kinetics of formation of methane and ethane gas hydrates. Chemical Engineering Science, 42(11), 2647-2658. doi:http://dx.doi.org/10.1016/0009-2509(87)87015-X

English, N. J., & MacElroy, J. M. D. (2015). Perspectives on molecular simulation of clathrate hydrates: Progress, prospects and challenges. Chemical Engineering Science, 121, 133-156. doi:10.1016/j.ces.2014.07.047

Erto, A., Silvestre-Albero, A., Silvestre-Albero, J., Rodríguez-Reinoso, F., Balsamo, M., Lancia, A., Montagnaro, F. (2015). Carbon-supported ionic liquids as

innovative adsorbents for CO_2 separation from synthetic flue-gas. J. Colloid Interface Sci. 448, 41-50.

Eslamimanesh, A., Mohammadi, A. H., Richon, D., Naidoo, P., & Ramjugernath, D. (2012). Application of gas hydrate formation in separation processes: A review of experimental studies. The Journal of Chemical Thermodynamics, 46, 62-71. doi: 10.1016/j.jct.2011.10.006

Falabella, B. J. (1975). A Study of Natural Gas Hydrates. (7605849 Ph.D.), University of Massachusetts Amherst, Ann Arbor. Retrieved from https://search.proquest.com/docview/302746250?accountid=14723

Falenty, A., Salamatin, A. N., & Kuhs, W. F. (2013). Kinetics of CO_2-hydrate formation from ice powders: Data summary and modeling extended to low temperatures. The Journal of Physical Chemistry C, 117(16), 8443-8457. doi:10.1021/jp310972b

Fan, S., Li, S., Wang, J., Lang, X., Wang, Y. (2009). Efficient capture of CO_2 from simulated flue gas by formation of TBAB or TBAF semiclathrate hydrates. Energy & fuels 23, 4202-4208. doi: 10.1021/ef9003329

Favre, E. (2007). Carbon dioxide recovery from post-combustion processes: Can gas permeation membranes compete with absorption? Journal of Membrane Science, 294(1-2), 50-59. doi: 10.1016/j.memsci.2007.02.007

Gholinezhad, J., Chapoy, A., & Tohidi, B. (2011). Separation and capture of carbon dioxide from CO_2/H_2 syngas mixture using semi-clathrate hydrates. Chemical Engineering Research and Design, 89(9), 1747-1751. doi: http://dx.doi.org/10.1016/j.cherd.2011.03.008

Giavarini, C., Maccioni, F., Politi, M., & Santarelli, M. L. (2007). CO_2 Hydrate: Formation and Dissociation Compared to Methane Hydrate. Energy & Fuels, 21(6), 3284-3291. doi: 10.1021/ef070080t

Giavarini, C., Maccioni, F., & Santarelli, M. L. (2003). Formation Kinetics of Propane Hydrates. Industrial & Engineering Chemistry Research, 42(7), 1517-1521. doi: 10.1021/ie0207764

Gupta, A., Lachance, J., Sloan Jr, E.D., Koh, C.A. (2008). Measurements of methane hydrate heat of dissociation using high pressure differential scanning calorimetry. Chem. Eng. Sci. 63, 5848-5853.

Handa, Y.P. (1986). Calorimetric determinations of the compositions, enthalpies of dissociation, and heat capacities in the range 85 to 270 K for clathrate hydrates of xenon and krypton. . J. Chem. Thermodyn. 18, 891-902.

Hashimoto, S., Murayama, S., Sugahara, T., & Ohgaki, K. (2006). Phase Equilibria for H_2 + CO_2 + Tetrahydrofuran + Water Mixtures Containing Gas Hydrates. Journal of Chemical & Engineering Data, 51(5), 1884-1886. doi: 10.1021/je0602364

Hashemi, S., Macchi, A., & Servio, P. (2007). Gas hydrate growth model in a semibatch stirred tank reactor. Industrial & Engineering Chemistry Research, 46(18), 5907-5912. doi:10.1021/ie061048+

Hashimoto, S., Sugahara, T., Moritoki, M., Sato, H., & Ohgaki, K. (2008). Thermodynamic stability of hydrogen tetra-n-butyl ammonium bromide mixed gas hydrate in nonstoichiometric aqueous solutions. Chemical Engineering Science, 63(4), 1092-1097. doi: http://dx.doi.org/10.1016/j.ces.2007.11.001

Hawkins, R. E., & Davidson, D. W. (1966). Dielectric Relaxation in the Clathrate Hydrates of Some Cyclic Ethers. The Journal of Physical Chemistry, 70(6), 1889-1894. doi: 10.1021/j100878a033

He, Z., Linga, P., & Jiang, J. (2017). What are the key factors governing the nucleation of CO_2 hydrate? Phys Chem Chem Phys, 19(24), 15657-15661. doi:10.1039/c7cp01350g

Hendriks, E. M., Edmonds, B., Moorwood, R. A. S., & Szczepanski, R. (1996). Hydrate structure stability in simple and mixed hydrates. Fluid Phase Equilibria, 117(1–2), 193-200. doi: http://dx.doi.org/10.1016/0378-3812(95)02953-2

Henning, R. W., Schultz, A. J., Thieu, V., & Halpern, Y. (2000). Neutron diffraction studies of CO_2 clathrate hydrate: Formation from deuterated ice. The Journal of Physical Chemistry A, 104(21), 5066-5071. doi:10.1021/jp0001642

Himmelblau, D.M., Riggs, J.B. (2012). Basic Principles and Calculations in Chemical Engineering. FT Press.

Ho, M. T., Allinson, G. W., & Wiley, D. E. (2008). Reducing the Cost of CO_2 Capture from Flue Gases Using Pressure Swing Adsorption. Industrial & Engineering Chemistry Research, 47(14), 4883-4890. doi: 10.1021/ie070831e

Jacobson, L. C., Hujo, W., & Molinero, V. (2010a). Amorphous precursors in the nucleation of clathrate hydrates. Journal of the American Chemical Society, 132(33), 11806-11811. doi:10.1021/ja1051445

Jacobson, L. C., Hujo, W., & Molinero, V. (2010b). Nucleation pathways of clathrate hydrates: Effect of guest size and solubility. The Journal of Physical Chemistry B, 114(43), 13796-13807. doi:10.1021/jp107269q

Kamath, V.A. (1984). Study of Heat Transfer Characteristics during Dissociation of Gas Hydrates in Porous Media, (Ph.D. Thesis).

Kang, S.-P., Lee, J.-W., & Ryu, H.-J. (2008). Phase behavior of methane and carbon dioxide hydrates in meso- and macro-sized porous media. Fluid Phase Equilibria, 274(1-2), 68-72. doi: 10.1016/j.fluid.2008.09.003

Kang, S.-P., Lee, J., & Seo, Y. (2013). Pre-combustion capture of CO_2 by gas hydrate formation in silica gel pore structure. Chemical Engineering Journal, 218, 126-132. doi: 10.1016/j.cej.2012.11.131

Kang, S., & Lee, H. (2000). Recovery of CO_2 from Flue Gas Using Gas Hydrate:? Thermodynamic Verification through Phase Equilibrium Measurements. Environmental science & technology, 34(20), 4397-4400. doi: 10.1021/es001148l

Kang, S. P., Lee, H., Lee, C. S., & Sung, W. M. (2001). Hydrate phase equilibria of the guest mixtures containing CO_2, N_2 and tetrahydrofuran. Fluid Phase Equilibria, 185(1–2), 101-109. doi: http://dx.doi.org/10.1016/S0378-3812(01)00460-5

Karanjkar, P. U., Lee, J. W., & Morris, J. F. (2012). Calorimetric investigation of cyclopentane hydrate formation in an emulsion. Chemical Engineering Science, 68(1), 481-491. doi: 10.1016/j.ces.2011.10.014

Karpiński, P. H. (1980). Crystallization as a mass transfer phenomenon. Chemical Engineering Science, 35(11), 2321-2324. doi:https://doi.org/10.1016/0009-2509(80)87010-2

Ke, W., Svartaas, T. M., & Chen, D. (2018). A Review of Gas Hydrate Nucleation Theories and Growth Models. Journal of Natural Gas Science and Engineering. doi:https://doi.org/10.1016/j.jngse.2018.10.021

Kelland, M. A. (2006). History of the development of low dosage hydrate inhibitors. Energy & Fuels, 20(3), 825-847. doi: Doi 10.1021/Ef050427x

Khurana, M., Yin, Z., & Linga, P. (2017). A review of clathrate hydrate nucleation. ACS Sustainable Chemistry & Engineering. doi:10.1021/acssuschemeng.7b03238

Kim, H.C., Bishnoi, P.R., Heidemann, R.A., Rizvi, S.S.H. (1987). Kinetics of methane hydrate decomposition. Chem. Eng. Sci. 42, 1645-1653.

Kim, S. M., Lee, J. D., Lee, H. J., Lee, E. K., & Kim, Y. (2011). Gas hydrate formation method to capture the carbon dioxide for pre-combustion process in IGCC plant. International Journal of Hydrogen Energy, 36(1), 1115-1121. doi: 10.1016/j.ijhydene.2010.09.062

Kimuro, H., Yamaguchi, F., Ohtsubo, K., Kusayanagi, T., & Morishita, M. (1993). CO_2 clathrate formation and its properties in a simulated deep ocean. Energy Conversion and Management, 34(9–11), 1089-1094. doi: http://dx.doi.org/10.1016/0196-8904(93)90057-H

Klaassen, R., Feron, P. H. M., & Jansen, A. E. (2005). Membrane Contactors in Industrial Applications. Chemical Engineering Research and Design, 83(3), 234-246. doi: http://dx.doi.org/10.1205/cherd.04196

Kvamme, B., Graue, A., Aspenes, E., Kuznetsova, T., Granasy, L., Toth, G., . . . Tegze, G. (2004). Kinetics of solid hydrate formation by carbon dioxide: Phase field theory of hydrate nucleation and magnetic resonance imaging. Physical Chemistry Chemical Physics, 6(9), 2327-2334. doi:10.1039/B311202K

Kumar, A., Sakpal, T., Linga, P., & Kumar, R. (2013). Influence of contact medium and surfactants on carbon dioxide clathrate hydrate kinetics. Fuel, 105, 664-671. doi: 10.1016/j.fuel.2012.10.031

Kumar, R., Englezos, P., Moudrakovski, I., & Ripmeester, J. A. (2009). Structure and composition of CO_2/H_2 and $CO_2/H_2/C_3H_8$ hydrate in relation to simultaneous CO_2 capture and H_2 production. AIChE Journal, 55(6), 1584-1594. doi: 10.1002/aic.11844

Kumar, R., Linga, P., Ripmeester, J., & Englezos, P. (2009). Two-Stage Clathrate Hydrate/Membrane Process for Precombustion Capture of Carbon Dioxide and Hydrogen. Journal of Environmental Engineering, 135(6), 411-417. doi: doi:10.1061/(ASCE)EE.1943-7870.0000002

Kumar, R., Linga, P., Ripmeester, J. A., & Englezos, P. (2009). Two-Stage Clathrate Hydrate/Membrane Process for Precombustion Capture of Carbon Dioxide and Hydrogen. J. Environ. Eng. (Reston, VA, U. S.), 135(6), 411-417. doi: 10.1061/(ASCE)EE.1943-7870.0000002

Kumar, R., Wu, H.-j., & Englezos, P. (2006). Incipient hydrate phase equilibrium for gas mixtures containing hydrogen, carbon dioxide and propane. Fluid Phase Equilibria, 244(2), 167-171. doi: http://dx.doi.org/10.1016/j.fluid.2006.04.008

Lee, H. J., Lee, J. D., Linga, P., Englezos, P., Kim, Y. S., Lee, M. S., & Kim, Y. D. (2010). Gas hydrate formation process for pre-combustion capture of carbon dioxide. Energy, 35(6), 2729-2733. doi: 10.1016/j.energy.2009.05.026

Lekse, J., Taylor, C. E., & Ladner, E. P. (2007). Effect of bubble size and density on methane conversion to hydrate. Journal of Petroleum Science and Engineering,56(1–3),97-100.doi: http://dx.doi.org/10.1016/j.petrol.2005.08.007

Lederhos, J. P., Long, J. P., Sum, A., Christiansen, R. L., & Sloan, E. D. (1996). Effective kinetic inhibitors for natural gas hydrates. Chemical Engineering Science, 51(8), 1221-1229. doi:https://doi.org/10.1016/0009-2509(95)00370-3

Li, S., Fan, S., Wang, J., Lang, X., & Liang, D. (2009). CO_2 capture from binary mixture via forming hydrate with the help of tetra-n-butyl ammonium bromide. Journal of Natural Gas Chemistry, 18(1), 15-20. doi: http://dx.doi.org/10.1016/S1003-9953(08)60085-7

Li, S., Fan, S., Wang, J., Lang, X., & Wang, Y. (2010). Clathrate Hydrate Capture of CO_2 from Simulated Flue Gas with Cyclopentane/Water Emulsion. Chinese Journal of Chemical Engineering, 18(2), 202-206. doi: http://dx.doi.org/10.1016/S1004-9541(08)60343-2

Li, X.-S., Xia, Z.-M., Chen, Z.-Y., & Wu, H.-J. (2011). Precombustion Capture of Carbon Dioxide and Hydrogen with a One-Stage Hydrate/Membrane Process in the Presence of Tetra-n-butylammonium Bromide (TBAB). Energy & fuels, 25(3), 1302-1309. doi: 10.1021/ef101559h

Li, X.-S., Xia, Z.-M., Chen, Z.-Y., Yan, K.-F., Li, G., & Wu, H.-J. (2010a). Equilibrium Hydrate Formation Conditions for the Mixtures of CO_2+ H_2+ Tetrabutyl Ammonium Bromide. Journal of Chemical & Engineering Data, 55(6), 2180-2184.

Li, X.-S., Xia, Z.-M., Chen, Z.-Y., Yan, K.-F., Li, G., & Wu, H.-J. (2010b). Gas Hydrate Formation Process for Capture of Carbon Dioxide from Fuel Gas Mixture. Industrial & Engineering Chemistry Research, 49(22), 11614-11619. doi: 10.1021/ie100851u

Li, X.-S., Xu, C.-G., Chen, Z.-Y., & Cai, J. (2012). Synergic effect of cyclopentane and tetra-n-butyl ammonium bromide on hydrate-based carbon dioxide separation from fuel gas mixture by measurements of gas uptake and X-ray diffraction patterns. International Journal of Hydrogen Energy, 37(1), 720-727. doi: 10.1016/j.ijhydene.2011.09.053

Li, X.-S., Xu, C.-G., Chen, Z.-Y., & Wu, H.-J. (2010). Tetra-n-butyl ammonium bromide semi-clathrate hydrate process for post-combustion capture of carbon dioxide in the presence of dodecyl trimethyl ammonium chloride. Energy, 35(9), 3902-3908. doi: 10.1016/j.energy.2010.06.009

Li, X.-S., Xu, C.-G., Chen, Z.-Y., & Wu, H.-J. (2011). Hydrate-based pre-combustion carbon dioxide capture process in the system with tetra-n-butyl ammonium bromide solution in the presence of cyclopentane. Energy, 36(3), 1394-1403. doi: 10.1016/j.energy.2011.01.034

Li, X.-S., Zhan, H., Xu, C.-G., Zeng, Z.-Y., Lv, Q.-N., & Yan, K.-F. (2012). Effects of Tetrabutyl-(ammonium/phosphonium) Salts on Clathrate Hydrate Capture of CO2from Simulated Flue Gas. Energy & fuels, 26(4), 2518-2527. doi: 10.1021/ef3000399

Li, X., Xu, C., Chen, Z., Wu, H., & Cai, J. (2011). Effect of temperature fluctuation on hydrate-based CO_2 separation from fuel gas. Journal of Natural Gas Chemistry, 20(6), 647-653. doi: 10.1016/s1003-9953(10)60254-x

Liang, S., Liang, D., Wu, N., Yi, L., & Hu, G. (2016). Molecular Mechanisms of Gas Diffusion in CO_2 Hydrates. The Journal of Physical Chemistry C, 120(30), 16298-16304. doi:10.1021/acs.jpcc.6b03111

Lievois, J.S., Perkins, R., Martin, R.J., Kobayashi, R. (1990). Development of an automated, high pressure heat flux calorimeter and its application to measure the heat of dissociation and hydrate numbers of methane hydrate. Fluid Phase Equilib. 59, 73-97.

Linga, P., Adeyemo, A., & Englezos, P. (2007). Medium-Pressure Clathrate Hydrate/Membrane Hybrid Process for Postcombustion Capture of Carbon Dioxide. Environmental science & technology, 42(1), 315.

Linga, P., Daraboina, N., Ripmeester, J. A., & Englezos, P. (2012). Enhanced rate of gas hydrate formation in a fixed bed column filled with sand compared to a stirred vessel. Chemical Engineering Science, 68(1), 617-623. doi: 10.1016/j.ces.2011.10.030

Linga, P., Kumar, R., & Englezos, P. (2007a). The clathrate hydrate process for post and pre-combustion capture of carbon dioxide. Journal of Hazardous Materials, 149(3), 625-629. doi: http://dx.doi.org/10.1016/j.jhazmat.2007.06.086

Linga, P., Kumar, R., & Englezos, P. (2007b). Gas hydrate formation from hydrogen/carbon dioxide and nitrogen/carbon dioxide gas mixtures. Chemical Engineering Science, 62(16), 4268-4276. doi: 10.1016/j.ces.2007.04.033

Lirio, C. F. d. S., Pessoa, F. L. P., & Uller, A. M. C. (2013). Storage capacity of carbon dioxide hydrates in the presence of sodium dodecyl sulfate (SDS) and tetrahydrofuran (THF). Chemical Engineering Science, 96, 118-123. doi: 10.1016/j.ces.2012.10.022

Liu, N., Chen, W., Liu, D., & Xie, Y. (2011). Characterization of CO_2 hydrate formation by temperature vibration. Energy Conversion and Management, 52(6), 2351-2354. doi: 10.1016/j.enconman.2010.12.037

Luo, Y. T., Zhu, J. H., Fan, S. S., & Chen, G. J. (2007). Study on the kinetics of hydrate formation in a bubble column. Chemical Engineering Science, 62(4), 1000-1009. doi: http://dx.doi.org/10.1016/j.ces.2006.11.004

Luzinova, Y., Dobbs, G. T., Raichlin, Y., Katzir, A., & Mizaikoff, B. (2011). Infrared spectroscopic monitoring of surface effects during gas hydrate formation in the presence of detergents. Chemical Engineering Science, 66(22), 5497-5503. doi: 10.1016/j.ces.2011.06.039

Maghsoodloo Babakhani, S., Bouillot, B., Ho-Van, S., Douzet, J., & Herri, J.-M. (2018). A review on hydrate composition and capability of thermodynamic modeling to predict hydrate pressure and composition. Fluid Phase Equilibria, 472, 22-38. doi:10.1016/j.fluid.2018.05.007

Malegaonkar, M. B., Dholabhai, P. D., & Bishnoi, P. R. (1997). Kinetics of carbon dioxide and methane hydrate formation. The Canadian Journal of Chemical Engineering, 75(6), 1090-1099. doi:10.1002/cjce.5450750612

Mano, H., Kazama, S., & Haraya, K. (2003). Development of CO_2 Separation Membranes (1) Polymer Membrane. In J. Gale & Y. Kaya (Eds.), Greenhouse Gas Control Technologies - 6th International Conference (pp. 1551-1554). Oxford: Pergamon.

Mansourizadeh, A., & Ismail, A. F. (2009). Hollow fiber gas–liquid membrane contactors for acid gas capture: A review. Journal of Hazardous Materials, 171(1–3), 38-53. doi: http://dx.doi.org/10.1016/j.jhazmat.2009.06.026

Mao, W. L., Mao, H.-k., Goncharov, A. F., Struzhkin, V. V., Guo, Q., Hu, J., . . . Zhao, Y. (2002). Hydrogen Clusters in Clathrate Hydrate. Science, 297(5590), 2247-2249. doi: 10.1126/science.1075394

Meisen, A., & Shuai, X. (1997). Research and development issues in CO_2 capture. Energy Conversion and Management, 38, Supplement(0), S37-S42. doi: http://dx.doi.org/10.1016/S0196-8904(96)00242-7

Meysel, P., Oellrich, L., Raj Bishnoi, P., & Clarke, M. A. (2011). Experimental investigation of incipient equilibrium conditions for the formation of semi-clathrate hydrates from quaternary mixtures of (CO_2+N_2+TBAB+H_2O). The Journal of Chemical Thermodynamics, 43(10), 1475-1479. doi: 10.1016/j.jct.2011.04.021

Millward, A. R., & Yaghi, O. M. (2005). Metal−Organic Frameworks with Exceptionally High Capacity for Storage of Carbon Dioxide at Room Temperature. Journal of the American Chemical Society, 127(51), 17998-17999. doi: 10.1021/ja0570032

Mochizuki, T., & Mori, Y. H. (2006). Clathrate-hydrate film growth along water/hydrate-former phase boundaries—numerical heat-transfer study. Journal of Crystal Growth, 290(2), 642-652. doi:http://dx.doi.org/10.1016/j.jcrysgro.2006.01.036

Mohammadi, A. H., Eslamimanesh, A., Belandria, V., Richon, D., Naidoo, P., & Ramjugernath, D. (2012a). Phase equilibrium measurements for semi-clathrate hydrates of the (CO_2 + N_2 + tetra-n-butylammonium bromide) aqueous solution system. J. Chem. Thermodyn., 46, 57-61. doi: 10.1016/j.jct.2011.10.004

Mohammadi, A. H., Eslamimanesh, A., Belandria, V., Richon, D., Naidoo, P., & Ramjugernath, D. (2012b). Phase equilibrium measurements for semi-clathrate hydrates of the (CO_2+N_2+tetra-n-butylammonium bromide) aqueous solution system. The Journal of Chemical Thermodynamics, 46, 57-61. doi: 10.1016/j.jct.2011.10.004

Mohammadi, A. H., Eslamimanesh, A., & Richon, D. (2013). Semi-clathrate hydrate phase equilibrium measurements for the CO_2+H_2/CH_4+tetra-n-butylammonium bromide aqueous solution system. Chemical Engineering Science, 94, 284-290. doi: 10.1016/j.ces.2013.01.063

Mondal, M. K., Balsora, H. K., & Varshney, P. (2012). Progress and trends in CO_2 capture/separation technologies: A review. Energy, 46(1), 431-441. doi: 10.1016/j.energy.2012.08.006

Mori, Y. H. (2001). Estimating the thickness of hydrate films from their lateral growth rates: application of a simplified heat transfer model. Journal of Crystal Growth, 223(1), 206-212. doi:https://doi.org/10.1016/S0022-0248(01)00614-5

Mullin, J. W. (2001). Nucleation. In Crystallization (Fourth Edition ed., pp. 181-215). Oxford: Butterworth-Heinemann.

Nakajima, M., Ohmura, R., & Mori, Y. H. (2008). Clathrate Hydrate Formation from Cyclopentane-in-Water Emulsions. Industrial & Engineering Chemistry Research, 47(22), 8933-8939. doi: 10.1021/ie800949k

Natarajan, V., Bishnoi, P. R., & Kalogerakis, N. (1994). Induction phenomena in gas hydrate nucleation. Chemical Engineering Science, 49(13), 2075-2087. doi:https://doi.org/10.1016/0009-2509(94)E0026-M

Okabe, K., Matsumiya, N., Mano, H., & Teramoto, M. (2003). Development of CO_2 Separation Membranes (2) Facilitated Transport Membrane. In J. Gale & Y. Kaya (Eds.), Greenhouse Gas Control Technologies - 6th International Conference (pp. 1555-1558). Oxford: Pergamon.

Okutani, K., Kuwabara, Y., & Mori, Y. H. (2008). Surfactant effects on hydrate formation in an unstirred gas/liquid system: An experimental study using methane and sodium alkyl sulfates. Chemical Engineering Science, 63(1), 183-194. doi: http://dx.doi.org/10.1016/j.ces.2007.09.012

Olajire, A. A. (2010). CO_2 capture and separation technologies for end-of-pipe applications – A review. Energy, 35(6), 2610-2628. doi: 10.1016/j.energy.2010.02.030

Oshima, M., Shimada, W., Hashimoto, S., Tani, A., & Ohgaki, K. (2010). Memory effect on semi-clathrate hydrate formation: A case study of tetragonal tetra-n-butyl ammonium bromide hydrate. Chemical Engineering Science, 65(20), 5442-5446. doi: 10.1016/j.ces.2010.07.019

Ostroverkhov, V., Waychunas, G. A., & Shen, Y. R. (2005). New Information on Water Interfacial Structure Revealed by Phase-Sensitive Surface Spectroscopy. Physical Review Letters, 94(4), 046102.

Ou, W., Lu, W., Qu, K., Geng, L., & Chou, I. M. (2016). In situ Raman spectroscopic investigation of flux-controlled crystal growth under high pressure: A case study of carbon dioxide hydrate growth in aqueous solution. International Journal of Heat and Mass Transfer, 101, 834-843. doi:10.1016/j.ijheatmasstransfer.2016.05.082

Oyama, H., Shimada, W., Ebinuma, T., Kamata, Y., Takeya, S., Uchida, T., . . . Narita, H. (2005). Phase diagram, latent heat, and specific heat of TBAB semiclathrate hydrate crystals. Fluid Phase Equilibria, 234(1-2), 131-135. doi: 10.1016/j.fluid.2005.06.005

Park, S., Lee, S., Lee, Y., Lee, Y., & Seo, Y. (2013). Hydrate-based pre-combustion capture of carbon dioxide in the presence of a thermodynamic promoter and porous silica gels. International Journal of Greenhouse Gas Control, 14(0), 193-199. doi: http://dx.doi.org/10.1016/j.ijggc.2013.01.026

Peng, D.-Y., Robinson, D.B. (1976). A new two-constant equation of state. Ind. Eng. Chem. Fundam. 15, 59-64.

Radhakrishnan, R., & Trout, B. L. (2002). A new approach for studying nucleation phenomena using molecular simulations: Application to CO_2 hydrate clathrates. The Journal of Chemical Physics, 117(4), 1786-1796. doi:10.1063/1.1485962

Ratcliffe, C.I., Ripmeester, J.A. (1986). Proton and carbon-13 NMR studies on carbon dioxide hydrate. J. Phys. Chem. 90, 1259-1263.

Ramezan, M., Skone, T. J., Nsakala, N. Y., Liljedahl, G. N., Gearhart, L. E., Hestermann, R., & Rederstorff, B. (2007). Carbon dioxide capture from existing coal-fired power plants. National Energy Technology Laboratory, DOE/NETL Report, (401/110907).

Ribeiro Jr, C. P., & Lage, P. L. C. (2008). Modelling of hydrate formation kinetics: State-of-the-art and future directions. Chemical Engineering Science, 63(8), 2007-2034. doi:http://dx.doi.org/10.1016/j.ces.2008.01.014

Ripmeester, J. A., & Alavi, S. (2016). Some current challenges in clathrate hydrate science: Nucleation, decomposition and the memory effect. Current Opinion in Solid State and Materials Science, 20(6), 344-351. doi:10.1016/j.cossms.2016.03.005

Robinson, D. B., & Peng, D.-Y. (1978). The characterization of the heptanes and heavier fractions for the GPA Peng-Robinson programs. Tulsa, Okla.: Gas Processors Association.

Rojas, Y., & Lou, X. (2010). Instrumental analysis of gas hydrates properties. Asia-Pacific Journal of Chemical Engineering, 5(2), 310-323. doi: 10.1002/apj.293

Rueff, R.M., Dendy Sloan, E., Yesavage, V.F. (1988). Heat capacity and heat of dissociation of methane hydrates. AIChE journal 34, 1468-1476.

Sabil, K. M., Witkamp, G.-J., & Peters, C. J. (2010). Estimations of enthalpies of dissociation of simple and mixed carbon dioxide hydrates from phase equilibrium data. Fluid Phase Equilibria, 290(1–2), 109-114. doi: http://dx.doi.org/10.1016/j.fluid.2009.07.006

Selim, M. S., & Sloan, E. D. (1989). Heat and mass transfer during the dissociation of hydrates in porous media. AIChE Journal, 35(6), 1049-1052. doi:10.1002/aic.690350620

Satyapal, S., Filburn, T., Trela, J., & Strange, J. (2001). Performance and properties of a solid amine sorbent for carbon dioxide removal in space life support applications. Energy & Fuels, 15(2), 250-255.doi: 10.1021/ef0002391

Seo, Y.-T., Moudrakovski, I. L., Ripmeester, J. A., Lee, J.-w., & Lee, H. (2005). Efficient Recovery of CO_2 from Flue Gas by Clathrate Hydrate Formation in Porous Silica Gels. Environmental science & technology, 39(7), 2315-2319. doi: 10.1021/es049269z

Seo, Y., & Kang, S.-P. (2010). Enhancing CO_2 separation for pre-combustion capture with hydrate formation in silica gel pore structure. Chemical Engineering Journal, 161(1-2), 308-312. doi: 10.1016/j.cej.2010.04.032

Shi, B.-H., Fan, S.-S., & Lou, X. (2014). Application of the shrinking-core model to the kinetics of repeated formation of methane hydrates in a system of mixed dry-water and porous hydrogel particulates. Chemical Engineering Science, 109, 315-325. doi:http://dx.doi.org/10.1016/j.ces.2014.01.035

Shi, B.-H., Gong, J., Sun, C.-Y., Zhao, J.-K., Ding, Y., & Chen, G.-J. (2011). An inward and outward natural gas hydrates growth shell model considering intrinsic kinetics, mass and heat transfer. Chemical Engineering Journal, 171(3), 1308-1316. doi:http://dx.doi.org/10.1016/j.cej.2011.05.029

Shi, B.-H., Yang, L., Fan, S.-S., & Lou, X. (2017). An investigation on repeated methane hydrates formation in porous hydrogel particles. Fuel, 194, 395-405. doi:10.1016/j.fuel.2017.01.037

Singh, R., & Shukla, A. (2014). A review on methods of flue gas cleaning from combustion of biomass. Renewable and Sustainable Energy Reviews, 29(0), 854-864. doi: http://dx.doi.org/10.1016/j.rser.2013.09.005

Skovborg, P., Ng, H. J., Rasmussen, P., & Mohn, U. (1993). Measurement of induction times for the formation of methane and ethane gas hydrates. Chemical

Engineering Science, 48(3), 445-453. doi:https://doi.org/10.1016/0009-2509(93)80299-6

Sloan, E. D. (2003). Fundamental principles and applications of natural gas hydrates. Nature, 426(6964), 353-363.

Sloan, E. D., & Koh, C. A. (2008). Clathraye Hydrates of Natural Gases (third ed. Vol. 119). New York: Taylor & Francis Group.

Spencer, D.F. (1999). Integration of an advanced CO_2 separation process with methods for disposing of CO_2 in oceans and terrestrial deep aquifers. Greenhouse Gas Control Technologies, 89, Elsevier.

Spigarelli, B. P., & Kawatra, S. K. (2013b). Opportunities and challenges in carbon dioxide capture. Journal of CO_2 Utilization(0). doi: http://dx.doi.org/10.1016/j.jcou.2013.03.002

Staykova, D. K., Kuhs, W. F., Salamatin, A. N., & Hansen, T. (2003). Formation of porous gas hydrates from ice powders: Diffraction experiments and multistage model. The Journal of Physical Chemistry B, 107(37), 10299-10311. doi:10.1021/jp027787v

Stewart, C., & Hessami, M.-A. (2005). A study of methods of carbon dioxide capture and sequestration—the sustainability of a photosynthetic bioreactor approach. Energy Conversion and Management, 46(3), 403-420. doi: http://dx.doi.org/10.1016/j.enconman.2004.03.009

Strobel, T. A., Koh, C. A., & Sloan, E. D. (2009). Thermodynamic predictions of various tetrahydrofuran and hydrogen clathrate hydrates. Fluid Phase Equilibria, 280(1-2), 61-67. doi: 10.1016/j.fluid.2009.02.012

Suginaka, T., Sakamoto, H., Iino, K., Sakakibara, Y., & Ohmura, R. (2013). Phase equilibrium for ionic semiclathrate hydrate formed with CO_2, CH_4, or N_2 plus tetrabutylphosphonium bromide. Fluid Phase Equilibria, 344, 108-111. doi: 10.1016/j.fluid.2013.01.018

Sun, C.-Y., Chen, G.-J., Ma, C.-F., Huang, Q., Luo, H., & Li, Q.-P. (2007). The growth kinetics of hydrate film on the surface of gas bubble suspended in water or aqueous surfactant solution. Journal of Crystal Growth, 306(2), 491-499. doi: http://dx.doi.org/10.1016/j.jcrysgro.2007.05.037

Sun, Q., & Kang, Y. T. (2016). Review on CO_2 hydrate formation/dissociation and its cold energy application. Renewable and Sustainable Energy Reviews, 62, 478-494. doi:10.1016/j.rser.2016.04.062

Sun, Z.-G., Fan, S.-S., Guo, K.-H., Shi, L., Guo, Y.-K., & Wang, R.-Z. (2002). Gas Hydrate Phase Equilibrium Data of Cyclohexane and Cyclopentane. Journal of Chemical & Engineering Data, 47(2), 313-315. doi: 10.1021/je0102199

Tajima, H., Yamasaki, A., & Kiyono, F. (2004). Energy consumption estimation for greenhouse gas separation processes by clathrate hydrate formation. Energy, 29(11), 1713-1729. doi: http://dx.doi.org/10.1016/j.energy.2004.03.003

Tam, S. S., Stanton, M. E., Ghose, S., Deppe, G., Spencer, D. F., Currier, R. P., . . . Devlin, D. J. (n.d.). A High Pressure Carbon Dioxide Separation Process for IGCC Plants. Retrieved September 19, 2013, from http://www.netl.doe.gov/publications/proceedings/01/carbon_seq/1b4.pdf

Tang, J., Zeng, D., Wang, C., Chen, Y., He, L., & Cai, N. (2013a). Study on the influence of SDS and THF on hydrate-based gas separation performance. Chemical Engineering Research and Design. doi: 10.1016/j.cherd.2013.03.013

Tang, J., Zeng, D., Wang, C., Chen, Y., He, L., & Cai, N. (2013b). Study on the influence of SDS and THF on hydrate-based gas separation performance. Chemical Engineering Research and Design(0). doi: http://dx.doi.org/10.1016/j.cherd.2013.03.013

Teng, H., Kinoshita, C. M., & Masutani, S. M. (1995). Hydrate formation on the surface of a CO_2 droplet in high-pressure, low-temperature water. Chemical Engineering Science, 50(4), 559-564. doi:https://doi.org/10.1016/0009-2509(94)00438-W

Torré, J.-P., Dicharry, C., Ricaurte, M., Daniel-David, D., & Broseta, D. (2011). CO_2 capture by hydrate formation in quiescent conditions: In search of efficient kinetic additives. Energy Procedia, 4, 621-628. doi: 10.1016/j.egypro.2011.01.097

Torré, J.-P., Ricaurte, M., Dicharry, C., & Broseta, D. (2012). CO_2 enclathration in the presence of water-soluble hydrate promoters: Hydrate phase equilibria and kinetic studies in quiescent conditions. Chemical Engineering Science, 82(0), 1-13. doi: http://dx.doi.org/10.1016/j.ces.2012.07.025

Trueba, A. T., Radović, I. R., Zevenbergen, J. F., Peters, C. J., & Kroon, M. C. (2013). Kinetic measurements and in situ Raman spectroscopy study of the formation of TBAF semi-hydrates with hydrogen and carbon dioxide. International Journal of Hydrogen Energy. doi: 10.1016/j.ijhydene.2013.03.154

Uchida, T., Ebinuma, T., Kawabata, J. i., & Narita, H. (1999). Microscopic observations of formation processes of clathrate-hydrate films at an interface between water and carbon dioxide. Journal of Crystal Growth, 204(3), 348-356. doi:http://dx.doi.org/10.1016/S0022-0248(99)00178-5

Udachin, K.A., Ratcliffe, C.I., Ripmeester, J.A. (2001). Structure, composition, and thermal expansion of CO_2 hydrate from single crystal x-ray diffraction measurements. J. Phys. Chem. B, 105, 4200-4204.

Uddin, M., Coombe, D., Law, D., & Gunter, B. (2008). Numerical studies of gas hydrate formation and decomposition in a geological reservoir. Journal of Energy Resources Technology, 130(3), 032501-032501-032514. doi:10.1115/1.2956978

Unruh, C. H., & Katz, D. L. (1949). Gas Hydrates of Carbon Dioxide-Methane Mixtures. Journal of Petroleum Technology, 1(4), 83-86. doi: 10.2118/949983-G

Upadhyaya, A., Acosta, E. J., Scamehorn, J. F., & Sabatini, D. A. (2007). Adsorption of Anionic–Cationic Surfactant Mixtures on Metal oxide Surfaces. Journal of Surfactants and Detergents, 10(4), 269-277. doi: 10.1007/s11743-007-1045-3

Vatamanu, J., & Kusalik, P. G. (2010). Observation of two-step nucleation in methane hydrates. Phys Chem Chem Phys, 12(45), 15065-15072. doi:10.1039/c0cp00551g

Verrett, J., & Servio, P. (2016). Reaction rate constant of CO_2-Tetra-n-butylammounium bromide semi-clathrate formation. The Canadian Journal of Chemical Engineering, 94(11), 2138-2144. doi:10.1002/cjce.22612

Vysniauskas, A., & Bishnoi, P. R. (1983). A kinetic study of methane hydrate formation. Chemical Engineering Science, 38(7), 1061-1072. doi:https://doi.org/10.1016/0009-2509(83)80027-X

Walsh, M. R., Beckham, G. T., Koh, C. A., Sloan, E. D., Wu, D. T., & Sum, A. K. (2011). Methane hydrate nucleation rates from molecular dynamics simulations:

Effects of aqueous methane concentration, interfacial curvature, and system size. The Journal of Physical Chemistry C, 115(43), 21241-21248. doi:10.1021/jp206483q

Wang, M., Joel, A.S., Ramshaw, C., Eimer, D., Musa, N.M. (2015). Process intensification for post-combustion CO_2 capture with chemical absorption: A critical review. Appl. Energy 158, 275-291

Warrier, P., Khan, M. N., Srivastava, V., Maupin, C. M., & Koh, C. A. (2016). Overview: Nucleation of clathrate hydrates. J Chem Phys, 145(21), 211705. doi:10.1063/1.4968590

Wataru, S., Takao, E., Hiroyuki, O., Yasushi, K., Satoshi, T., Tsutomu, U., . . . Hideo, N. (2003). Separation of Gas Molecule Using Tetra- n -butyl Ammonium Bromide Semi-Clathrate Hydrate Crystals. Japanese Journal of Applied Physics, 42(2A), L129.

Xu, C.-G., Cai, J., Li, X.-S., Lv, Q.-N., Chen, Z.-Y., & Deng, H.-W. (2012). Integrated Process Study on Hydrate-Based Carbon Dioxide Separation from Integrated Gasification Combined Cycle (IGCC) Synthesis Gas in Scaled-Up Equipment. Energy & fuels, 26(10), 6442-6448. doi: 10.1021/ef3011993

Xu, C.-G., Li, X.-S., Lv, Q.-N., Chen, Z.-Y., & Cai, J. (2012). Hydrate-based CO_2 (carbon dioxide) capture from IGCC (integrated gasification combined cycle) synthesis gas using bubble method with a set of visual equipment. Energy, 44(1), 358-366. doi: 10.1016/j.energy.2012.06.021

Xu, C., Li, X., Cai, J., & Chen, Z. (2012). Hydrate-based carbon dioxide capture from simulated integrated gasification combined cycle gas. Journal of Natural Gas Chemistry, 21(5), 501-507. doi: 10.1016/s1003-9953(11)60397-6

Yang, D., Le, L. A., Martinez, R. J., Currier, R. P., & Spencer, D. F. (2011). Kinetics of CO_2 hydrate formation in a continuous flow reactor. Chemical Engineering Journal, 172(1), 144-157. doi:10.1016/j.cej.2011.05.082

Yang, M., Song, Y., Jiang, L., Wang, X., Liu, W., Zhao, Y., . . . Wang, S. (2013). Dynamic measurements of hydrate based gas separation in cooled silica gel. Journal of Industrial and Engineering Chemistry. doi: 10.1016/j.jiec.2013.03.031

Yang, M., Song, Y., Liu, W., Zhao, J., Ruan, X., Jiang, L., & Li, Q. (2013). Effects of additive mixtures (THF/SDS) on carbon dioxide hydrate formation and dissociation in porous media. Chemical Engineering Science, 90, 69-76. doi: 10.1016/j.ces.2012.11.026

Yin, Z., Khurana, M., Tan, H. K., & Linga, P. (2018). A review of gas hydrate growth kinetic models. Chemical Engineering Journal, 342, 9-29. doi:10.1016/j.cej.2018.01.120

Yoon, J.-H., Yamamoto, Y., Komai, T., Haneda, H., Kawamura, T. (2003). Rigorous approach to the prediction of the heat of dissociation of gas hydrates. Ind. Eng. Chem. Res. 42, 1111-1114.

Yoslim, J., Linga, P., & Englezos, P. (2010). Enhanced growth of methane–propane clathrate hydrate crystals with sodium dodecyl sulfate, sodium tetradecyl sulfate, and sodium hexadecyl sulfate surfactants. Journal of Crystal Growth, 313(1), 68-80. doi: 10.1016/j.jcrysgro.2010.10.009

Yue, M. B., Chun, Y., Cao, Y., Dong, X., & Zhu, J. H. (2006). CO_2 Capture by As-Prepared SBA-15 with an Occluded Organic Template. Advanced Functional Materials, 16(13), 1717-1722. doi: 10.1002/adfm.200600427

Zhang, J., & Lee, J. W. (2008). Enhanced Kinetics of CO_2 Hydrate Formation under Static Conditions. Industrial & Engineering Chemistry Research, 48(13), 5934-5942. doi: 10.1021/ie801170u

Zhang, J., Yedlapalli, P., & Lee, J. W. (2009). Thermodynamic analysis of hydrate-based pre-combustion capture of CO_2. Chemical Engineering Science, 64(22), 4732-4736. doi: 10.1016/j.ces.2009.04.041

Zhang, J. S., & Lee, J. W. (2008). Equilibrium of Hydrogen + Cyclopentane and Carbon Dioxide + Cyclopentane Binary Hydrates†. Journal of Chemical & Engineering Data, 54(2), 659-661. doi: 10.1021/je800219k

Zheng, J. M., Chin, W. C., Khijniak, E., Khijniak, E., Jr., & Pollack, G. H. (2006). Surfaces and interfacial water: evidence that hydrophilic surfaces have long-range impact. Adv Colloid Interface Sci, 127(1), 19-27. doi: 10.1016/j.cis.2006.07.002

Every reasonable effort has been made to acknowledge the owners of copyright material. I would be pleased to hear from any copyright owner who has been omitted or incorrectly acknowledged.